STATE OF ALASKA

DEPARTMENT OF NATURAL RESOURCES

DIVISION OF GEOLOGICAL AND GEOPHYSICAL SURVEYS

Steve Cowper, *Governor*

Judith M. Brady, *Commissioner*

Robert B. Forbes, *Director and State Geologist*

March 1988

This report is a preliminary publication of DGGS. The author is solely responsible for its content and will appreciate candid comments on the accuracy of the data as well as suggestions to improve the report.

Report of Investigations 88-3

A GELOGICAL, GEOCHEMICAL, AND GEOPHYSICAL SURVEY OF THE GEOTHERMAL RESOURCES AT HOT SPRINGS BAY VALLEY, AKUTAN ISLAND, ALASKA

Edited by
Roman J. Motyka and Christopher J. Nye

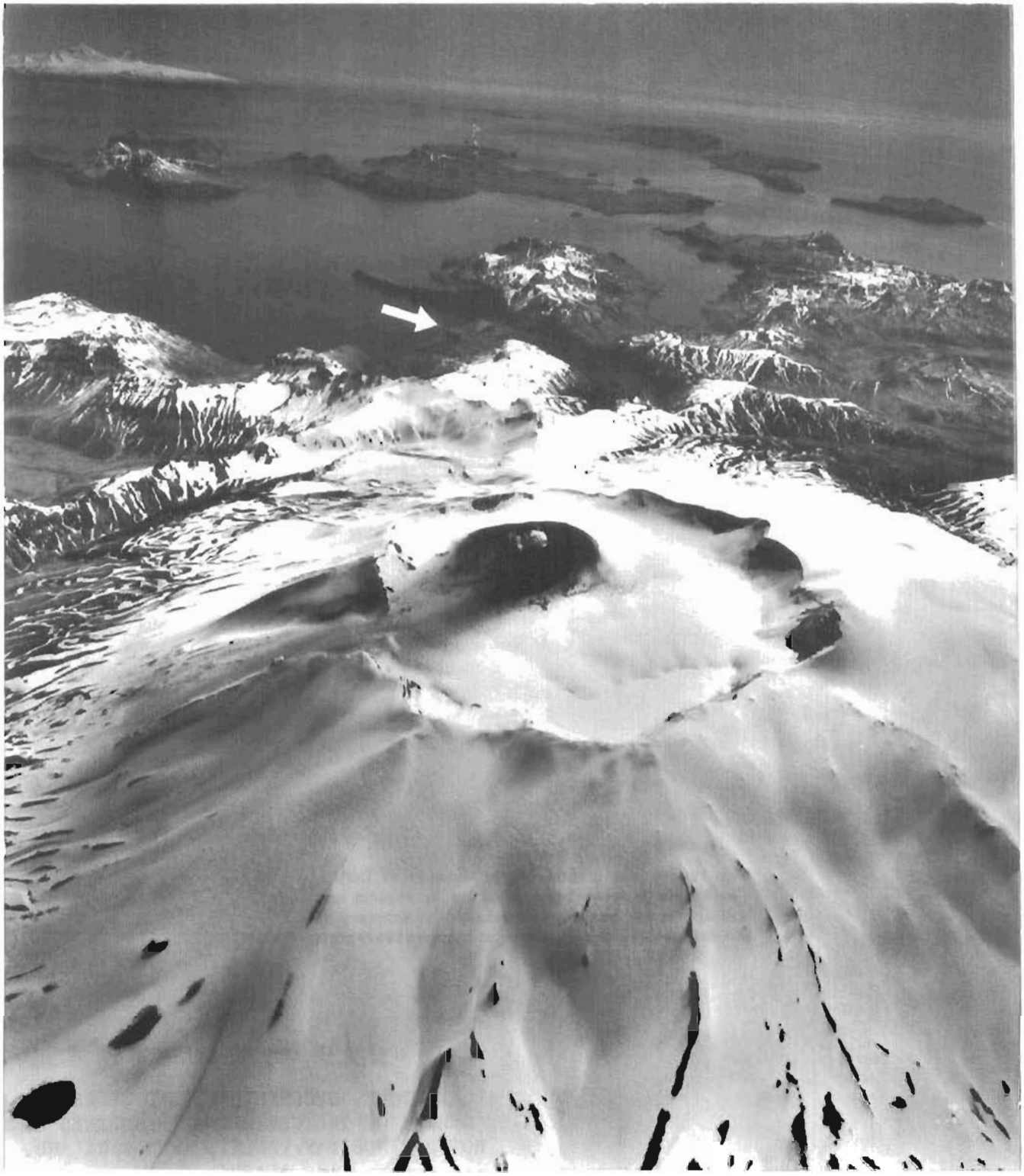

Aerial view of Akutan Volcano, looking east-northeast. The summit caldera is about 2 km in diameter; the active cinder cone within the caldera is the source of recent eruptions. Hot Springs Bay is northeast of the volcano (arrow); Akutan Harbor indents the eastern end of the island. Akun and Unimak Islands can be seen in the background and far background, respectively. Photo taken by North Pacific Aerial Surveys, Anchorage, Alaska on June 7, 1983.

A GEOLOGICAL, GEOCHEMICAL, AND GEOPHYSICAL SURVEY OF THE GEOTHERMAL RESOURCES AT HOT SPRINGS BAY VALLEY, AKUTAN ISLAND, ALASKA

Edited by

Roman J. Motyka[1] and Christopher J. Nye[2]

[1]Alaska Division of Geological and Geophysical Surveys, 400 Willoughby Ave., 3rd floor, Juneau, Alaska 99801

[2]Alaska Division of Geological and Geophysical Surveys, 794 University Ave., Suite 200, Fairbanks, Alaska 99709 (current address: Geophysical Institute, University of Alaska-Fairbanks, Fairbanks, Alaska 99775)

STATE OF ALASKA
Department of Natural Resources
DIVISION OF GEOLOGICAL & GEOPHYSICAL SURVEYS

According to Alaska Statute 41, the Alaska Division of Geological and Geophysical Surveys is charged with conducting 'geological and geophysical surveys to determine the potential of Alaskan land for production of metals, minerals, fuels, and geothermal resources; the locations and supplies of ground water and construction materials; the potential geologic hazards to buildings, roads, bridges, and other installations and structures; and shall conduct such other surveys and investigations as will advance knowledge of the geology of Alaska.'

In addition, the Division of Geological and Geophysical Surveys shall collect, record, evaluate, and distribute data on the quantity, quality, and location of underground, surface, and coastal water of the state; publish or have published data on the water of the state and require that the results and findings of surveys of water quality, quantity, and location be filed; require that water-well contractors file basic water and aquifer data, including but not limited to well location, estimated elevation, well-driller's logs, pumping tests, flow measurements, and water-quality determinations; accept and spend funds for the purposes of this section, AS 41.08.017 and 41.08.035, and enter into agreements with individuals, public or private agencies, communities, private industry, and state and federal agencies; collect, record, evaluate, archive, and distribute data on seismic events and engineering geology of the state; and identify and inform public officials and industry about potential seismic hazards that might affect development in the state.

Administrative functions are performed under the direction of the Director, who maintains his office in Fairbanks. The locations of DGGS offices are listed below:

.794 University Avenue
(Suite 200)
Fairbanks, 99709
(907)474-7147

.400 Willoughby Avenue
(3rd floor)
Juneau, 99801
(907)465-2533

.18225 Fish Hatchery Road
P.O. Box 772116
Eagle River, 99577
(907)696-0070

This report is for sale by DGGS for $7.50. DGGS publications may be inspected at the following locations. Mail orders should be addressed to the Fairbanks office.

.794 University Avenue
(Suite 200)
Fairbanks, 99709

.400 Willoughby Avenue
(3rd floor)
Juneau

.U.S. Geological Survey
Public Information Office
701 C Street
Anchorage

.Information Specialist
U.S. Geological Survey
4230 University Drive, Room 101
Anchorage

CONTENTS

ILLUSTRATIONS

Page

SHEETS

TABLES

CHAPTER 1

INTRODUCTION AND SUMMARY OF GEOTHERMAL INVESTIGATIONS IN HOT SPRINGS BAY VALLEY, AKUTAN ISLAND, ALASKA

by

Roman J. Motyka,[1] Eugene M. Wescott,[2] Donald L. Turner,[2] Samuel E. Swanson,[2] Roger D. Allely,[3] and Mark Larsen[3]

[1]Alaska Division of Geological and Geophysical Surveys, 400 Willoughby Ave., 3rd floor, Juneau, Alaska 99801
[2]Geophysical Institute, University of Alaska-Fairbanks, Fairbanks, Alaska 99775
[3]Alaska Division of Geological and Geophysical Surveys, 18225 Fish Hatchery Road, P.O. Box 772116, Eagle River, Alaska 99577

INTRODUCTION

Regional and site-specific exploration and assessment of geothermal resources in Alaska were initiated in 1979 by the Alaska Division of Geological and Geophysical Surveys (DGGS) and the Geophysical Institute, University of Alaska, under a program jointly sponsored and funded by the U.S. Department of Energy and the State of Alaska. Impetus for the program was derived in part from federal policy for finding ways of decreasing national dependency on fossil-fuel energy sources and from a State policy of fostering energy and economic independence in rural areas of Alaska. Early in the study, it was recognized that the best potential for finding high-temperature geothermal resources---those capable of generating electrical power---lies in the Aleutian arc of active volcanism. State and local governments, Aleutian Islands area native corporations, and industry all expressed strong interest in the development of such resources as a means of providing stable and economical electrical power to support the State's growing fishing industry. The Bering Sea fishery is acknowledged to be one of the richest in the world. In addition, oil and gas exploration in the Bering Sea region has intensified in recent years, increasing the demand for land-based support facilities.

An extensive geothermal reconnaissance of the Aleutian arc was made in 1980 by DGGS. Using chemical and isotopic geothermometry and the existence of persistent fumarole fields as indicators, at least 13 sites were identified as potential locations of high-temperature hydrothermal systems (T >150°) (Motyka and others, 1981; Motyka, 1982). One of the most promising sites for future development is Hot Springs Bay valley on Akutan Island. Preliminary geothermometry applied to waters obtained from Akutan hot springs indicated reservoir temperatures of 170-190°C (Motyka and others, 1981), sufficient for electrical-power generation. The thermal waters could also be used for space heating and for industrial direct-use application. The resource is close to potential users located in Akutan village, 6 km away, and to Akutan Harbor, one of the few sheltered, deep-water harbors in the Aleutians. Several fish-processing plants operate in the area, and a state-supported bottom-fish processing plant has recently been constructed near Akutan village. For these reasons, Hot Springs Bay valley was chosen for more detailed geothermal exploration. Most field surveys were accomplished during July 1981. This report describes these surveys and the results of the investigations.

REGIONAL SETTING

Akutan Island is located in the eastern Aleutian Islands between Unimak and Unalaska Islands (figs. 1-1 and 1-2). The Aleutian Chain is composed predominately of volcanic rocks, and most of the major islands, including Akutan, have active volcanoes. The volcanic arc lies immediately north of the Aleutian Trench, a convergent boundary between the North American and the Pacific lithospheric plates. This convergence produces a seismically active belt with much of the seismicity originating from the Benioff zone, the subcrustal region where the Pacific plate is being actively subducted under the North American plate. The eruption of Aleutian magmas, including those of Akutan Island, appears to be intimately related to this subduction process.

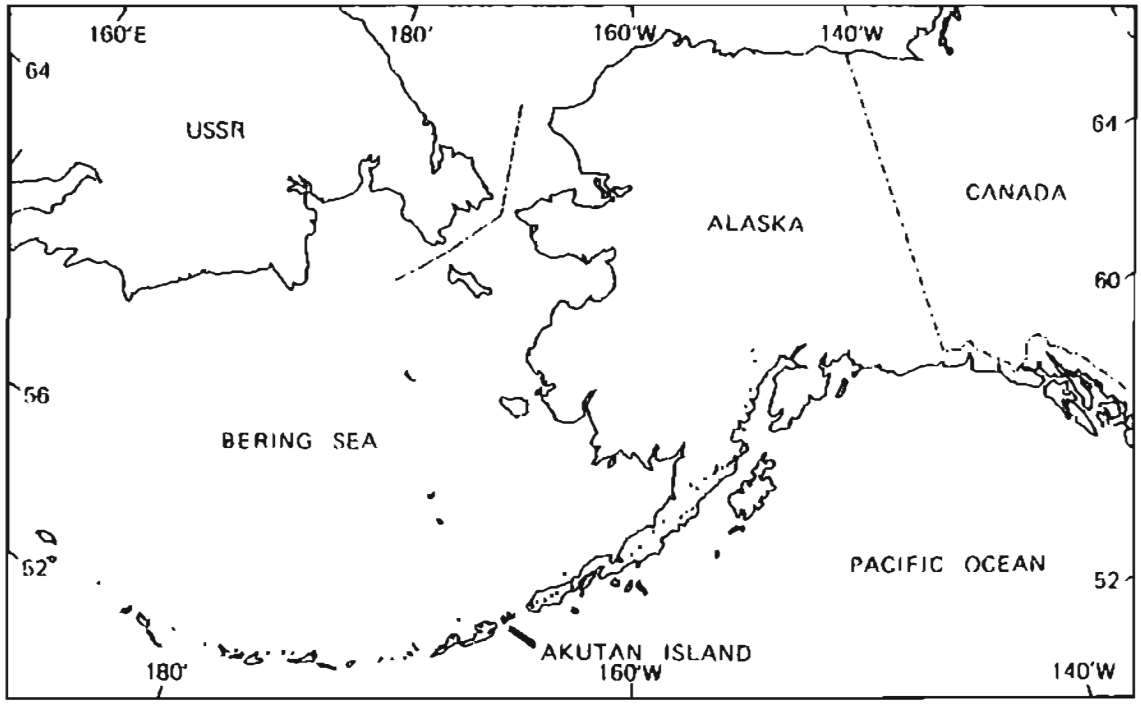

Figure 1-1. Position of Akutan Island within the Aleutian Arc. Dots represent locations of volcanoes along the arc.

Akutan Island is mountainous and rugged with shorelines dominated by steep cliffs and rocky headlands. Akutan volcano (1,300 m), a composite shield volcano, has erupted numerous times in recorded history and remains active, with several eruptions occurring during the past decade. Portions of the island not covered by recent volcanic flows show signs of extensive glaciation, including serrated ridges, cirques, hanging valleys, and broad U-shaped valleys. The east end of the island is bisected by Akutan Harbor, a deep, 8-km-long fjord. The lower elevations of the island are covered by a thin mantle of soil and recent volcanic ash commonly blanketed by lush, verdant tundra vegetation.

The Akutan hot springs are located in Hot Springs Bay valley, about 4 km northwest of Akutan Harbor and 10 km northeast of the active Akutan volcano (fig. 1-2, sheet 1). In addition to the hot springs, a fumarole field occurs several kilometers up-valley from the springs at about 350 m elevation on the flank of Akutan volcano. The glacial valley containing the hot springs has been carved from a sequence of interbedded volcanic breccias, debris flows, and lava flows that are at least 700 m thick in places. Although the valley is relatively close to the volcano, an intervening valley and ridge help form barriers to lava flows or debris flows from the active vent.

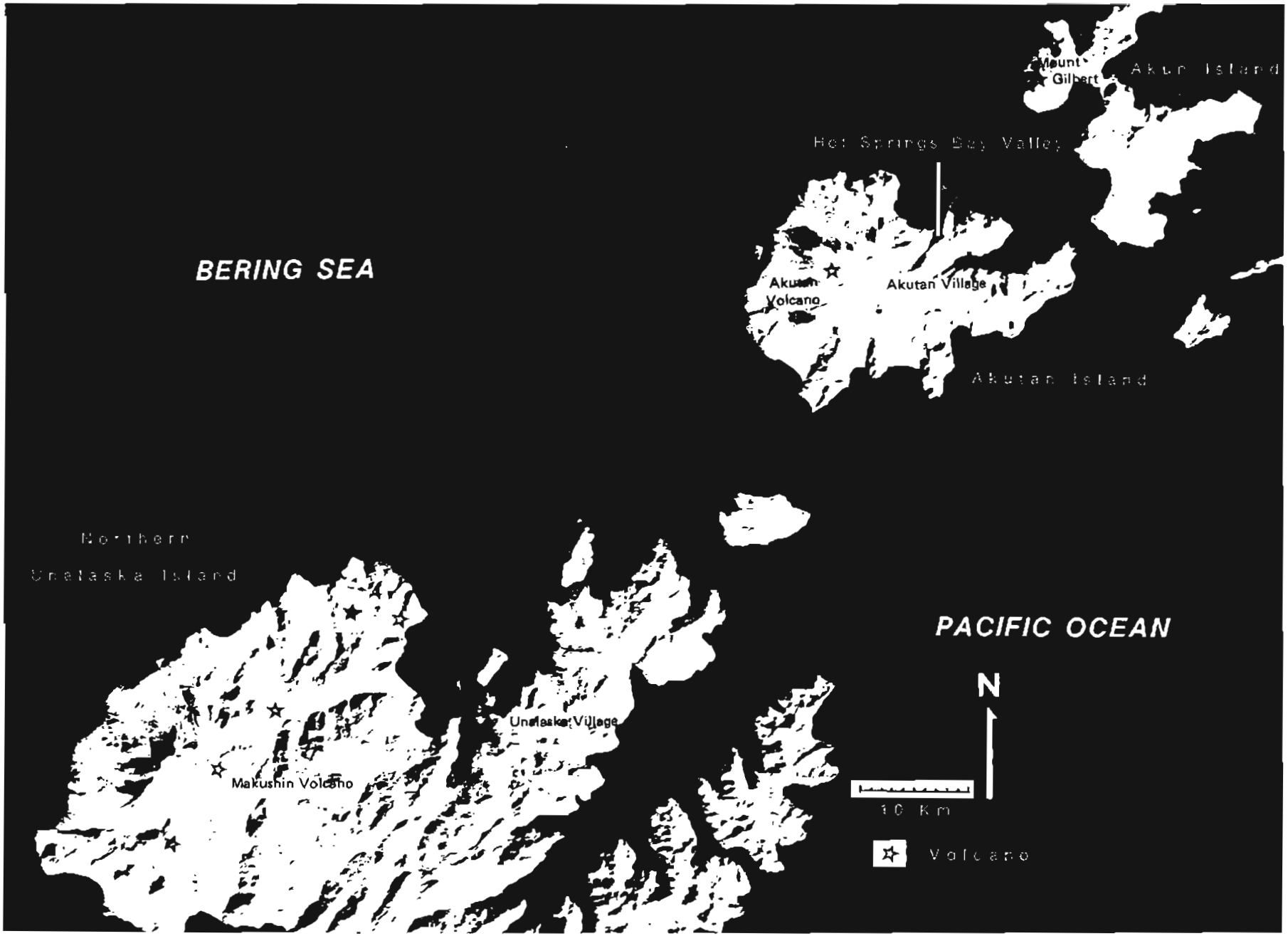

Figure 1-2. ERTS-LANDSAT image #2413-21234-7 1 taken March 10, 1976, showing Akutan Island and vicinity.

Akutan village, the only habitation on the island, is located on the east coast of the island at the base of a steep ridge bordering the north shore of Akutan Harbor (fig. 1-2, sheet 1). The village was established in 1879 as a fur storage and trading post; in 1912 a whale-processing station was built across the bay from Akutan village and operated until 1939 (Morgan, 1980). The present population of about 120 inhabitants depends on subsistence fishing and hunting, commercial fishing, and fish processing for its livelihood. Several floating fish-processing facilities now operate in the protected waters of Akutan Harbor and bring a seasonal influx of 200-700 nonresident workers. Boats and amphibious aircraft are the only means of transportation into Akutan village, which has no airstrip.

PROGRAM OBJECTIVES

The primary objectives of the Akutan geothermal study were to evaluate the size, temperature, depth and chemical characteristics of possible high-temperature geothermal resources of the area. These objectives were approached by the following methods:

1. The construction of a topographic base map using land surveying techniques.

2. Reconnaissance geologic mapping of northern Akutan Island.

3. Detailed geologic mapping of Hot Springs Bay valley.

4. Detailed geophysical surveys of lower Hot Springs Bay valley, including interpretation and analysis.

5. Geochemical soil surveys of lower Hot Spring Bay valley, including interpretation and analysis.

6. Sampling, analysis, and geochemical interpretation of hot springs water and fumarolic gases.

The geology of northern Akutan Island and Hot Springs Bay valley was mapped with the aid of helicopter and inflatable raft. Shoreline, valley and ridge traverses were also conducted.

Funding and logistical limitations restricted detailed geophysical and geochemical-soil surveys to lower Hot Springs Bay valley. Geophysical surveys included shallow-ground conductivity measurements using a Geonics EM-31 meter, Schlumberger vertical electrical soundings, co-linear dipole-dipole sections, and seismic-refraction profiles. Gravity profiling and VLF measurements were carried out but did not produce usable results. The depth of geophysical investigations was limited to about 150 m because of equipment and methodological limitations.

Helium and mercury soil surveys were conducted in the vicinity of the hot springs located in the lower valley. Water from the springs was sampled in 1980 and 1981. Fumarolic gases and waters at the head of the valley were sampled in 1981 and 1983. Water samples were analyzed for major and minor

element species and stable isotope composition; the gases were analyzed for major, minor, and trace constituents, and for $^{13}C/^{12}C$ and $^{3}He/^{4}He$ ratios.

TOPOGRAPHIC BASE MAP

Until recently vertical aerial photography has been lacking for most of Akutan Island, and, as a result, topographic coverage on U.S. Geological Survey and U.S. Coast and Geodetic Survey maps is nonexistent or unreliable, except for the coastline and areas immediately adjacent to it.[1] To facilitate geological mapping of Hot Springs Bay valley and establish accurate locations of the various geophysical and geochemical surveys it was necessary to construct a topographic map of the valley. This program was accomplished in the following manner:

1. A base network was established on the valley floor and a theodolite-distance-ranger survey was made of selected points in and around the valley.

2. Surveyed positions were plotted on a base map and contours between points were sketched in the field.

3. Oblique aerial photos were taken of the valley and were subsequently used to define valley drainages and to modify contours sketched in the field.

4. The coastline used on the map was adapted from available U.S. Coast Guard nautical charts.

The geodetic survey was accomplished by R.D. Allely and M. Larsen of DGGS. Contouring and drainage locations were interpreted by R.D. Allely. The final version of the topographic map was drafted by G. LaRoche, also of DGGS (sheet 1). Contours appearing on the map are within about 6 m (20 ft) for steeply sloping areas, and about 1.5 m (5 ft) or less for the valley floor area.

The geophysical grid used in this study was surveyed by theodolite and distance-ranger. This grid and lower valley topography are plotted on sheet 2.

STREAM HYDROLOGY

The principal stream draining Hot Springs Bay valley is Hot Springs Creek (sheet 1). Two tributaries, one of which flows through a fumarole field, have their sources on the flanks of Akutan volcano and coalesce near the head of the valley. A second but much smaller creek drains the southeast side of the valley and eventually joins Hot Springs Creek immediately upval-

---

[1]North Pacific Aerial Surveys (NPAS) of Anchorage acquired photogrammetric-quality vertical aerial photos of Akutan Island on June 7, 1983. A proposal has been submitted to the U.S. Geological Survey by NPAS to produce topographic maps of the island.

ley of a prominent sand dune about 1 km from the coast. A small tributary to Hot Springs Creek, informally called west fork, flows past group A hot springs and joins the main branch just above group B springs (sheet 1).

Only two stream flow measurements are available for Hot Springs Creek. Baker and others (1978) measured a stream flow of 57,800 lpm on May 21, 1977, at a point approximately 30 m upstream of the mean high tide mark. Our measurement on July 8, 1981, found a stream flow of 60,300 lpm at a point immediately downstream from the prominent inland sand dune.

SUMMARY OF RESULTS

Northern Akutan Island is composed of three distinct volcanogenic units. The oldest, informally termed the Hot Springs Bay volcanics in this report, is a sequence of volcanic debris flows and volcanic breccias with minor intercalated lava flows of Tertiary (?) age that have been intruded by dikes, sills, and plugs. This unit is overlain by the informally named Akutan volcanics which consists of lava flows of Pleistocene age with minor dike and sill intrusions. Lava flows of Holocene age (including some historic flows) from Akutan volcano and Lava Point cinder cone overlie both of the preceding units, and volcanic debris flows and pyroclastic deposits of Holocene age fill several glacially-scoured valleys. The volcanic rocks at Akutan are primarily tholeiitic basalts and andesites with major element chemistry consistent with simple low-pressure crystal fractionation of a single magmatic system.

The Hot Springs Bay valley walls consist mostly of thick, poorly bedded debris flows with the high parts of ridges capped by basalt and andesite flows of the Akutan volcanics. The valley is floored by a Holocene volcanic debris flow which appears to be acting as an impermeable cap over the subsurface hydrothermal system. The outline of low resistivity from EM-31 surveys and helium and mercury soil surveys suggest that thermal waters ascend along buried stream channels which cut through the less permeable volcanic debris flows and allow the waters to emerge at the surface as springs along the present stream banks.

The electrical resistivity and seismic refraction surveys were able to distinguish three subsurface units: 1) an uppermost low-velocity, high-resistivity layer about 30-40 m thick believed to be composed of Holocene volcanic debris flows and valley alluvium; 2) a porous, medium-velocity, low-resistivity middle layer, 30-100 m thick that could be either hydrothermally cemented till and glaciofluvial deposits or an ash flow tuff; and 3) a high-velocity bedrock layer thought to be similar to the Hot Springs Bay valley volcanics exposed in the adjacent walls. The zone of low resistivity in the middle layer appears to be restricted to the northwest corner of the lower valley and extends under the region of hot spring activity.

The results of fluid analyses, geothermometry, and application of mixing models provide evidence that thermal fluids emanating at the surface of Hot Springs Bay valley are derived in part from a deep hot-water reservoir (or reservoirs) having a temperature of 200°C. Similarities in gas composition,

$^3He/^4He$ ratios, and geothermometric temperature estimates suggest that reservoirs supplying thermal fluids to the fumaroles and the hot springs are interconnected. If so, a deep reservoir system may extend over a distance of more than 4 km. Depth to the reservoir (or reservoir system) is unknown, but based on exploration at Makushin geothermal area on neighboring Unalaska Island (Motyka and others, 1988), it may lie within 1 km or less of the surface.

Thermal spring water chemistry and mixing models suggest that the reservoir contains moderately concentrated NaCl waters with Cl^- concentrations of 1,100 ppm and SiO_2 concentrations of 260 ppm. The similarity of stable isotope compositions of the thermal spring waters to surface stream waters indicate the reservoir is recharged by local meteoric waters. The relatively heavy carbon-13 composition of the fumarolic carbon dioxide (11 per mil), and the $^3He/^4He$ ratios of 6.0-7.0 reflect a probable magmatic influence on the geothermal system, perhaps associated with the active volcanism at nearby Akutan Volcano.

Fumaroles at the head of the valley are probably fed directly by gases and steam boiling off the deep hot-water reservoir. Thermal waters ascending from the reservoir in the lower part of the valley appear to pass through and mix with low-enthalpy thermal waters contained in a shallow reservoir before emerging from springs. Geophysical evidence for the existence of this shallow reservoir is the zone of low resistivity that appears to underlie the region of hot spring activity. The low-enthalpy thermal water in the shallow reservoir is thought to be derived from the mixing of cold meteoric waters infiltrating beneath the valley floor and thermal waters ascending from the deep reservoir.

Heat discharge at the surface by spring flow from spring groups A through D referenced to 10°C is estimated at 2.2-4.1 MW. Substantially more thermal water is probably discharging at the beach and directly into the sea beyond the limit of the volcanic debris flow confining unit as evidenced by sand temperatures and hot water outflow at the shoreline.

ACKNOWLEDGMENTS

Funding for the Akutan geothermal investigations came from the U.S. Department of Energy, Grant No. DE-FC07-79ET27105, and from the State of Alaska, Department of Natural Resources Geothermal Program.

The authors wish to extend special acknowledgment to S.A. Liss and G. LaRoche of DGGS for their cartographic contributions to this report.

This report benefited greatly from the technical reviews provided by Duncan Foley, University of Utah Research Institute in Salt Lake City, Utah, and James Munter, DGGS.

One of us (R.J. Motyka) wishes to acknowledge the help of W. Evans and C.J. Janik, U.S. Geological Survey, Menlo Park, California, and D.S. Sheppard, New Zealand Department of Sciences and Industrial Research, Aukland, New Zealand, in performing gas analyses.

REFERENCES CITED

Baker, R.O., Lebida, R.C., Pyle, W.D., and Britch, R.P., 1978, An investigation of selected Alaska geothermal spring sources as possible salmon hatchery sites: National Technical Information Service IDO/1624-1, 173 p.

Morgan, L., ed., 1980, The Aleutians: Alaska Geographic, v. 7, no. 3, p. 224.

Motyka, R.J., 1982, High temperature hydrothermal resources in the Aleutian arc: Alaska Geological Society Symposium on Western Alaska Geology and Resource Potential, Anchorage, Proceedings, p. 87-99.

Motyka, R.J., Moorman, M.A., and Liss, S.A., 1981, Assessment of thermal spring sites, Aleutian arc, Atka Island to Becharof Lake - preliminary results and evaluation: Alaska Division of Geological and Geophysical Surveys Alaska Open-file Report 144, 173 p.

Motyka, R.J., Queen, L.D., Janik, C.J., Sheppard, D.S., Poreda, R.J., and Liss, S.A., 1988, Fluid geochemistry and fluid-mineral equilibria in test wells and thermal gradient holes of the Makushin geothermal area, Unalaska Island, Alaska: Alaska Division of Geological and Geophysical Surveys, Report of Investigations [in preparation].

CHAPTER 2

GEOLOGY OF NORTHERN AKUTAN ISLAND

by

Samuel E. Swanson[1] and Jay D. Romick[2]

[1]Geophysical Institute, University of Alaska-Fairbanks, Fairbanks, Alaska 99775
[2]Alaska Division of Geological and Geophysical Surveys, 794 University Ave., Suite 200, Fairbanks, Alaska 99709 (Current address: Department of Geological Sciences, Cornell University, Ithaca, N.Y. 14853)

INTRODUCTION

Akutan Island is located in the eastern Aleutian chain at lat 54°05' N., long 165°55' W., about 45 km northeast of Unalaska Island. The island is 29 km long, 21 km wide, and is oriented roughly east-west (fig. 2-1). It is dominated by Akutan Volcano, a 1,300-m-high composite volcano. Central and eastern Akutan consists of steep ridges separating glacially-scoured valleys which predate the formation of Akutan Volcano. The radial drainage pattern of these valleys suggests an old topographic high in the same area that is now occupied by Akutan Volcano. Western Akutan has gentle topography dissected by streams flowing off the west flanks of the volcano.

The summit of Akutan Volcano is capped by a 2-km-diam caldera. Within the caldera is a cinder cone, which existed prior to 1931 (Finch, 1935), and a small lake. The caldera is breached on the north side. Northwest of Akutan Volcano are two small eruptive centers, an old eroded volcanic center consisting primarily of lava flows (Lava Peak), and a cinder cone (near Lava Point) which developed sometime before 1870 (Byers and Barth, 1953).

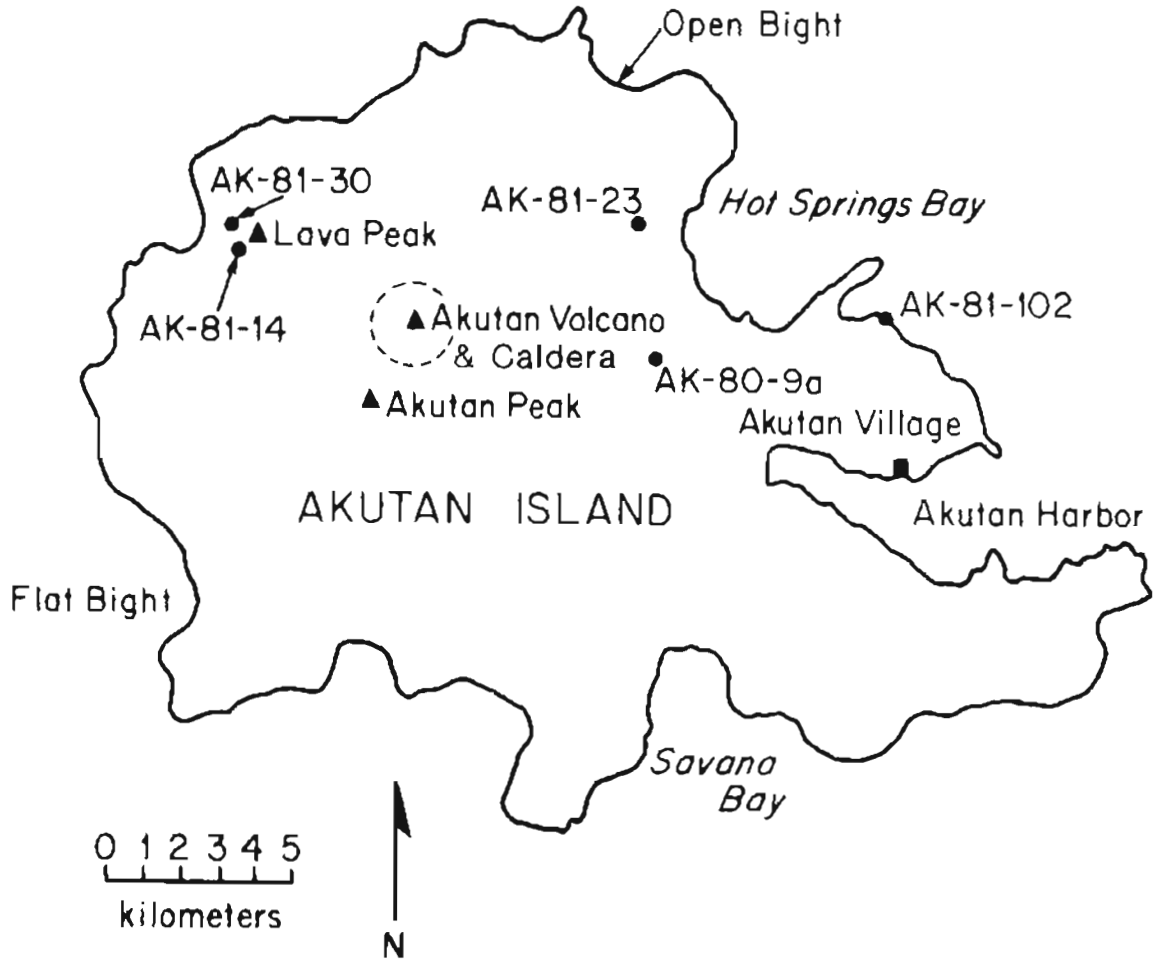

Figure 2-1. Map of Akutan Island showing location of radiometrically dated samples in table 2-1.

Very little geologic information about Akutan Island has been published. Russians visited the island in the 1850's. R.H. Finch conducted the first scientific exploration of the island in 1931, and briefly described the geology and topography of the island (Finch, 1935). Finch noted that Dr. T.A. Jaggar had visited the island in 1907 and 1927 and had made some correlations between the volcaniclastic units on Akutan and those on the Alaska Peninsula, but nothing was published regarding that correlation.

Byers and Barth conducted field work on Akutan Island in 1948 as part of the U.S. Geological Survey study of the Aleutian Islands after World War II, but no official report was issued. They prepared a geologic map of Akutan Island, which is in the U.S. Geological Survey archives in Menlo Park. Byers and Barth (1953) published some information on Akutan Island in a paper discussing both Akutan and Akun islands, but their major emphasis was on the recent 1947 and 1948 eruptions rather than past volcanic activity and geology.

Motyka and others (1981) briefly described Akutan geology in their report on the geothermal resources of the island. Perfit and Gust (1981) published some isotope and microprobe analyses of samples from Akutan Island, and discussed their results relative to other Aleutian Islands. McCulloch and Perfit (1981) published isotope and rare earth element data for Akutan lavas.

Much of the geology and petrology described here is summarized from Romick (1982). Readers interested in detailed descriptions of the analytical methods used and of the mineralogy and geochemistry of Akutan volcanic rocks are referred to Romick (1982).

GENERAL GEOLOGY

Figure 2-2 is a map of the general geology of Akutan Island modified from Byers and Barth (1948 unpublished map). Akutan Island consists of volcaniclastic debris flows interbedded with subordinate lava flows which are overlain in places by younger volcanic deposits associated with Akutan Volcano. The volcaniclastic material and flows are exposed principally on central and eastern Akutan Island and are here referred to informally as Hot Springs Bay volcanics. They consist primarily of volcaniclastic deposits locally in excess of 700 m thick (Motyka and others, 1981). The Hot Springs Bay volcanics are slightly to moderately altered to chlorite and carbonate. The volcaniclastic rocks contain numerous dikes, especially near Hot Springs Bay. Dikes located around Hot Springs Bay valley strike primarily northwest, while those located to the west of Hot Springs Bay valley are oriented primarily northeast; however, dike orientations span 180°. Small gabbroic bodies intrude the Hot Springs Bay volcanics. The orientation and arrangement of several small curvilinear intrusions exposed south of Open Bight (fig. 2-2) suggest that they may be ring dikes associated with an older caldera system. Bedding attitudes also suggest an older center of volcanic activity near Open Bight (Byers and Barth, unpublished data).

The Hot Springs Bay volcanics are unconformably overlain by a unit, here called the Akutan volcanics, which is dominantly composed of basalt and andesite flows of Quaternary age. These flows are generally unaltered and

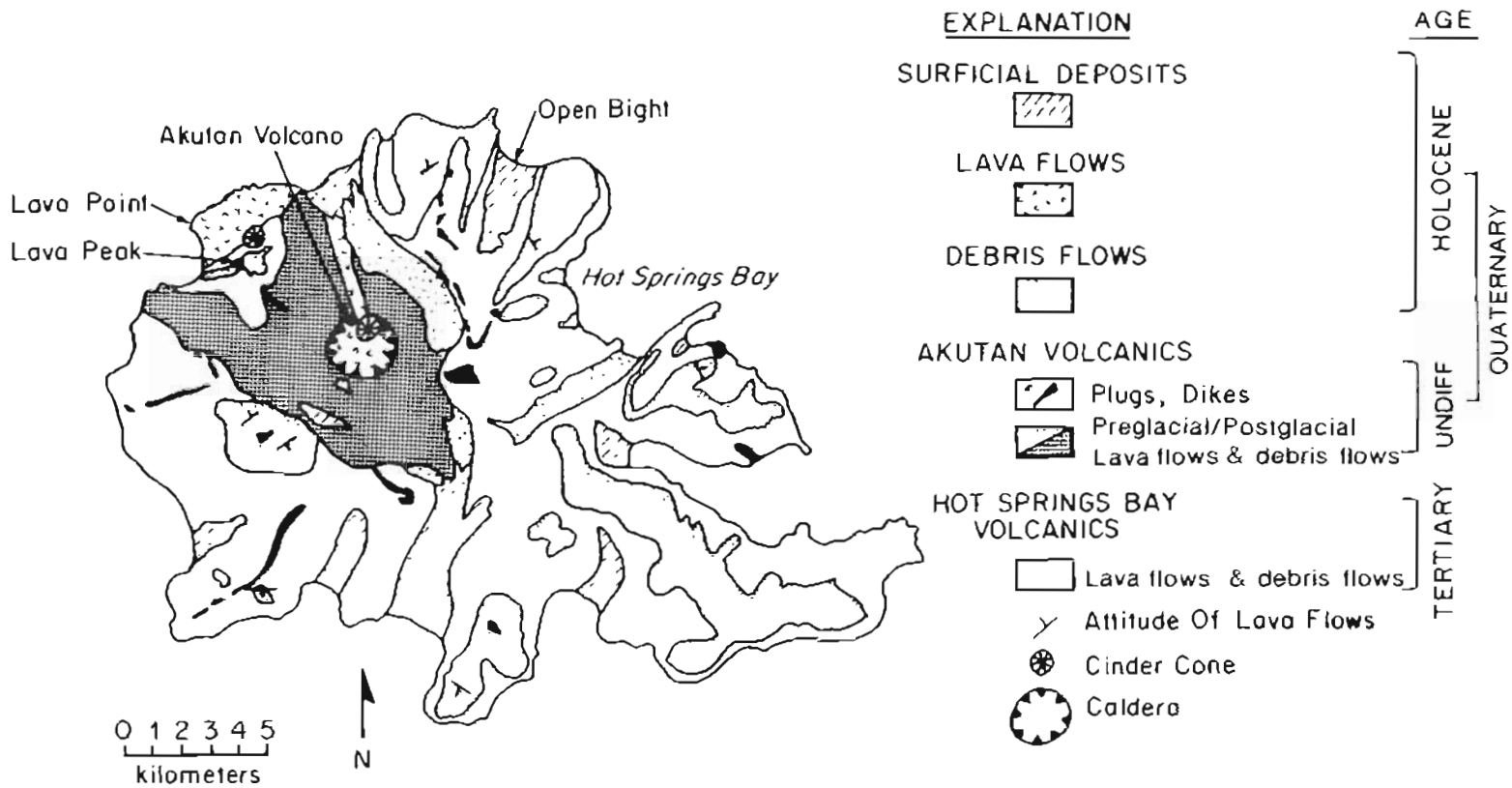

Figure 2-2. Generalized geology of Akutan Island modified from Byers and Barth (1948, unpublished map).

cap ridges between glacially-scoured valleys as well as forming the relatively uneroded flanks of Akutan Volcano.

On northwestern Akutan Island a high ridge, here called Lava Peak, is made up of at least 19 flows and seven dikes, all assigned to the Akutan Volcanics. Eleven nearly flat-lying flows of the Hot Springs Bay volcanics are unconformably overlain by eight or more flows which dip to the west. East of the peak a baked, autobrecciated zone appears to be the core of an eroded volcanic center.

Dikes intrude the lower eleven flows and are only exposed on the north side of the Lava Peak. A large dike exposed east of Lava Peak also intrudes the lower 11 lava flows, but is truncated by the upper sequence of flows. The dike is the backbone of the ridge to the east of Lava Peak and may have been a feeder dike from Akutan Volcano. There are several flows to the south of Lava Peak which are topographically lower than the Lava Peak rocks and are mantled by Holocene tephra deposits from Akutan Volcano.

North of Lava Peak is a cinder cone and lava flow (Lava Point flow) which may have formed in 1852 (Simkin and others, 1981). The cone is approximately 100 m high and 300 m across at the base. The lava flow is about 4 km^2 in area, and forms Lava Point (fig. 2-2).

Other Holocene-age volcanic deposits include several historic flows, the most recent of which formed in 1978, and pyroclastic deposits. The 1978 lava flow followed two stream drainages down the north flank of the volcano and came to within 1 km of the coast. Ash eruptions interspersed with these flows have mantled some of the deposits on western Akutan Island, and have occasionally reached Akutan Village on the east side of the island (Finch, 1935; Byers and Barth, 1953). Table 2-1 lists dates of documented volcanic activity on Akutan Island since 1790.

IGNEOUS ROCKS

Hot Springs Bay Volcanics

The Hot Springs Bay volcanics are inferred to underlie most of the island and are exposed on about half the island (fig. 2-2). The base of the section is not exposed, but the unit is at least 700 m thick in places. Typical exposures of these rocks are found in the sea cliffs surrounding Hot Springs Bay and most of our data from this unit are taken from these outcrops.

Volcanic Breccia

Volcanic breccia is the dominant lithology, but dikes of porphyritic basalt and andesite are also found within this unit. Outcrops of the breccia are limited to the sea cliffs; inland, the breccia forms rounded, grass-covered slopes. The dikes are more resistant and often form outcrops on an otherwise grassy hillside.

Table 2-1. Volcanic activity on Akutan Island since 1790.

Date	Type of Eruption	Location
1790	Smoking	
1828	Smoking	
1838	Smoking	
1845	Smoking	
March 1848	Small explosive eruption	
1852	Parasitic cone eruption	NW of summit
1862	Smoking	
1865	Glow seen from Unimak Pass	
1867	?	
1883	Small steam and ash eruption	
1887	Lava flow	
1892	?	
1896	Glowing	
1907	Continuously active	
Feb.22, 1908	Lava flow	
1911	Ash fell on Akutan Village	
1912	Smoking	
1928	Smoke and "flaming"	
May 1929	Explosive eruption and lava flow	
1931	Explosive eruption	
1946-47	Lava flow and explosive eruption	
1948	Explosive eruption	
Oct. 1951	Explosive eruption	
1953	?	
1972	Explosive eruption	
1974	Parasitic cone, ash eruption and lava flow	West flank?
1976-77	Explosive eruptions	
Sep.25, 1978	Lava flow and ash eruptions	
1980	Explosive eruption	

Sources: Finch (1935), Byers and Barth (1953), and Simkin and others (1981).

The volcanic breccia of the Hot Springs Bay unit is a poorly sorted and poorly stratified rock composed of fragments of basalt and andesite. Internal bedding is lacking, but individual layers (flows?) are marked by slight breaks in slope or erosional surfaces. Angular to rounded blocks up to 3 m in diameter are enclosed in a matrix as fine as clay-sized. Lack of thermally-altered contacts or breadcrust bombs indicates the breccias were not hot at the time of emplacement. The breccias of the Hot Springs Bay unit are interpreted to be mudflow deposits. Carbonate and chlorite alteration is pervasive throughout the breccia.

Dikes

Vertical dikes intrude the volcanic breccias. The dikes range in thickness from 0.3 to 10 m, but nesting of dikes-within-dikes locally produces

thicknesses up to 13 m. Contact metamorphism of the enclosing breccias by the dikes is limited to a zone of thermal alteration 1-4 cm wide adjacent to the dikes. Strike of the dikes is generally to the northwest, but the attitudes are quite variable; individual dikes can change strike over 90° in a single outcrop. Flow-banding, defined by mineralogical layering or vesicule alignment, is common in some of the dikes and is parallel to the margins of the dikes.

Porphyritic basalt is the dominant lithology found in the dikes. Phenocrysts of plagioclase set in a fine-grained matrix of plagioclase, chlorite and carbonate (altered clinopyroxene) constitute the most common mineralogy. Phenocrysts of olivine, clinopyroxene and, rarely, hornblende also occur in the dikes, but the common alteration of mafic minerals makes recognition of these phases difficult. Phenocrystic and groundmass olivine and augite are commonly replaced by fine-grained carbonate or chlorite. This replacement is so complete in many samples that plagioclase is the only recognizable primary phase. Carbonate-filled amygdules are also common in the dikes. The alteration pattern is similar to that found in the host volcanic breccias and probably represents a single alteration event.

Age

The Hot Springs Bay volcanics are the oldest rocks exposed in the study area. A marked unconformity separates the volcanic breccias and dikes of the Hot Springs Bay volcanics from the overlying Akutan volcanics. Dikes of the Hot Springs Bay volcanics exposed in the sea cliffs between Sandy Cove (sheet 1) and Hot Springs Bay are also truncated by an unconformity and overlain by Akutan Volcanics.

The Hot Springs Bay volcanics of Akutan Island are similar and may be equivalent to the Miocene to Pliocene Unalaska Formation (Drewes and others, 1961; Nye and others, 1984) on Unalaska Island. Volcaniclastic sediments with minor lava flows characterize both the Unalaska Formation and the Hot Springs Bay volcanics. Dikes and other intrusives as old as 1.5 m.y. (table 2-2) cut both units, and lava flows of Quaternary age unconformably overlie both units.

Intrusive Rocks

Three phaneritic intrusive igneous rocks were sampled on Akutan Island. One of the intrusions is a 150-m-wide plug exposed in Sandy Cove. This mass shows columnar jointing and one side of the plug intrudes along a bedding surface in the Hot Springs Bay volcanics in a sill-like fashion. A smaller plug of gabbro, intrusive into the Hot Springs Bay volcanics, is located on the coast about 4 km northwest of Hot Springs Bay valley. The third sample is a small block of diorite collected from the 1978 tephra deposits near Lava Peak.

The gabbro is an equigranular rock consisting of ophitic plagioclase and clinopyroxene with crystal diameters of about 2-4 mm. The diorite block from the 1978 tephras is also composed of augite and plagioclase, but has a cumulate texture and a smaller grain size (1-2 mm). The Sandy Cove plug is

Table 2-2. Whole-rock ^{40}K–^{40}Ar ages for Akutan lavas.[a]

Sample[b]	Material dated	Map unit	K_2O (wt %)	$^{40}Ar(rad)$ (mol/g x10^{-11})	$\frac{^{40}Ar(rad)}{^{40}Ar(total)}$	Age (m.y.)
AK-81-14	lava flow	Akutan volcanics	0.691	0.133	0.085	1.1 ± 0.2
AK-81-30	dike	Hot Springs Bay volcanics	0.648	0.175	0.238	1.5 ± 0.1
AK-81-23	lava flow	" "	1.23	0.305	0.100	1.4 ± 0.2
AK-80-9a	lava flow	" "	0.806	0.159	0.136	1.1 ± 0.1
AK-81-102	plug	" "	0.731	0.141	0.074	1.1 ± 0.1

[a] R.L. Armstrong, University of British Columbia, analyst. Constants used: $\lambda_e + \lambda_{e'} = 0.581 \times 10^{-10}\ yr^{-1}$; $\lambda_B = 4.962 \times 10^{-10}\ yr^{-1}$; $^{40}K/K_{total} = 1.167 \times 10^{-4}$ mol/mol.

[b] Sample location is shown on figure 2-1.

composed of phenocrysts of augite and plagioclase in a holocrystalline groundmass of plagioclase, augite and opaque minerals.

The gabbroic and dioritic rocks from Akutan are similar in texture and mineralogy to some of the mafic phases of Neogene plutons on Unalaska Island (Drewes and others, 1961; Perfit and others, 1980). The plug at Sandy Cove is more similar to the dikes in the Akutan volcanics.

A whole-rock K-Ar age determination on the plug in Sandy Cove yields an age of 1.1 ± 0.1 m.y. (table 2-2). This age is identical, within experimental error, to ages of both lava flows and dikes in the Akutan volcanics, indicating affiliation with the younger volcanics.

Akutan Volcanics

A series of lava flows, informally referred to as the Akutan volcanics, unconformably overlies the Hot Springs Bay volcanics. An unconformity also separates the Akutan volcanics from overlying Holocene volcanic deposits. Resistant ridge-capping lava flows dominate the Akutan volcanics. Individual flows either rest directly on other flows or are separated by thin layers of volcanic breccia. The lava flows form steep slopes with good exposure. Dikes are also found within the Akutan volcanics, but are not as abundant as in the Hot Springs Bay volcanics.

Flows

Lava flows of the Akutan volcanics range in thickness from 2 to 31 m. Top and bottom surfaces of the lava flows are often brecciated and many flows

have baked contacts. Flow banding, defined by vesicles and phenocrysts, is found in some of the flows. Columnar jointing, oriented perpendicular to the flow surface, is developed in some lava flows. Within thicker flows, columnar jointing is only developed in the upper portion of the flows.

The Akutan volcanics consist of porphyritic basalt and andesite. Most of the rocks contain over 10 percent phenocrysts set in a holocrystalline groundmass, but at least one lava flow near Akutan Village contains only rare phenocrysts of plagioclase. Plagioclase is the most abundant phenocryst mineral and is found in all of the samples examined. Other phenocryst minerals, in decreasing order of abundance, include augite, olivine, and hypersthene and opaque minerals set in a groundmass of plagioclase, augite, and opaques. Feldspars in the groundmass are often aligned to form a trachytic texture.

Intrusions

Dikes and small plugs intrude the lava flows of the Akutan volcanics (fig. 2-2). The dikes range in thickness from 0.5 to 15 m, and plugs up to 0.5 km in diameter intrude the lava flows. Some thicker dikes in the Lava Point area show columnar jointing with the columns oriented perpendicular to the walls of the dike. Flow banding defined by oriented vesicules and phenocrysts parallels the margins of some dikes.

Porphyritic olivine basalt is the most common lithology found in the dikes, but about one-third of the dikes do not contain any olivine. Common phenocryst phases include plagioclase, augite, and olivine set in a matrix of plagioclase, augite, and opaque minerals. Minor quartz, calcite, and chlorite veinlets are found in dikes south of Open Bight.

Dikes and plugs that are believed to be correlative with the intrusions in the Akutan volcanics of Lava Peak are found in the breccias of the Hot Springs Bay volcanics (fig. 2-2). These intrusions are distinguished from those of the Hot Springs Bay volcanics by a general lack of alteration and a finer grain size.

Byers and Barth (1948) believed the circular outcrop pattern shown by some of these intrustions (for instance, southwest of Open Bight) is related to a ring-dike structure. This pattern is most apparent east of Akutan Volcano where series of disconnected dikes form a semi-circular pattern about the present summit caldera (fig. 2-2). Another series of dikes form ridges that radiate from Akutan Volcano to the south, southwest and west (fig. 2-2). The radial dike pattern may also be related to an earlier caldera-forming event.

Alteration

Alteration is uncommon in the western Akutan volcanics, but is more prevalent on the eastern side of Akutan Island. Alteration in the samples from western Akutan is confined to oxidation of some olivine phenocrysts. On eastern Akutan Island, chlorite and carbonate are sometimes found in the

groundmass. Some olivine on eastern Akutan is partially replaced by chlorite.

Age

The Akutan volcanics unconformably overlie the Hot Springs Bay volcanics and are dissected by at least one major period of glaciation. Exposures in the sea cliffs southeast of Hot Springs Bay and dikes in the Hot Springs Bay volcanics are truncated by an unconformity which is, in turn, covered by lava flows of the Akutan volcanics. There is little relief on the unconformity and the lava flows above appear to parallel the crude bedding in the underlying breccias.

The lack of widespread alteration and the stratigraphic position suggest that the Akutan volcanics are significantly younger than the Hot Springs Bay volcanics. Radiometric ages measured by the K-Ar method on whole-rock samples from the Akutan volcanics range from 1.1 ± 0.2 to 1.5 ± 0.1 m.y. (table 2-2). Near Lava Peak a lava flow near the base of the section is dated at 1.1 ± 0.1 m.y. A lava flow west of Hot Springs Bay that overlies breccias of the Hot Springs Bay volcanics yields an age of 1.4 ± 0.2 m.y., which is consistent with the results from Lava Peak.

Holocene Volcanic Deposits

Lava Point

A cinder cone developed in 1852(?) just northeast of Lava Peak. A lava flow erupted from the base of the cone, covering about 4 km^2, and makes up what is called Lava Point (Byers and Barth, 1953) (fig. 2-2). The lava flow is very blocky, and has two lobes which flowed into the sea. Erosion has exposed numerous lava tubes on the northern border of the flow which have developed into spectacular bridges and caves along the coastline. The rock is very vesicular, and contains plagioclase phenocrysts with subordinate mafic minerals, all set in a glassy groundmass. The groundmass contains flow-aligned plagioclase laths, some opaque minerals, and a great deal of brown glass.

Akutan

In 1978 a lava flow erupted in the summit caldera, flowed down the north flank of Akutan Volcano in two lobes, and came within 1 km of the coast. The flow consists of very blocky (aa) lava ranging from vesicular to very glassy in texture. In hand specimen the rocks are aphanitic with occasional plagioclase phenocrysts. In thin section plagioclase makes up about 32 percent of the rock, while clinopyroxene, olivine, and opaque minerals make up less than 7 percent. The groundmass has a trachytic texture and consists of plagioclase laths and brown glass.

Several other historic lava flows from Akutan Volcano have occurred (table 2-1) and the relatively uneroded shape of most of the volcano indicates that a large portion of the modern edifice is of Holocene age.

GEOMORPHOLOGY AND SURFICIAL DEPOSITS

Glacial Landforms

Glacial landforms including U-shaped valleys, cirques and arêtes are very prominent on the higher slopes of the central part of Akutan Island. The bottoms of major valleys formed by glacial action have been modified by stream erosion and the deposition of postglacial volcanic debris flows. Stream erosion in the upper reaches of the glaciated valleys has produced incised, V-shaped stream channels over 150 m deep. Lower portions of the major valleys are filled with volcaniclastic debris.

Only one small glacier exists on Akutan Island. This glacier covers about 1 km^2 between 1,100 m (3,600 ft) and 825 m (2,700 ft) elevation on a pinnacle on the rim of the caldera of Akutan Volcano.

Several well-defined cirques occur on Akutan Island. Major valleys, such as those behind Open Bight or Hot Springs Bay valley, are headed by cirques. Smaller valleys, such as the one behind Sandy Cove, are also headed by small cirques. Cirques on Akutan Island are restricted to elevations higher than 365 m (1,200 ft), similar to those on Unalaska Island (Drewes and others, 1961), indicating a snowline of 365 m (1,200 ft) at the time of glaciation.

Till was not identified during the course of the present study. However, Byers and Barth (1948) identified a small moraine associated with the glacier on Akutan Peak. The extensive deposits of recent tephra and volcaniclastic debris that fill most of the valleys would conceal any till that might be present. Morphology of the major valleys suggests that the valley glaciers must have terminated offshore from the present coastline, and, thus, terminal moraines for these glaciers are not found.

Stream Erosion and Deposits

Postglacial stream erosion has produced V-shaped canyons up to 150 m deep on the rugged upper slopes of Akutan Island. Stream channels choked with large boulders completely cover the canyon bottoms. Terrace remnants of outwash gravels are found along the stream channels where the stream gradient rapidly decreases. In the lower portion of the major valleys, streams meander in response to a gentle gradient and expose volcaniclastic valley-fill debris in the stream banks (Swanson and others, this report).

Marine Deposits

Beach deposits ranging from boulders to sand are common around Akutan Island. Steep cliffs immediately adjacent to the shoreline promote boulder beaches that are only exposed at low tide. Beach deposits further removed from the cliffs range from cobbles to sand. Bars and spits are found across the mouths of some bays (for example, Hot Springs Bay and Open Bight), thus isolating lagoons or lakes from the sea.

Eolian Deposits

Dunes have formed behind some of the sand beaches, such as at Hot Springs Bay. The presence of dunes is controlled by the availability of sand. Dunes reach a height of 10 m and are stabilized by a lush growth of grasses.

Volcaniclastic Deposits

Layers of volcanic ash and lapilli with occasional bombs are widespread on the western half of Akutan Island. Thickness of the deposits is quite variable and ranges from 0 on steep slopes to over 30 m in some valley bottoms. Thick accumulations of volcaniclastic debris in valleys are probably material from adjacent slopes that was remobilized by fluid mudflows. Bedding is crudely developed within these deposits, but local channeling does reveal fluvial reworking of the deposits. Older, but postglacial, volcaniclastic deposits with some cementation are found in Hot Springs Bay valley (Swanson and others, chap. 3, this report).

GEOCHEMISTRY

Major oxide analyses for over 30 samples of Akutan lava flows, dikes and plugs are available (Romick, 1982). Figure 2-3 shows a silica variation diagram of the major oxides for samples from the Hot Springs Bay and Akutan volcanics plus the historic lava flows on Akutan. Silica ranges from 49 to 63 weight percent on Akutan. Samples of lava flows and intrusions from the Akutan volcanics show a well-defined fractionation trend that includes the historic lavas on Akutan. FeO^* ($FeO + 0.899\ Fe_2O_3$), Mg, and Ca decrease with increasing Si, while Na and K increase. Aluminum decreases slightly with increasing fractionation and Ti remains unchanged over the observed range of Si contents. The Hot Springs Bay volcanics show a similar pattern of chemical variation, but the scatter is much greater than the Akutan trend (fig. 2-3). The variable alteration to calcite, chlorite and clays of the Hot Springs Bay volcanics results in scatter in the Al, Fe, Mg, and Ca contents of these rocks. Further discussions of the mineralogy and petrology will not deal with the Hot Springs Bay volcanics because the rocks are extensively altered, making recognition of primary mineralogic and geochemical trends difficult, and because these rocks are old and are thus unrelated to the current magmatic/geothermal system.

Akutan volcanic rocks have been characterized as tholeiitic (Perfit and Gust, 1981; McCulloch and Perfit, 1981; Kay and others, 1982). Rather weak Fe-enrichment is found in the Akutan volcanic rocks (fig. 2-4). The increase in FeO^* (total Fe)/MgO ratios with increasing SiO_2 (fig. 2-5) is similar to the tholeiitic trend described by Kay and others (1982) for other Aleutian volcanoes.

Patterns of chemical variation (figs. 2-3, 2-4, and 2-5) permit the interpretation that the Akutan volcanics and the recent lava flows at Lava Point and from Akutan Volcano are comagmatic. The relatively smooth curvilinear patterns of variation are typical of the trends produced by

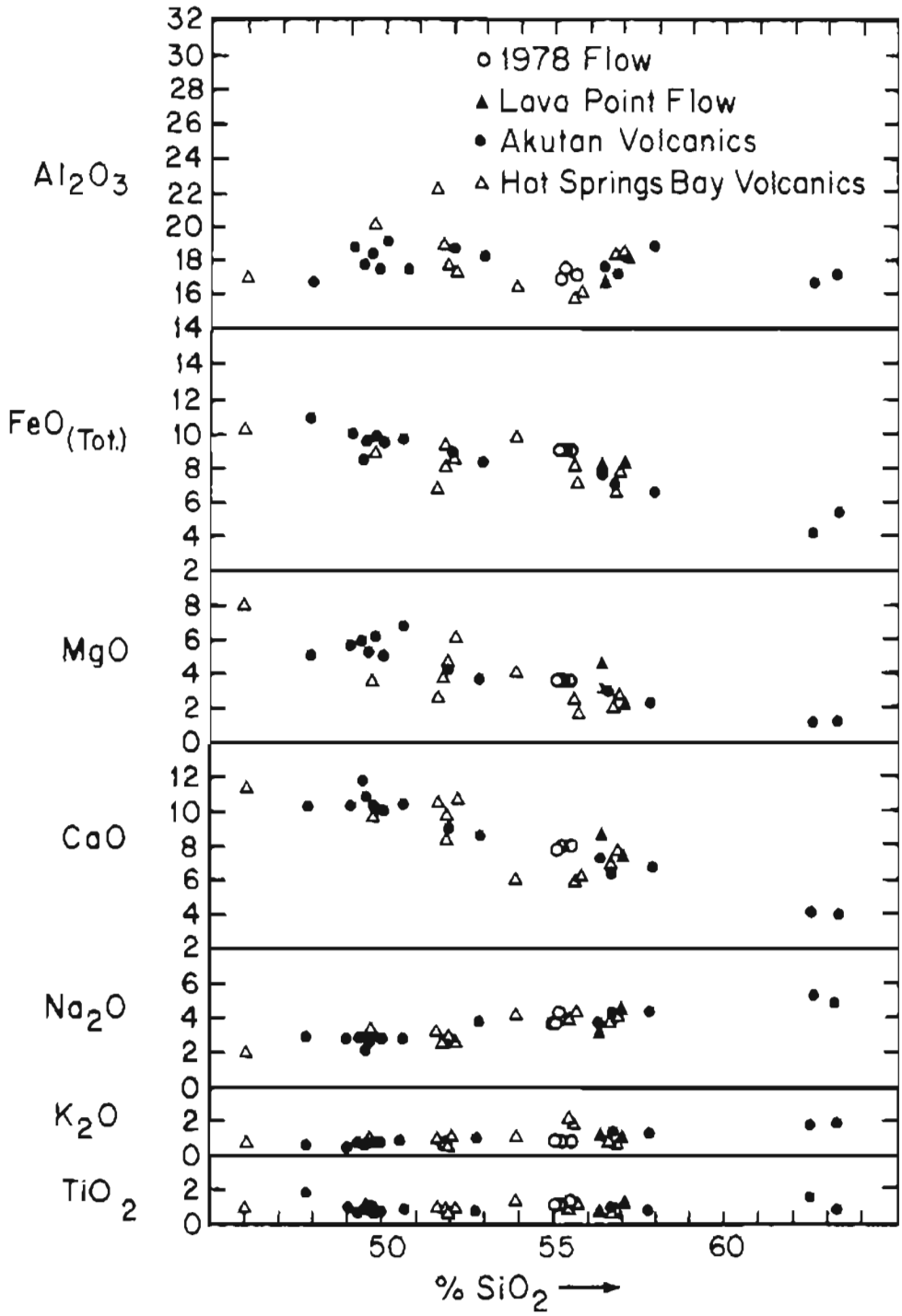

Figure 2-3. Harker silica variation diagram for Akutan volcanic rocks.

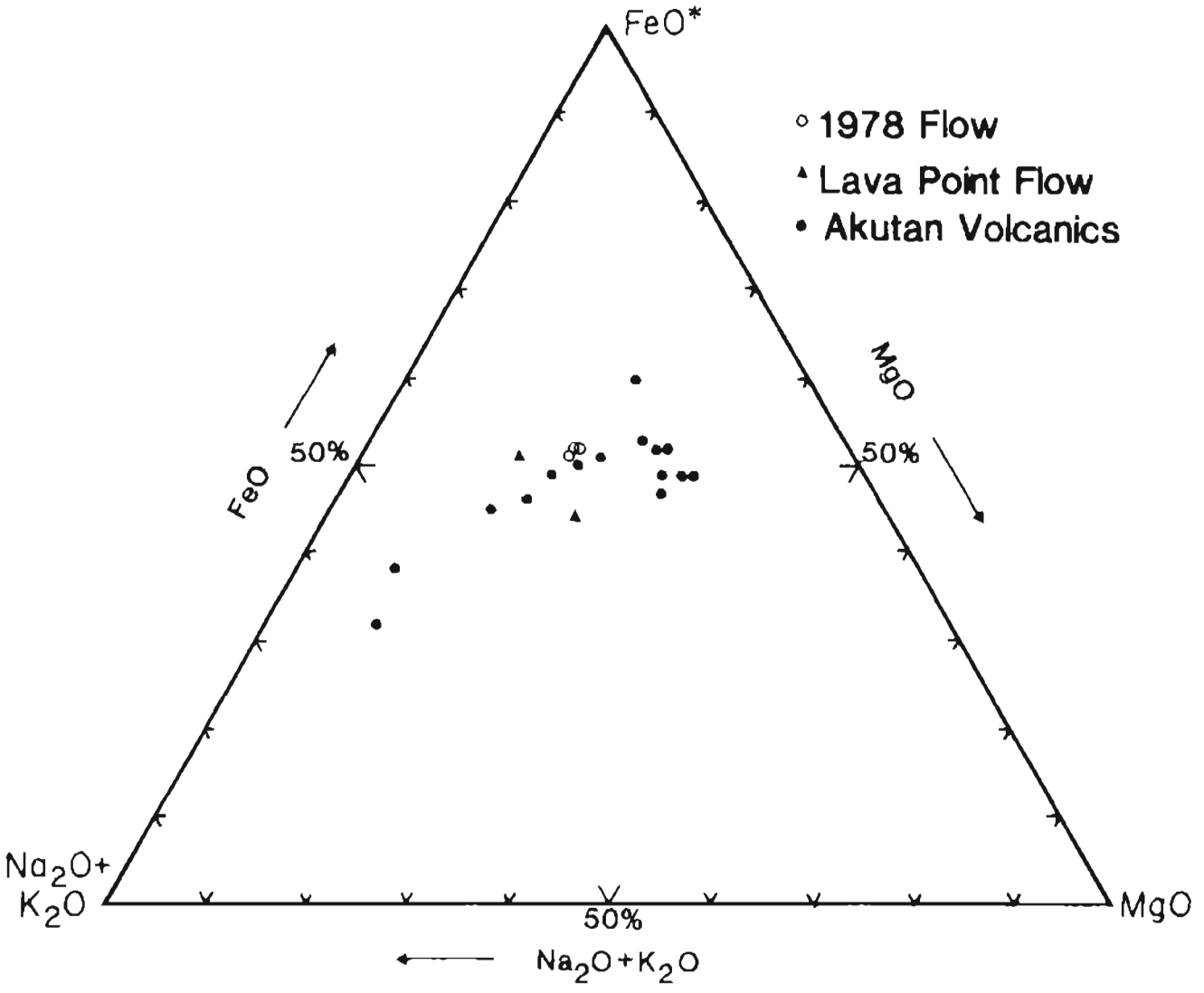

Figure 2-4. AFM diagram for Akutan volcanic rocks. A = $Na_2O + K_2O$ (alkalis); F = iron oxides; M = magnesium oxides.

fractionation in crystal-liquid systems. This relatively simple pattern of chemical variation is consistent with the apparently simple modern-day volcanic plumbing system of one central vent (Akutan Volcano) and one satellite vent (Lava Point).

INTERPRETATION

The rather simple pattern of chemical variation (fig. 2-3 and 2-4) can be explained by the extraction of phases rich in Ca, Fe, and Mg, resulting in a decrease in these components with increasing Si. The removal of the commonly observed phenocryst assemblage plagioclase + olivine + augite could produce this pattern of variation in the Akutan lavas. Hypersthene replaces olivine in the phenocryst assemblage in bulk compositions with more than 52 weight percent SiO_2. This change in phenocryst mineralogy does not change the overall pattern of fractionation (decreasing Ca, Fe, Mg, increasing Si),

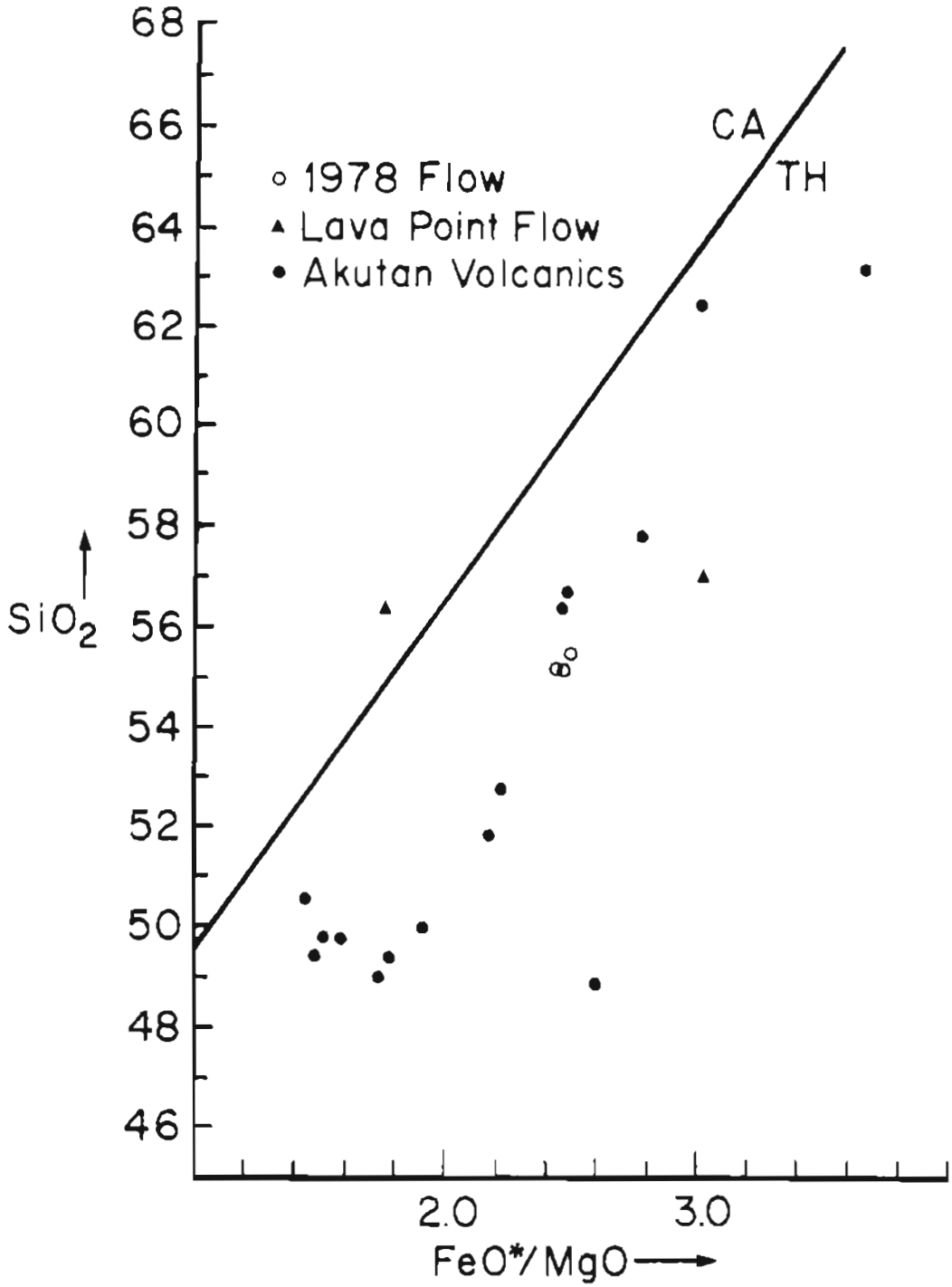

Figure 2-5. FeO^*/MgO vs. SiO_2 diagram for Akutan volcanic rocks. ($FeO^* = FeO + 0.899\ Fe_2O_3$). Calc-alkaline (CA)/tholeiitic(TH) dividing line is after Miyashiro (1974).

but it may explain a discontinuity in the pattern of MgO variation at about 52 weight percent SiO_2 (fig. 2-3).

Phase equilibria studies in a haplobasalt system ($CaAl_2Si_2O_8$ - $CaMgSi_2O_6$ - Mg_2SiO_4 - SiO_2) have revealed a crystallization sequence similar to that found in the volcanic rocks of Akutan (Presnall and others, 1978). Low pressure, one atmosphere, experimental studies show that bulk compositions low in Si will initially crystallize some combination of plagioclase, olivine and augite (clinopyroxene). Increasing fractionation in the experimental systems results in a reaction of olivine (in the presence of plagioclase and augite) with the silicate liquid to produce hypersthene (orthopyroxene).

Compositional and textural data from the phenocrysts are consistent with low pressure fractionation. The phenocrysts show a very restricted range of compositions. Such a restricted compositional range argues for a simple, near-surface crystallization history. Zones of glass inclusions within Akutan plagioclase are interpreted to have formed as a result of the fast growth of plagioclase at a somewhat undercooled temperature. Such dramatic temperature fluctuations within a crystallizing magma chamber also indicate a near-surface environment.

Shallow-level fractionation of the Akutan lavas suggests the existence of a shallow-level magma chamber under Akutan Volcano. Partial draining and collapse of such a magma chamber could explain the small caldera on Akutan Volcano as well as the compositional and mineralogic trends within the lavas. High heat flow associated with a shallow magma may produce the thermal anomalies on Akutan that are located east of the active volcanic vents.

REFERENCES CITED

Byers, F.M., Jr., and Barth, T.F.W., 1948, Geology of Akutan Island, unpublished geologic map and field notes: U.S. Geological Survey Archives, Menlo Park, California.

Byers, F.M., Jr., and Barth, T.F.W., 1953, Volcanic activity on Akun and Akutan Island: Pacific Science Conference Proceedings, 7th, 1949, New Zealand, v. 2, p. 382-397.

Drewes, Harold, Fraser, G.F., Snyder, G.L., and Barnett, H.F. Jr., 1961, Geology of Unalaska Island and adjacent insular shelf, Aleutian Islands, Alaska: U.S. Geological Survey Bulletin, v. 1028-5, p. 583-676.

Finch, R.H., 1935, Akutan Volcano: Zeitschrift fur Vulkanologie, Bd. XVI, p. 155-160.

Kay, S.M., Kay, R.W., and Citron, G.P., 1982, Tectonic controls on tholeiitic and calc-alkaline magmatism in the Aleutian arc: Journal of Geophysical Resources, v. 87, p. 4051-4072.

McCulloch, M., and Perfit, M.R., 1981, $^{143}Nd/^{144}Nd$, $^{87}Sr/^{86}Sr$ and trace element constraints on the petrogenesis of the Aleutian island arc magmas: Earth and Planetary Science Letters, v. 56, p. 167-179.

Miyashiro, A., 1974, Volcanic rock series in island arcs and active continental margins: American Journal of Science, v. 247, p. 321-355.

Motyka, R.J., Moorman, M.A., and Liss, S.A., 1981, Assessment of thermal spring sites Aleutian Arc, Atka Island to Becherof Lake - preliminary results and evaluation: Alaska Division of Geological and Geophysical Surveys Open-file Report 144, 173 p.

Nye, C.J., Queen, L.D., and Motyka, R.J., 1984, Geologic map of the Makushin geothermal area, Unalaska Island, Alaska: Alaska Division of Geological and Geophysical Surveys Report of Investigations 84-2, 2 sheets, scale 1:24,000.

Perfit, M.R., Brueckner, H.K., Lawrence, J.R., and Kay, R.W., 1980, Trace element and isotopic variations in a zoned pluton and associated rocks, Unalaska Island, Alaska: A model for fractionation in the Aleutian calc-alkaline suite: Contributions to Mineralogy and Petrology, v. 73, p. 69-87.

Perfit, M.R., Gust, D.A., 1981, Petrochemistry and experimental crystallization of basalts from the Aleutian Islands, Alaska: (abs), 1981 IAVCEI Symposium, Arc Volcanism, Tokyo and Hokane, Japan, p. 288-289.

Presnall, D.C., Dixon, S.A., Dixon, J.R., O'Donnell, T.H., Brenner, N.L., Schrock, R.L., and Dycus, D.W., 1978, Liquidus phase relations on the join diopside-forsterite-anorthite from 1 atm to 20 kbar: Their bearing on the generation and crystallization of basaltic magma: Contributions to Mineralogy and Petrology, v. 66, p. 203-220.

Romick, J.D., 1982, The igneous petrology and geochemistry of northern Akutan Island, Alaska: Master's thesis, University of Alaska, Fairbanks, 151 p.

Simkin, Tom, Siebert, Lee, McCelland, Lindsey, Bridge, David, Newhall, Christopher, and Latter, J.H., 1981, Volcanoes of the world: The Smithsonian Institution, Hutchinson Ross Publishing Co., Stroudsburg, Pennsylvania, 232 p.

CHAPTER 3

GEOLOGY OF HOT SPRINGS BAY VALLEY AKUTAN ISLAND, ALASKA

by

Samuel E. Swanson,[1] Donald L. Turner,[1] Jay D. Romick,[2] and Roman J. Motyka[3]

[1]Geophysical Institute, University of Alaska-Fairbanks, Fairbanks, Alaska 99775
[2]Alaska Division of Geological and Geophysical Surveys, 794 University Ave., Suite 200, Fairbanks, Alaska 99709 (Current address: Department of Geological Sciences, Cornell University, Ithaca, N.Y. 14853)
[3]Alaska Division of Geological and Geophysical Surveys, 400 Willoughby Ave., 3rd Floor, Juneau, Alaska 99801

INTRODUCTION

Hot Springs Bay valley is located on the eastern side of Akutan Island in the eastern Aleutian Islands. The valley is 4.2 km long and 0.9 km wide and trends approximately northeast. Steep valley walls rise almost 500 m above a flat valley floor (sheet 1). Hot Springs Creek meanders over the gently sloping floor of Hot Springs Bay valley and drains into the sea at Hot Springs Bay. Helicopter and Zodiac raft-supported geologic mapping of Hot Springs Bay valley has produced a 1:20,000 scale geologic map (sheet 1). The valley walls are composed of volcanic breccia with minor intercalated lava flows. Lava flows are more abundant on the higher slopes. Dikes from 15 cm to 5 m thick intrude the layered sequence in the valley walls. Two small gabbroic bodies intrude the flows, along the coast north and south of Hot Springs Bay valley (sheet 1). Outcrops of valley fill consist of volcanic debris flows, dune sands and contemporary beach deposits.

VALLEY WALLS

Preglacial Debris Flows

Much of the lower valley wall adjacent to Hot Springs Bay valley is composed of volcanic debris flow deposits of the informally named Hot Springs Bay volcanics (Swanson and Romick, chap. 2, this report). Individual flows lack internal stratification. Bedding attitudes can, however, be determined from occasional layers of pyroclastic material or lava flows. The deposits are unsorted and comprised of angular blocks up to 1 m in diameter in a sand-size matrix. Petrologically the flows are best termed volcanic breccia. Different textural varieties of basalt and basaltic-andesite comprise the blocks in the debris flows. Blocks within the debris flows do not show any evidence, such as oxidized rims or radial fractures, that the flows were hot at the time of emplacement. These flows probably represent remobilized debris from the upper slopes of Akutan volcano.

Basalt and Basaltic-Andesite Lava Flows

Lava flows are more abundant on the higher elevations surrounding Hot Springs Bay valley (sheet 1). The lava flows tend to be more resistant to erosion than the breccias and therefore form caps on ridges. Flows range in thickness from 3.5 to 10 m and some show crudely developed columnar jointing perpendicular to the base. Lava flows dip at shallow (3°-5°) angles toward the sea.

Phenocrysts of augite, plagioclase and minor olivine in a moderately altered matrix characterize the lava flows in the lower walls of the valley. The groundmass is holocrystalline and in places plagioclase microlites define a flow banding, resulting in a trachytic texture. Olivine phenocrysts are partially altered to iddingsite and augite, and the groundmass is often altered to a mixture of carbonate and chlorite. The groundmass plagioclase is commonly unaltered.

In the upper parts of the valley walls the lava flows are less altered and do not contain olivine. Flows that cap the ridge immediately north of

the valley (sheet 1) have a very fine-grained matrix and contain about 15 percent phenocrysts. Plagioclase is the dominant phenocryst phase, followed by augite and hypersthene which also form phenocrysts. Opaque minerals are unusually abundant in these lavas and constitute about 2 percent of the rocks. Except for rare carbonate amygdules these lavas show no sign of alteration.

The upper flows unconformably overlie the Hot Spring Bay volcanics and are informally referred to as the Akutan volcanics (Swanson and Romick, chap. 2, this report).

Dikes and Other Intrusions

Numerous dikes are exposed in the sea cliffs and hillsides around Hot Springs Bay valley (sheet 1). The dikes intrude the near-horizontal lava and breccia flows and are often well-exposed because they are more resistant to erosion than the volcanic breccias. Dikes are more abundant in the lower portion of the stratigraphic section. At least one dike exposed in the walls of Hot Springs Bay valley is truncated against the bottom surface of a lava flow, indicating the lava flows in the upper part of the section post-date at least some of the dikes.

Orientation of the dikes varies considerably, but they generally trend northwesterly to westerly around Hot Springs Bay valley. Dips of the dikes are variable, but typically occur at a high angle. Dike thickness ranges from 0.4 to 5.0 m. Nesting of dikes within dikes has been noted in some localities, resulting in an aggregate thickness of up to 13 m.

Dike rocks are typically fine-grained to aphanitic with occasional phenocrysts of plagioclase and, more rarely, augite, olivine or hornblende. The matrix is sometimes trachytic and usually a holocrystalline mixture of plagioclase, augite and opaque minerals, but glass was noted in the groundmass of some dike samples. Mineral banding exists in some dikes; augite and olivine are concentrated toward the dike interiors and plagioclase is concentrated near the margins. The banding may be the result of flow differentiation during dike emplacement.

Dike alteration in the vicinity of Hot Springs Bay valley is variable, but generally more pervasive than elsewhere on Akutan Island. Commonly pyroxene and olivine (when present) are at least partially altered to an assemblage of chlorite plus carbonate. Degree of alteration varies greatly, both across the width of individual dikes and between adjacent dikes only a few meters apart.

A small plug of augite gabbro is exposed in the sea cliff north of Hot Springs Bay valley (sheet 1). The rock is fine grained, ophitic, and appears to be a hypabyssal equivalent of many of the dikes.

SURFICIAL DEPOSITS

Sand Dunes

Two parallel sand dunes derived principally from beach deposits are present near the mouth of Hot Springs Bay valley (sheet 1). A dune about 7 m high is located behind the present beach. This dune is partially overgrown by grass, especially on the landward side, and is still active. A second, older, dune is located about 300 m up-valley from the beach dune and is about 130 m wide and 12 m high. The older dune is completely overgrown with grass. Studies of sea level changes in the Aleutian Islands (R.F. Black, personal commun., 1982; Black, 1982) suggest that the older dune was formed during a period of a 2-3-m higher-than-present sea-level stand that occurred between 10,000 and 3,000 years before present (ybp). Most of the Hot Springs Bay valley fill must have been in place at the time of sea level rise in order to form a platform for construction of the older sand dune. The active coastal dune began forming since 3,000 ybp as sea level slowly dropped to its present level. Both dunes are cut by Hot Springs Creek.

Postglacial Volcanic Debris Flows

Our geologic mapping shows that the present valley floor is completely covered by a volcanic debris flow of unknown thickness. Similar volcanic debris flows are exposed in several valleys on the western part of the island (Swanson and Romick, this report). These deposits are believed to have formed when water-saturated pyroclastic debris from the upper flanks of Akutan Volcano flowed down into the valleys that drain the volcano.

Two stream bank outcrops of debris flow deposits were found on the northwest side of Hot Springs Bay valley, one between springs C and D, (table 3-1) and one about 200 m up-valley from there. Several shallow auger holes near the center of the valley also encountered the same unit. The unit is highly indurated and gray where fresh, and brown where weathered. The matrix is clay-rich and encloses abundant dark-gray to black scoria ranging in size from 1.5 mm to 5 cm.

Numerous holes drilled for the helium soil gas survey in the western part of the valley encountered hard drilling and brought up cuttings of basaltic scoria in a gray, clay-rich matrix, indicating the presence of this unit. Two 2-m-deep seismic shot holes located, respectively, 500 m and 845 m up valley from the older dune, also encountered hard drilling and brought up similar cuttings. Both shots blew out large fragments of the massive debris flow unit. These ranged up to 0.7 m across in the southernmost shot hole. The fragments were fresh, indurated, gray in color and contained abundant dark-gray-to-black basaltic scoria in a clay-rich matrix. Where seen in the shot holes, the unit is megascopically indistinguishable from the unit in the cutbank outcrops described previously.

In order to determine whether or not this volcanic debris flow flowed over the older dune near the mouth of the valley (sheet 1), six 1.2-m-deep holes were drilled along a traverse across the dune, spaced about 1-2 m apart in elevation. Cuttings and hard drilling indicative of the debris flow were

Table 3-1. Composition and thickness of volcanic debris flow deposit at outcrop between Springs C and D, Hot Springs Bay valley (location on sheet 1).

Layer	Description	Thickness (cm)
1	Tundra cap, active zone of plant growth	12
2	Soil, black, sandy	8
3	Soil, dark-brown, rich in organic matter	3
4	Soil, dark-grey	7
5	Soil, brown, clay-rich	4
6	Soil, very dark-brown, clay-rich	1
7	Lapilli breccia, gray, clay-rich matrix with black scoriaceous cinders up to 5 cm diam. Material is poorly sorted and does not show any stratification. Microscopically the matrix consists of about 99% fine-grained clay enclosing plagioclase (0.1-0.2 mm diam). The matrix is well indurated. Base of this unit is not exposed.	150
	Total exposed section	185 cm

present along the back side of the dune to within about 1.7 m of the top of the dune. Two additional holes were drilled at the seaward edge of the dune and at about 10 m farther seaward. Both holes produced cuttings indicative of the presence of the volcanic debris flow.

This evidence suggests that the debris flow overrode the ancient dune and that the still-fluid deposits then slumped off the top of the dune. An alternate possibility is that the lahar surged through a stream-cut channel in the dune and then flooded the area seaward of the dune. The presence of the deposit seaward of the ancient dune indicates the flow post-dates the sea-level recession of 2,000-3,000 ybp. Valley-dune topography constrains the thickness at the distal end of this debris flow to <3 m.

About 0.3 km up the east-west tributary valley at the head of the main valley (sheet 1), a volcanic debris flow deposit at least 3.6 m thick is exposed (table 3-2). The deposit is light brown, extremely well-bedded, poorly consolidated, and composed of lapilli and clasts up to 46 cm in diameter. The absence of draping of beds over large clasts and the lack of depression of underlying beds by these clasts indicate that this unit is not an air-fall deposit. The following evidence argues against this unit being a stream-laid deposit:

1. All clasts and matrix grains are sharply angular.

2. There is no cross-bedding or cut-and-fill structure in the entire 4 x 30 m exposure.

3. Bedding is continuous around the large clasts with no evidence of back eddy turbulence.

4. The deposit is very poorly sorted.

The continuous nature of the bedding suggests laminar flow of a wet mass of dominantly sand-size material containing a few larger clasts. This unit is interpreted as representing a proximal facies of the valley-filling lahar described previously. It appears that this debris flow came down the east-west tributary valley from the flanks of Akutan Volcano and completely covered the floor of Hot Springs Bay valley, probably flowing over previous debris flow deposits and valley fill alluvium deposited prior to the formation of the ancient dune discussed above.

J.W. Reeder (personal commun., 1985) reported finding a similar section in the same vicinity, consisting of soil overlain by pyroclastics which, in turn, are overlain by the volcanic debris flow. Reeder (1983) obtained ^{14}C dates on the underlying soil layer and on soil layers underlying similar pyroclastics at two other locations on Akutan Island. The three determinations yielded an average age of 5,200 ± 200 radiometric years before present (rybp). Thus the volcanic debris flow covering Hot Springs Bay valley is younger than 5,200 rybp, which is consistent with the coastal debris-flow and sea-level change relationships discussed previously.

Beach Deposits

Material on the beaches ranges in size from sand through boulders. On the geologic map (sheet 1) sand and gravel beaches have been mapped; boulder beaches have not been distinguished. Sand and gravel beaches typically form an apron leading to dunes behind the beach, thus leaving some of the sand from the beach-dune system exposed, even at high tide. Boulder beaches consist of blocks of volcanic rock derived from sea cliffs located immediately behind the beach. These boulder beaches typically are small and are exposed only at low tide.

GEOMORPHOLOGY

Recent studies of representative islands in the Aleutians have shown that ice caps covered all major islands in the late Wisconsinan Stage and extended considerable distances over the now submerged Aleutian platform (Gard, 1980; Black, 1982; Black, 1983). Thus, glacial erosion is largely responsible for the serrated ridges radiating from Akutan summit and for the large U-shaped valleys draining the interior of Akutan Island. Retreat of the Wisconsinan ice sheet in the Aleutian Islands is thought to have occurred about 10,000-12,000 ybp (Black, 1975), indicating a fairly young age for Hot Springs Bay valley. The V-shaped lower parts of the western tributary valleys to Hot Springs Bay valley are apparently due to postglacial downcutting by streams. The present valley floors were formed in part by in-filling of volcaniclastic, glaciofluvial, and alluvial deposits.

Table 3-2. Composition and thickness of volcanic debris flow deposit at outcrop in upper tributary of Hot Springs Bay valley (location on sheet 1).

Layer	Description	Thickness (cm)
1	Tundra cap, intergrown mass of modern roots	10
2	Soil, dark-brown to black	19
3	Soil, moderate olive brown, sandy	4
4	Soil, gray, sandy	2
5	Soil, light olive brown, sandy	11
6	Soil, gray, sandy	2
7	Soil, light olive brown, sandy	4
8	Lapilli breccia, light-brown, sand to silt-size matrix with black, angular scoriaceous cinders with some blocks to 46 cm. Planar bedding is not disrupted by the presence of large blocks. No clay-sized particles are present. Base of unit is not exposed.	300
	Total exposed section	352 cm

GEOLOGIC HISTORY

The earliest geologic event in the development of Hot Springs Bay valley was the deposition of a thick sequence of volcanic breccias. These deposits were probably formed by volcanic debris flows from an ancestral Akutan volcano. The debris flows were cool mudflows that formed from melted snow or rain which remobilized volcanic debris on the upper slopes of the volcano. These earliest deposits could not be dated directly.

A series of near-vertical dikes of basaltic andesite was intruded into the sequence of breccias. The strike of the dikes toward the present summit of Akutan Volcano suggest dike intrusion may be related to some event at the summit, such as caldera formation. Byers and Barth (1953) suggested such a relation in their 1948 reconnaissance of Akutan Island. Small plugs that intrude the lava flows and breccias probably are related to this period of dike emplacement.

An extensive period of erosion followed the dike intrusion in the lower portions of the section. A relatively flat erosion surface was produced, resulting in truncation of some dikes in the lower section. Extrusion of a series of basalt and basaltic-andesite lava flows of early Pleistocene age (Swanson and Romick, this report) marked the end of the erosional period.

Wisconsinan-age glaciation was widespread on Akutan Island. Glaciers heavily dissected the older series of breccias, lavas, and dikes. The glacier

that carved Hot Springs Bay valley probably overflowed the low divide that separates this valley from Akutan Harbor and flowed down that valley as well. Glaciers terminated seaward of the present beach line.

Following retreat of the Wisconsinan glaciers about 10,000-12,000 ybp, glaciofluvial deposits, alluvium, and cinder-laden lahars from the upper slopes of Akutan Volcano began to fill Hot Springs Bay valley. A general rise in sea level of 3 m resulted in sand dune formation in the lower section of the valley sometime between 10,000 and 3,000 ybp (Black, personal commun., 1982). Extensive postglacial valley-filling pyroclastic deposits and debris flows were emplaced in several valleys draining Akutan Volcano and may be related to the formation of Akutan Caldera. Carbon-14 dates obtained by Reeder (1983) show that these deposits are younger than 5,200 rybp. The volcanic debris flow that traveled down Hot Springs Bay valley was emplaced sometime after sea-level recession began 3,000 ybp.

REFERENCES CITED

Black, R.F., 1975, Late-Quaternary geomorphic processes: Effects on the ancient Aleuts of Umnak Island in the Aleutians: Arctic, v. 28, no. 3, p. 159-169.

Black, R.F., 1982, Holocene sea-level changes in the Aleutian Islands: New data from Atka Island: in Holocene sea level fluctuations, magnitude and causes: D.J. Colquhoun, Organizer, IGCP #61, p. 1-12.

Black, R.F., 1983, Glacial chronology of the Aleutian Islands: in 'Glaciation in Alaska': Alaskan Quaternary Center, University of Alaska Museum Occasional Paper No. 2, p. 5-10.

Byers, F.M., Jr., and Barth, T.F.W., 1953, Volcanic activity on Akun and Akutan Island: Pacific Science Congress Proceedings, 7th, New Zealand, 1949, Proceedings, v. 2. p. 382-397.

Gard, L.M., Jr., 1980, The Pleistocene geology of Amchitka Island, Aleutian Islands, Alaska: U.S. Geological Survey Bulletin 1478, 38 p.

Reeder, J.W., 1983, Preliminary dating of the caldera forming Holocene volcanic events for the eastern Aleutian Islands: Abstract, 96th Annual Meeting, Geological Society of America, v. 15, p. 668.

CHAPTER 4

GEOPHYSICAL SURVEYS
HOT SPRINGS BAY VALLEY, AKUTAN ISLAND, ALASKA

by

Eugene M. Wescott, William Witte, Donald L. Turner,
and Becky Petzinger

Geophysical Institute, University of Alaska-Fairbanks,
Fairbanks, Alaska 99775

INTRODUCTION

Geophysical methods were used at Hot Springs Bay valley to determine the thicknesses and physical properties of valley-filling sediments and volcanic debris flows, depth to bedrock, and to locate and delineate possible geothermal reservoirs. Several techniques were used to generate a wide range of information and compensate for the deficiency of current subsurface data in the area.

Near-surface (6-m) earth conductivities measured with a Geonics EM-31 noncontacting conductivity meter have been used elsewhere to map areas of anomalous temperatures (Wescott and Turner, 1981; Turner and Forbes, 1980; Osterkamp and others, 1983). EM-31 readings were taken at 25-m intervals along northwest-southeast oriented grid lines spaced 100 m apart. The grid system is shown on sheet 2. The electrical resistivity at greater depths was measured by Schlumberger vertical electrical soundings (VES) and by co-linear dipole-dipole sections. The layering of debris flows and sediments and depth to basement was investigated by use of the seismic refraction profile technique. Gravity profiling and very low frequency (VLF) measurements were carried out, but these techniques did not produce usable results.

Analysis of the results has produced an integrated model of the lower valley to a depth of about 150 m.

SHALLOW GROUND CONDUCTIVITY MEASUREMENTS

The specific conductances of waters from springs A_2 and D_2 are 1,775 and 700 mhos/cm at 25°C, respectively (Motyka and others, 1981). At the actual spring temperatures of 84° and 58.8°C, the reciprocals of the conductances (the resistivities) of the waters are 2.39 and 8.03 ohm-m, respectively, using the relationship of conductivity to temperature (T) where $\sigma_T = \sigma_{25}[1 + 0.023\ (T - 25)]$. The resistivities of formations filling the valley are in general much higher, so the presence of hot water near the surface should be apparent by low resistivity (high conductivity).

The Geonics EM-31 noncontacting terrain conductivity meter measures the apparent conductivity of the ground with an effective depth of penetration of about 6 m when the coils are horizontal. It operates by transmitting a 9.8 kHz signal into the ground via a self-contained dipole transmitter coil at one end of a boom which induces circular eddy current loops in the ground. The magnitude of these current loops is directly proportional to terrain conductivity in the vicinity of the loop. Each current loop generates a magnetic field proportional to the current in the loop. The receiver coil at the other end of the 4-m boom detects a portion of the induced magnetic field, which results in an output voltage proportional to terrain conductivity.

If the ground is homogeneous to about 6 m, the apparent conductivity is the true conductivity. However, if there are layers of different conductivity within the effective depth of penetration, the apparent conductivity will be an intermediate value.

The conductivity of water increases with temperature, and hot water is also likely to contain dissolved salts, further increasing its conductivity compared to cold water (Keller and Frischknecht, 1966).

In our investigations at Pilgrim Springs (Turner and Forbes, 1980), Chena Hot Springs (Wescott and Turner, 1981), and at Manley Hot Springs (East, 1982), the EM-31 has proven very useful for locating near-surface zones of anomalous temperatures, even where the salinity of the geothermal water is not high. The correlation between ground temperature and shallow conductivity has proven to be of sufficient reliability that the EM-31 method was selected to locate areas of near-surface temperature anomalies rather than making a more time-consuming ground temperature survey.

EM-31 readings were made along the northwest-southeast 100-m grid lines (sheet 2) at 25-m intervals, or closer in regions of steep gradients. The results of the survey, converted to resistivity values (units of ohm-m), have been contoured and are shown in figure 4-1. The lowest resistivity zone forms a discontinuous, sinuous pattern near the northwest edge of the valley from about 1,100 m southwest to 400 m northeast. The lowest resistivity, less than 10 ohm-m, forms narrow zones about 10 m wide near the A, C, and D hot springs, and a broad zone on the beach around the E springs.

The sinuous pattern of the anomaly suggests that the hot water may rise to or near the surface via an ancient stream channel which cuts through more impervious volcanic debris flow deposits covering a deeper reservoir (Swanson and others, chap. 3, this report).

Some EM-31 lines, not shown on the grid of figure 4-1, were run across the full width of the valley to determine if any other temperature anomalies existed. In all cases the resistivity was 100 ohm-m or greater all the way to the southeast edge of the valley. The anomalies seem to end at 1,100 m southwest, as no low resistivity readings were found further up the valley.

The highest near-surface resistivities were found on the dune formation near 0 southwest at greater than 500 ohm-m and also on the recent dune near 400 m northeast.

DEEP RESISTIVITY MEASUREMENTS

Schlumberger Vertical Electric Soundings

The Schlumberger vertical electric sounding (VES) technique uses four co-linear electrodes through which current is sent into the ground at the outermost electrodes (A and B) and the resulting voltage measured across the pair of electrodes (MN) in the center of AB, with MN << AB. To make a VES, the current electrodes AB are moved outwards while the potential electrodes remain fixed. The larger the spacing AB, the greater the depth of investigation. The apparent resistivity is calculated from the formula:

$$\rho = \pi \frac{AB^2}{MN} - \frac{MN}{4} \frac{V}{I} \qquad (4\text{-}1)$$

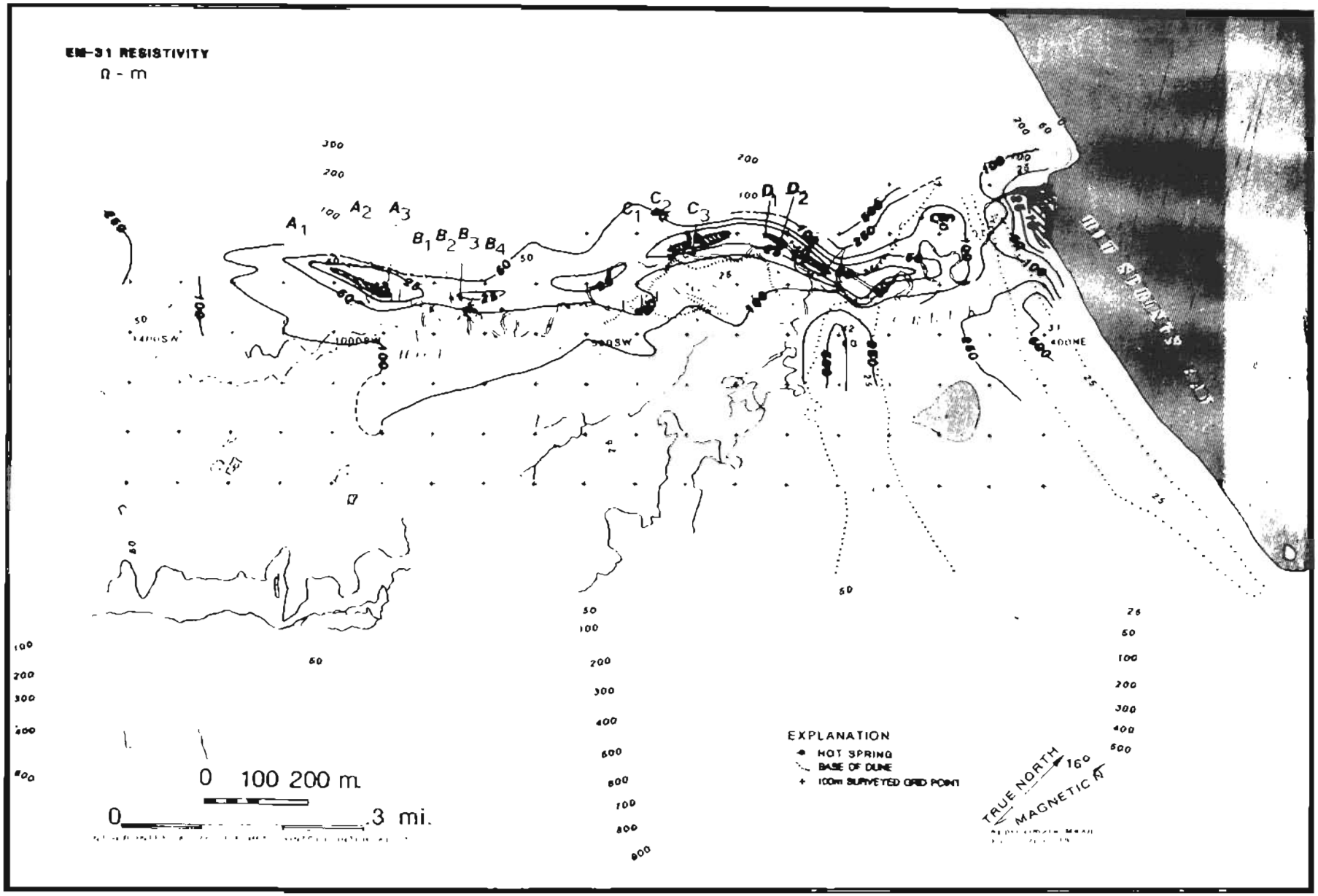

Figure 4-1. Map of Hot Springs Bay valley, Akutan Island, Alaska, with superimposed near-surface (6-m) electrical resistivity contours from an EM-31 ground conductivity survey. Cross-hatched areas indicate anomalously high ground temperatures (discussion in text).

where AB and MN are the current electrode and potential electrode separations, V is the voltage across MN and I is the current (Keller and Frischknecht, 1966). The apparent resistivity vs. ½ AB is plotted on log-log paper for interpretation by comparison with sets of theoretical curves or by computer modelling to give true resistivity vs. depth. The interpretation model assumes horizontal layers of uniform resistivity.

We carried out four Schlumberger VES measurements, with ½ AB spacings ranging from 0.68 m to 316 m located as shown in figure 4-2. VES 1 (see fig. 4-2) was run northeast-southwest along the same line as seismic profile B-B' (see fig. 4-10). It was centered at 0 northwest, 400 m southwest, and was carried out to a ½ AB spacing of 316 m. The data from table 4-1 are plotted on log-log paper in figure 4-3 along with a true resistivity-true depth model calculated by means of an automatic curve-fitting program (Zhody, 1974). The program uses various numbers of layers to approach a best fit. In the case of the model, the model VES curve is shown as well as the true resistivity vs. depth, with the spacing scale serving as depth in meters. The model indicates that the top of a low resistivity layer occurs at a depth of 52 m where the resistivity drops to 12 ohm-m, and is 42 m thick. The top of an even lower resistivity layer of 7 ohm-m is suggested by the data to occur at a depth of 148 m.

VES 2 (see fig. 4-2) was run parallel to and 75 m northwest of VES 1 and was centered at 75 m northwest, 275 m southwest. The maximum ½ AB spacing was 136 m. The location was chosen to sample the resistivity of the volcanic debris flow deposits, evident as a dry terrace and identified by shallow auger holes and a trench in the terrace bank (Swanson and others, this report). Figure 4-4 shows the observed apparent resistivity values from table 4-2, a model apparent resistivity curve and true resistivity vs. depth, with a depth scale equal to the ½ AB spacing scale. The model uses six layers to make a good fit to the data.

The volcanic debris flow unit has a resistivity of 181-517 ohm-m to a depth of 1 m. The resistivity decreases from 517 to 45 ohm-m from 1 to 20 m in depth. An underlying low resistivity layer has a resistivity of 10.5 ohm-m and occurs at a depth interval of 20-60 m. The resistivity of the underlying unit, which is probably bedrock, is much higher (1,524 ohm-m).

VES 3 was run on the stream terrace northwest of Hot Springs Creek between springs C and D (see fig. 4-2). As a result of space limitations the maximum ½ AB spacing was only 68 m. Figure 4-5 plots the observed apparent resistivity values (table 4-3), and a model using eight layers. In this situation the conditions for a one-dimensional interpretation are clearly violated by the occurrence of a steep hillside with high-resistivity bedrock, about 10 m northwest of the array. The high-resistivity bedrock unit probably slopes steeply beneath the array. Nevertheless, the interpretation utilizing a horizontal-layer model is valid for the near-surface layers and is probably an approximate representation of deeper layering. The model indicates a thin near-surface resistivity layer of 3 ohm-m occurring, with deeper layers of 6-4 ohm-m resistivity at a depth interval of 13.5-36.5 m.

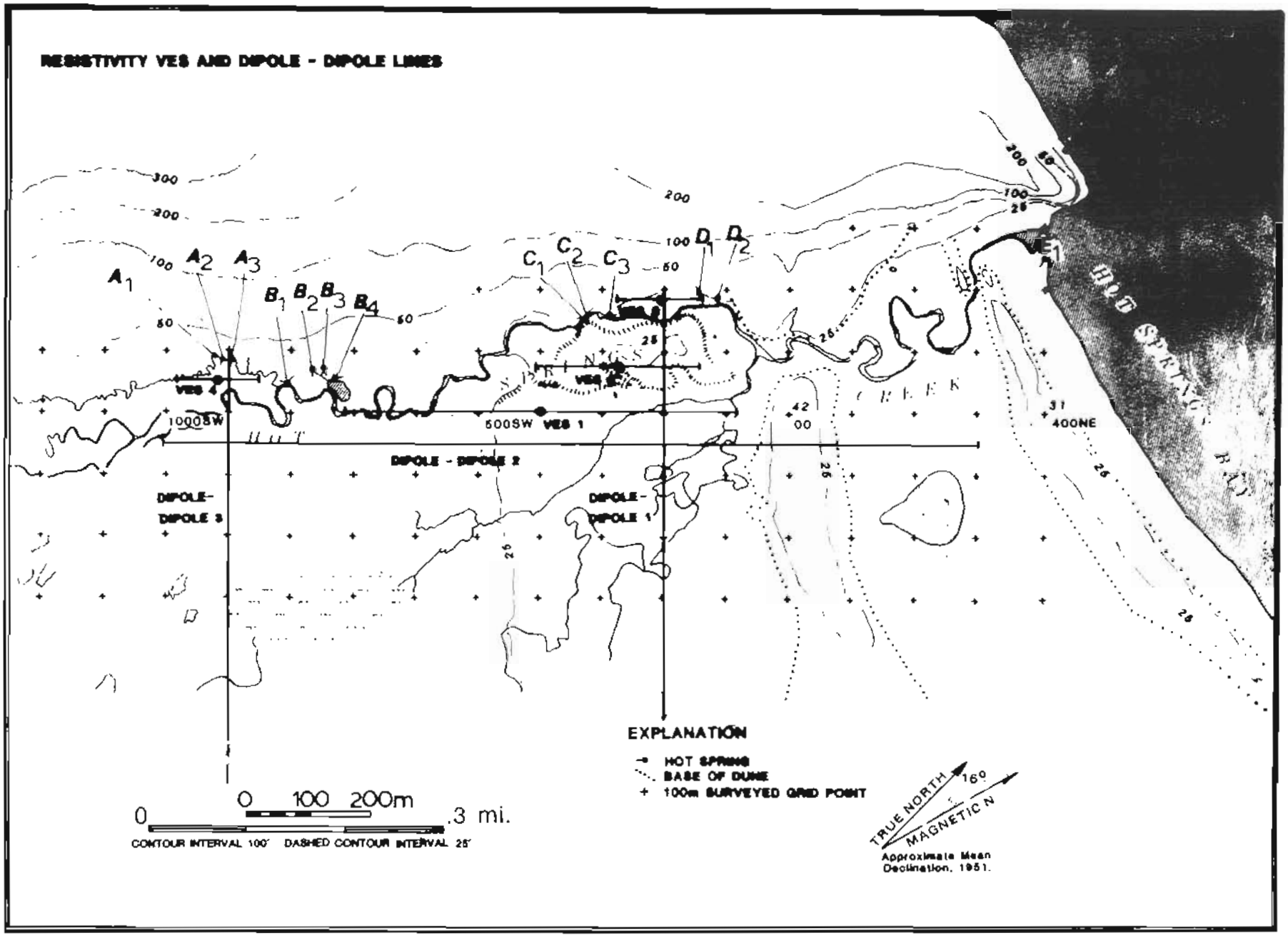

Figure 4-2. Map of Hot Springs Bay valley, Akutan Island, Alaska, with locations of four vertical electric soundings (VES) made using the Schlumberger array and locations of three dipole-dipole profile lines.

Table 4-1. Model input values for Schlumberger Akutan VES 1.

Layer	Depth to bottom of layer (m)	Thickness (m)	Resistivity (ohm-m)
1	0.3	0.3	107
2	1.0	1.0	179
3	3.0	1.5	165
4	5.0	3.0	206
5	11	6.0	105
6	14	2.5	33
7	34	21	74
8	52	18	50
9	95	42	12
10	150	55	21
11	∞	∞	7

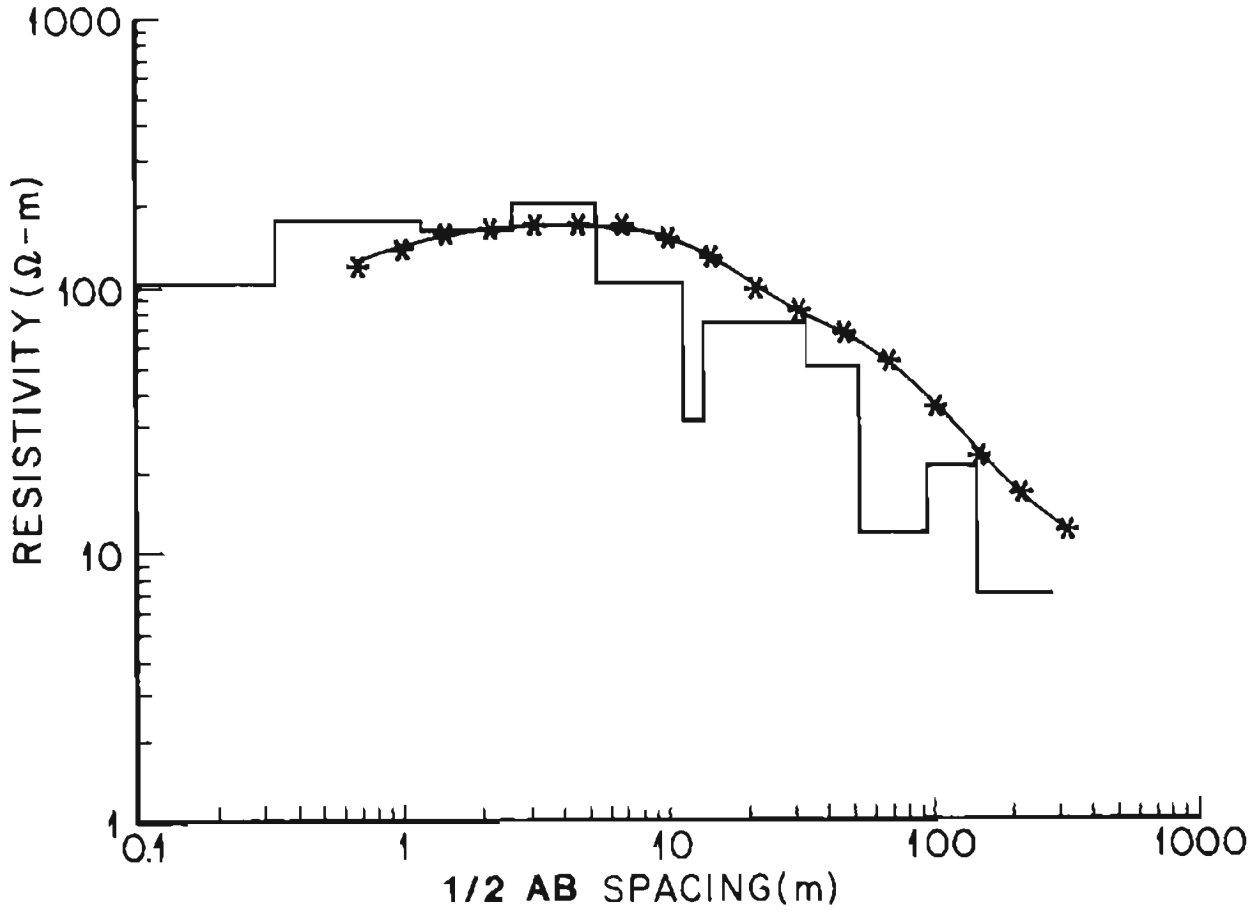

Figure 4-3. VES 1 plot of apparent resistivity vs. ½ AB spacing, Hot Springs Bay valley. Model input values are given in table 4-1. Observed data are denoted with asterisks and computed model results are shown by the curved solid line. The true resistivity vs. depth of the model is shown by straight line segments.

Table 4-2. Model input values for Schlumberger Akutan VES 2.

Layer	Depth to bottom of layer (m)	Thickness (m)	Resistivity (ohm-m)
1	0.4	0.4	181
2	1	0.6	517
3	4.5	3.5	121
4	20	15	44
5	60	40	10
6	∞	∞	1,524

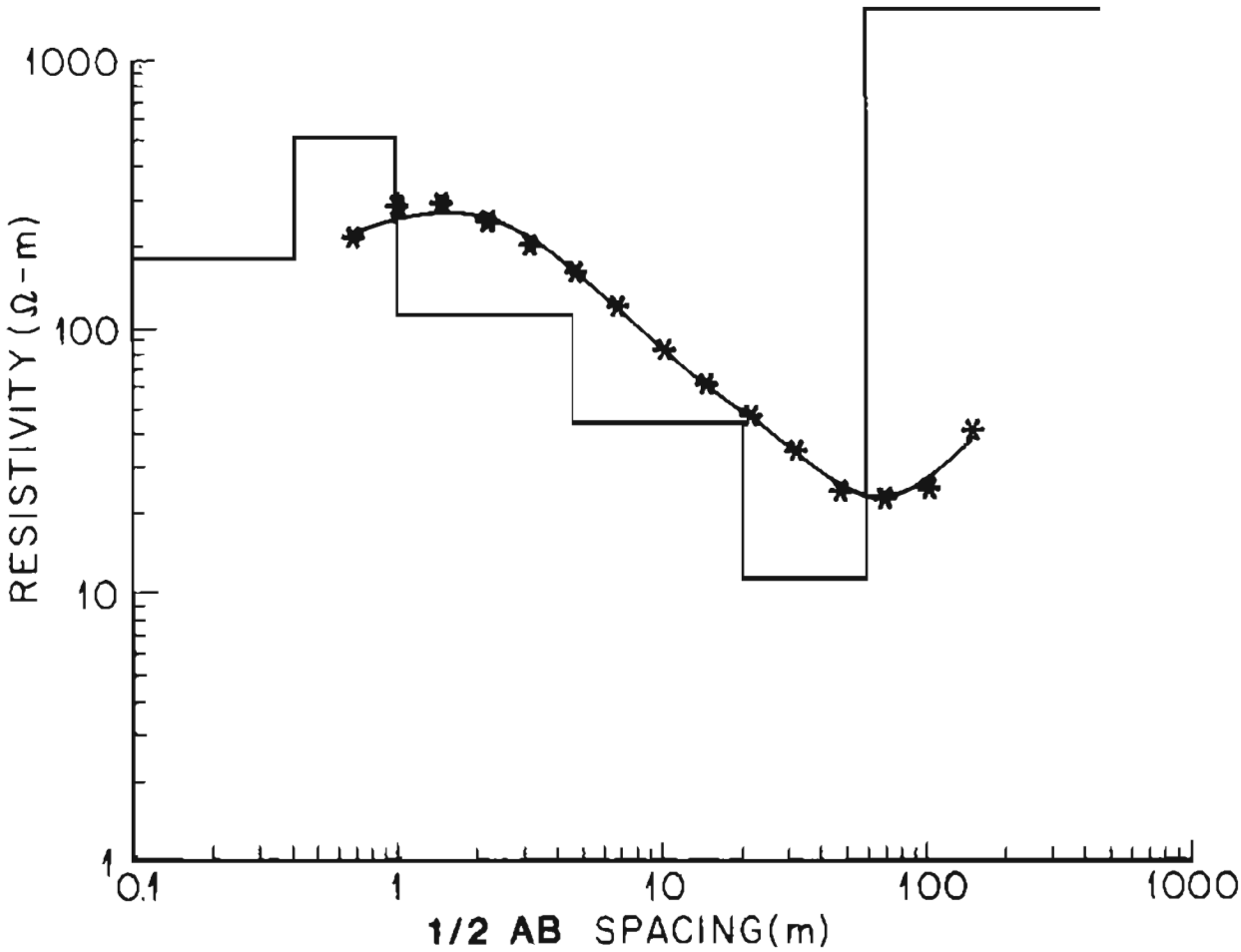

Figure 4-4. VES 2 plot of data and model results, Hot Springs Bay valley. Model input values are given in table 4-2.

Table 4-3. Model input values for Schlumberger Akutan VES 3.

Layer	Depth to bottom of layer (m)	Thickness (m)	Resistivity (ohm-m)
1	1.5	1.5	121
2	2.1	0.6	62
3	27	0.6	17
4	3.1	0.5	3
5	13.5	10	30
6	14.4	1.0	6
7	36.5	22	4
8	∞	∞	515

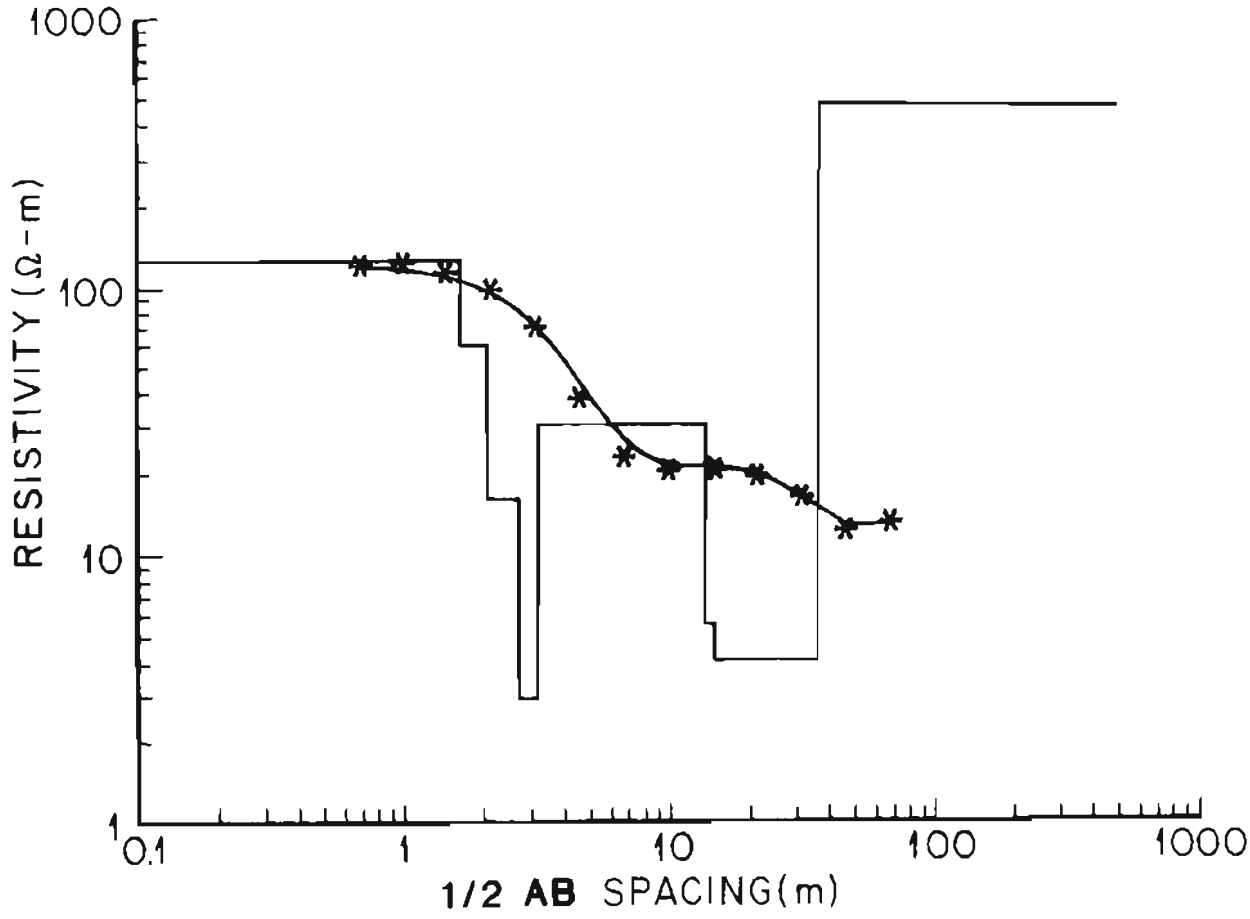

Figure 4-5. VES 3 plot of data and model results, Hot Springs Bay valley. Model input values are given in table 4-3.

A fourth VES was run in the vicinity of one of the springs in the A group (fig. 4-2). Figure 4-6 shows the observed apparent resistivities (values from table 4-4) and the results of a model with seven layers. The interpretation suggests a low resistivity layer of 2.2 ohm-m occurring at a depth of 9-13 m, underlain by a layer with a resistivity of 10 ohm-m. The resolution of the deepest layer is uncertain, because the maximum ½ AB spacing was 68 m.

Deep Resistivity Profiling

Deep electrical resistivity measurements were made using a Zonge Engineering and Research Organization GDP-12 induced polarization/resistivity receiver system. A Geotronics FT-4 transmitter capable of a 4 ampere square wave signal was used as the signal source. The Zonge system uses a pair of microprocessors to process the field data (stacking and averaging), to improve the signal-to-noise ratio and calculate the resistivity and phase shift. Although the system can be used with 16 different frequencies from 1/125 to 256 Hz to produce a complex resistivity curve, both Schlumberger VES and dipole-dipole measurements were made using only ¼ Hz frequencies because of time limitations.

As shown in figure 4-2, three dipole-dipole profiles were run along and across the valley. In the dipole-dipole electrode configuration, the computation of apparent resistivity is simplified if the receiving dipole is the same length as the transmitter, and separated from the transmitter by n times the dipole length. We used 100-m dipoles and generally extended each receiving spread out to $n = 5$. Figure 4-7 shows the dipole-dipole resistivity survey electrode configuration. The whole array can be moved horizontally to sample depth vs. horizontal distance. The results are usually presented as a pseudo-section, where the apparent resistivity values are plotted at the intersections of lines drawn at 45° from the horizontal between the center of the transmitter and the center of the receiver locations.

Apparao and Roy (1973) have defined the depth of investigation for homogeneous ground to be that depth which contributes the maximum to the signal measured at the ground surface. For the co-linear dipole-dipole configuration, their model studies indicate the depth of investigation as: $0.195\ (n + 2)a$, where 'a' is the dipole length. In our case the depth of investigation at $n = 5$ would be 137 m. However, the effects of deeper layers are evident in the data and the data can be interpreted through the use of models.

In common practice the nominal depth of investigation is usually assumed to be about half the distance between the transmitting and receiving dipoles. Thus the survey at $n = 5$ is assumed to have sampled to a depth of about 300 m, yet features of a few tens of meters in dimension could be distinguished.

Figure 4-8 shows all three pseudo-sections plotted to show where they intersect each other. A sharp resistivity discontinuity occurs at a pseudo-depth of 150 m in all three pseudo-sections, where the resistivity decreases from values in the tens of ohm-m to lower values. The longest pseudo-section

Table 4-4. Model input values for Schlumberger Akutan VES 4.

Layer	Depth to bottom of layer (m)	Thickness (m)	Resistivity (ohm-m)
1	0.3	0.3	210
2	0.5	0.2	35
3	2.8	2.3	150
4	4.5	1.7	360
5	9	4.7	68
6	13	3.5	2.2
7	∞	∞	10

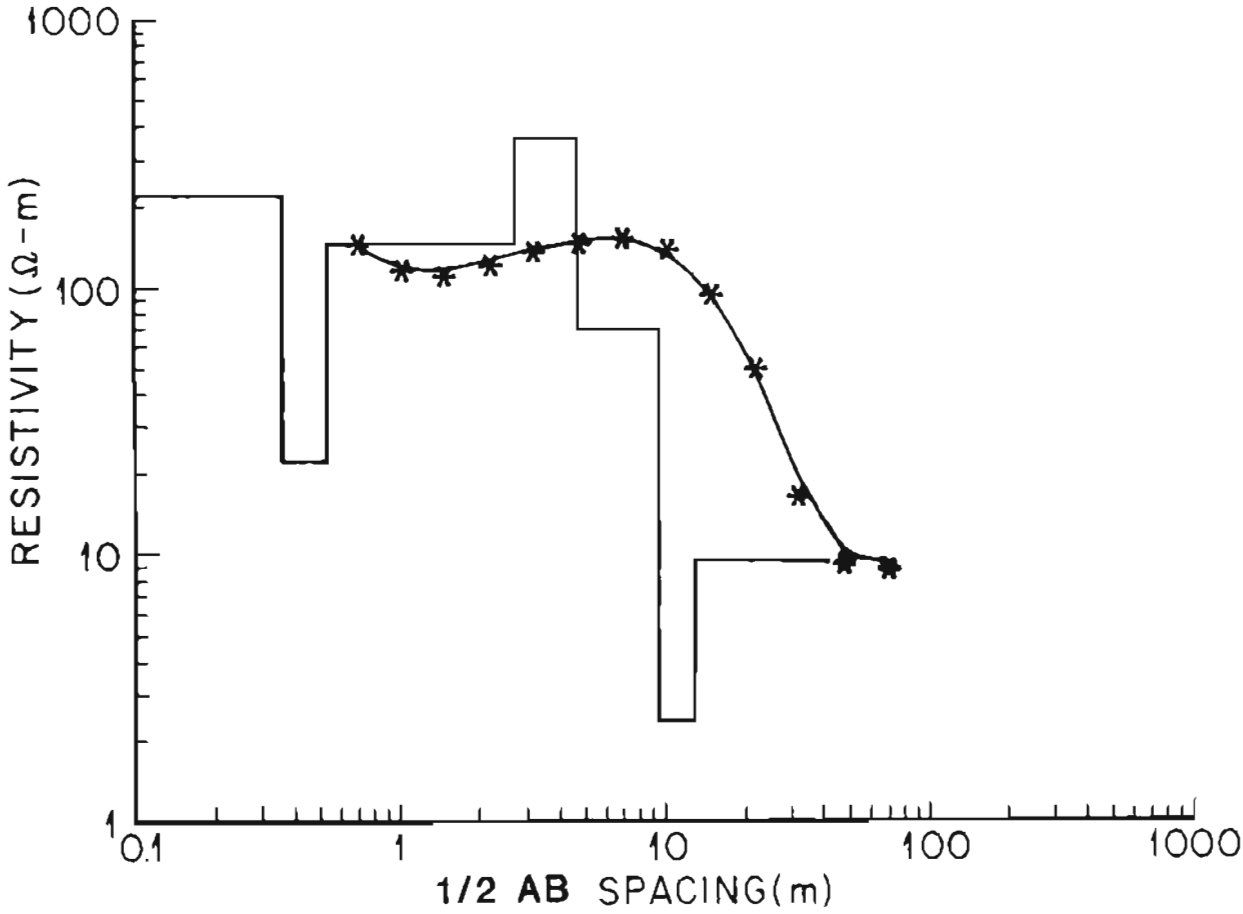

Figure 4-6. VES 4 plot of data and model results, Hot Springs Bay valley. Model input values are given in table 4-4.

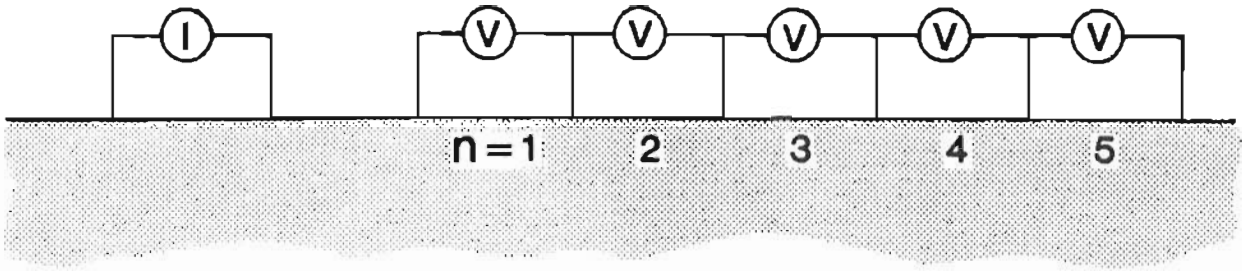

Figure 4-7. Typical electrode configuration for a dipole-dipole resistivity survey line.

(line 2) shows some very interesting effects. The inland dune which traverses the valley has a topographic high centered at 0 m southwest. Such a topographic feature will produce a type of anomaly which has been modelled for homogeneous ground by Fox and others (1978). The effect for a homogeneous medium would be to produce a small zone of apparently higher resistivity beneath station 0 with two zones of apparently lower resistivity sloping down at 45° away from station 0. Instead, the data collected on pseudo-section 2 show the resistivity decreases continuously towards the northeast. The minimum value is at a pseudo-depth of 200 m between station 0 and 100 m northeast. To the southwest of the dune there is a clear break in resistivity at a pseudo-depth of 150 m, with a low resistivity layer indicated below the upper layers.

Keller and Frischknecht (1966) have published two-layer tables for plotting a set of two-layer interpretation curves for the dipole-dipole array. Using the apparent resistivity vs. pseudo-depth at 400 m southwest as typical, the curve fitting for two layers suggests an upper layer 40 m thick of 100 ohm-m resistivity underlain by a layer of 11 ohm-m. Resistivity increases with depth below the second layer, indicating a third layer, higher in resistivity. This simple interpretation agrees fairly well with our VES 1 interpretation (fig. 4-3). As the resistivity decreases towards the northeast and the zone becomes apparently thicker, it is reasonable to suggest that the low resistivity layer increases in thickness towards the northeast, or the overlying resistive layer thins towards the northeast.

The interpretation of dipole-dipole pseudo-sections is not simple or straightforward except in simple horizontally-layered settings. Two- or three-dimensional resistivity configurations can be modelled to produce pseudo-sections for comparison with the observed data. For dipole-dipole 1, which extends completely across the valley (figs. 4-2 and 4-8), the situation is essentially two-dimensional, and we have made a number of two-dimensional model calculations using the computer code developed by Dey and Morrison (1975). This modelling program uses an array of discrete resistivity elements. Owing to the very large size of this array and the cost of computer runs for such a large program, the array was restricted to 113 x 16 elements. The smallest feature modelled is a resistivity element 10 m deep x 20 m wide. Numerous models were run, adjusting model resistivities by trial and error in

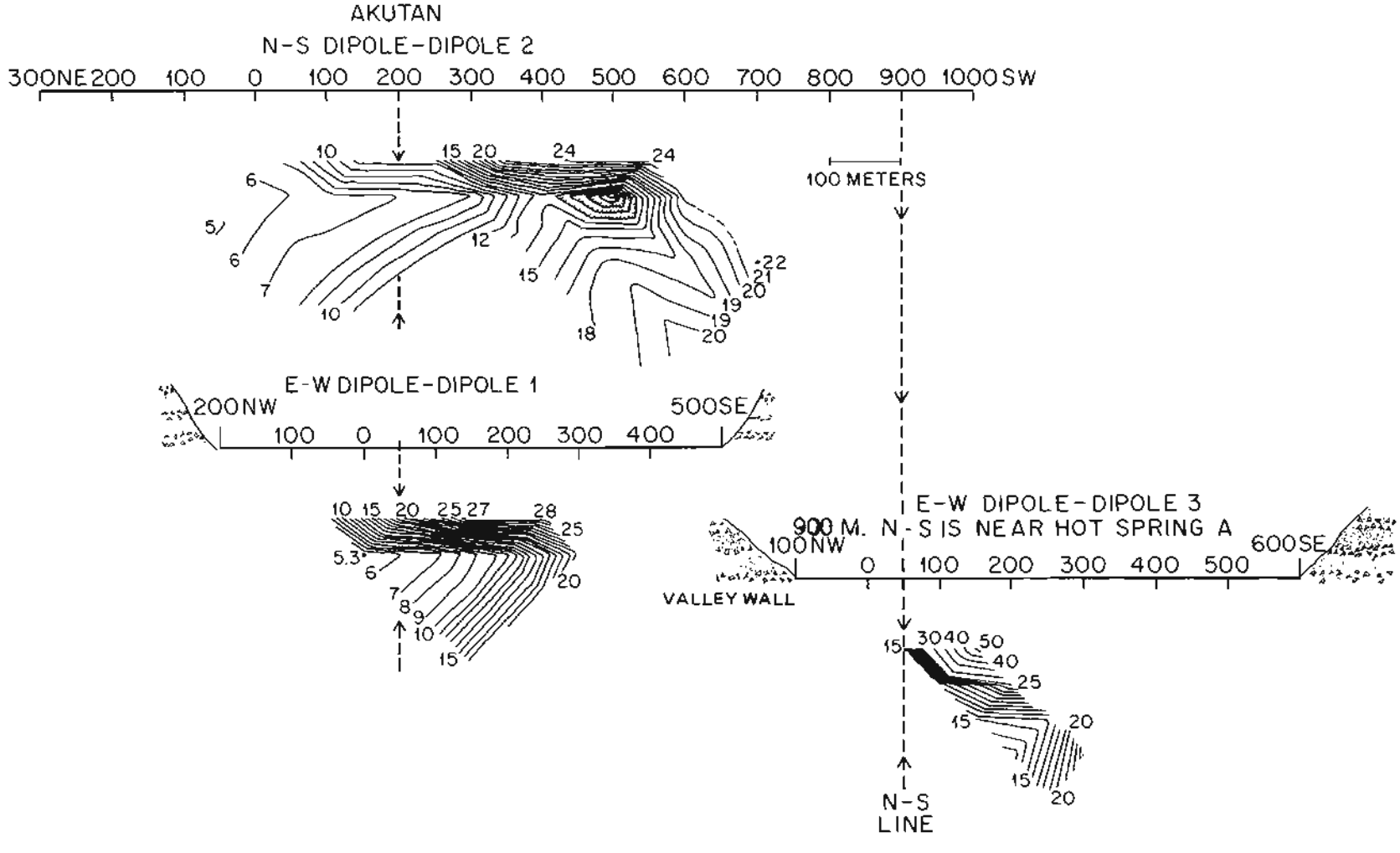

Figure 4-8. Three 100-m dipole-dipole resistivity pseudo-sections from Hot Springs Bay valley, plotted to show the intersection of lines 1 and 3 with line 2. The pseudo-depth scale is identical to the horizontal scale. Apparent resistivity contours are in ohm-m. Contour intervals are variable.

an attempt to obtain a good fit with the data. Those runs which had a fair fit to the data exhibited the same basic structure: a resistive cap layer 40-70 m thick underlain by a layer of low resistivity thinning out to the southeast and underlain by a more resistive basement. An exact fit to the observed psuedo-section was not obtained, perhaps because topographic effects of the valley walls were not incorporated. Figure 4-9 shows the observed data, a model pseudo-section and the model cross section with no vertical exaggeration.

Summary of Deep Resistivity Measurements

VES measurements 1 and 2 were far enough away from valley edges to provide a reasonable conceptualization of resistivity vs. depth of the valley subsurface between spring groups B and C. Both VES profiles show an upper layer about 10 m thick of moderate resistivity, about 120 ohm-m, underlain by layers of decreasing resistivity. VES 2, which is closer to the northwest valley side where the springs reach the surface, indicates a low resistivity zone of 10.5 ohm-m extending to a depth of 60 m. VES 1, nearer the center of the valley, shows slightly lower resistivity, which may well be influenced by the higher resistivity in the same layer towards the southeast side of the valley.

The dipole-dipole measurements require three-dimensional modelling for detailed interpretation, but by two-layer curve matching and two-dimensional cross-section modelling, results consistent with VES data were obtained. The uppermost layer has a model resistivity of about 100 ohm-m and a thickness of 40-70 m. The low resistivity layer may have a resistivity as low as 3 ohm-m towards the northwest side of the valley and 100 ohm-m towards the southeast side. The underlying basement rocks were modelled with 1,500 ohm-m.

SEISMIC REFRACTION PROFILING

Methods Used

The seismic refraction method can produce data on velocities, thicknesses, and attitudes of layers beneath a survey line if the velocities of each distinct layer increase with depth, and if distinct layers are of sufficient thickness. Thin layers or low-velocity layers may not be detected at all, or calculated depths of refractor boundaries may be erroneous. This problem, known as the hidden layer problem, is a serious drawback to the seismic refraction method. Seismic data collected during this investigation may have been affected by this problem. Analysis of first arrival times can also distinguish faults or other structural relief on a refractor boundary.

Two Geometrics Nimbus ES-1210F portable seismographs were used to investigate the structure of the valley. The Nimbus-12 seismograph is a 12-channel analog-to-digital recorder, with memory storage for stacking multiple shots or hammer strokes for signal-to-noise enhancement and post-shot variation of output amplitude for optimum traces. Twenty-four seismometers were laid out in a line with a 15-m spacing. Sixty percent seismic dynamite in 2-3-m holes served as the shot energy source. In the first shots, both seismographs were triggered by the same blaster, to produce

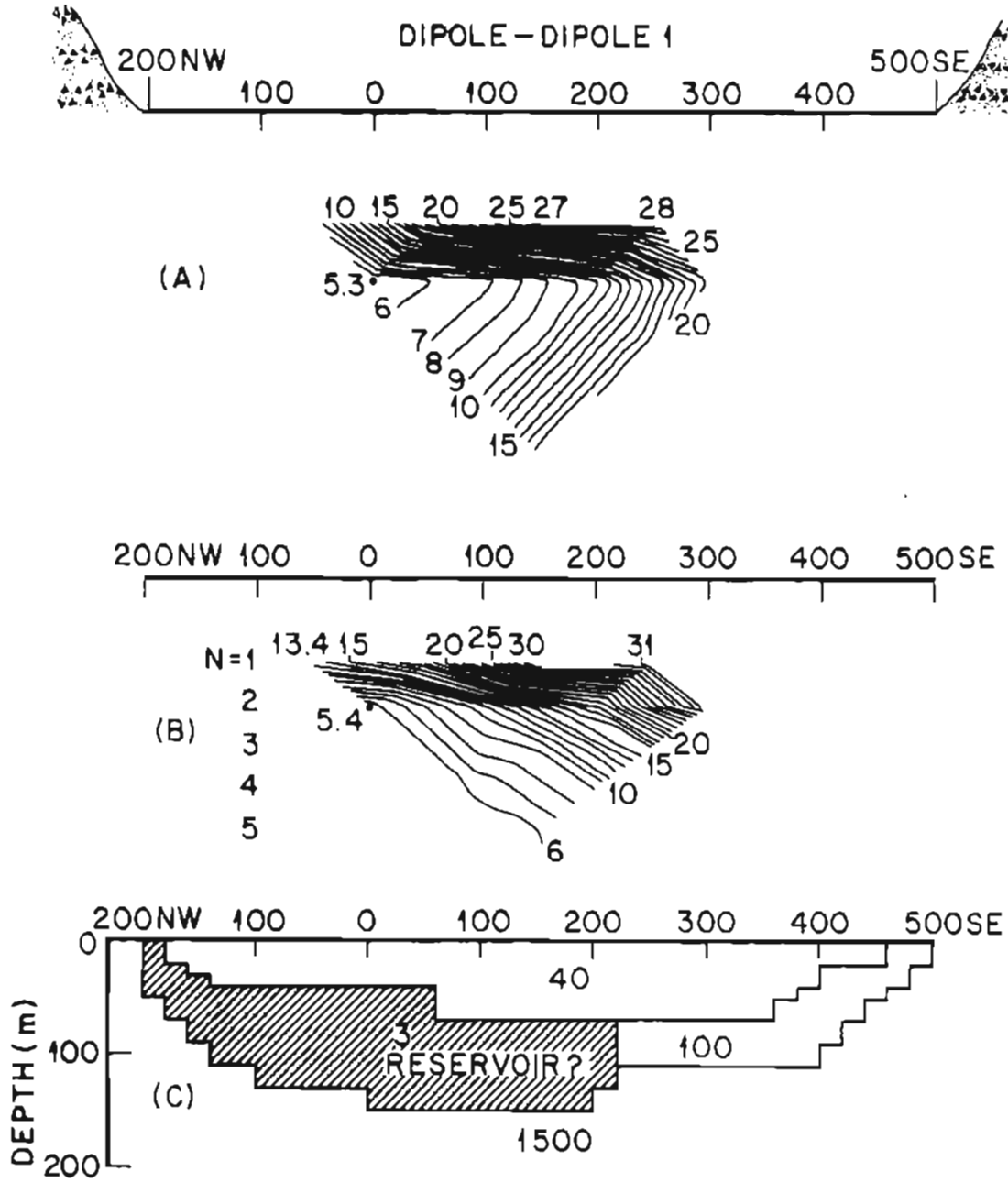

Figure 4-9. Three pseudo-section plots of dipole-dipole 1 profile across Hot Springs Bay valley. (A) shows pseudo-section produced from the observed data. (C) is a two-dimensional resistivity model cross section with its corresponding pseudo-section (B) shown above. No vertical exaggeration. Hatched area represents inferred geothermal reservoir.

a 24-channel record with a single shot. We found several instances where the seismographs did not trigger simultaneously, and all the later shots were single 12-channel spreads.

In order to detect dipping refractors, seismic spreads must be shot in both directions, and this was done in Hot Springs Bay valley. Figure 4-10 shows a map of Hot Springs Bay valley with the locations of three seismic refraction profile lines. B-B', the longest, was oriented northeast-southwest along the 0 baseline from 50 m southwest to 670 m southwest. Seven shots were used to obtain reversed travel times. We used a multi-layer dipping seismic refractor program (Campbell, 1981) to analyze the travel time curves. This program assumes that: 1) the velocity in all layers is constant within each layer; 2) all refractor interfaces are planar; and 3) no hidden layers exist. In reality, velocities may show variations laterally and with depth, interfaces are often curved or exhibit some topography, and hidden layers may occur in the area.

Results

Figure 4-11 shows the travel time curves and the calculated cross section for profile B-B'. Where the refractor interfaces are shown dashed, data are absent because the angle of incidence is less than the critical angle, and the energy is either reflected and appears as a second arrival, or is refracted downward. Three major refractors are evident from the data. The top unit varies in thickness from 45 m at 50 m southwest to 31 m near 670 m southwest, and has a velocity of about 1,630 m/s. The upper portion of this unit was observed to be a volcanic debris flow with apparent low porosity and permeability (Swanson and others, this report).

The second major unit has a velocity varying between 3,240 and 3,505 m/s. This velocity zone is of interest because it coincides with a low-resistivity layer found from Schlumberger VES measurements and dipole-dipole traverses. The depth to the base of this unit near the northeast end of the profile is about 135 m. The base slopes up the valley at about 7°, and has a depth of 78 m near 495 m southwest. The reversed shots 8, 9, and 10 covered a spread of only 165 m, which was not long enough to reach the bottom of the 3,505 m/s layer.

Beneath the second unit the velocity increases to 4,900 m/s. We have labeled the base layer as probable volcanic bedrock.

Profile A-A' was run along a line at 108 m southwest, perpendicular to profile B-B' (fig. 4-10). Figure 4-12 shows the first arrival travel time curves. The data are very clean, showing the presence of a thin (4-6 m) low-velocity (1,250 m/s) layer with two deeper layers indicated by the breaks in slope. The basal refractor appears to slope toward the center of the valley.

The velocity of the second layer is 1,960 m/s, which corresponds to the top volcanic debris flow unit in profile B-B' of 1,610 m/s. By the dipping refractor program (Campbell, 1981) the third layer would have a velocity of 4,550 m/s and the interface would dip at about 10° which would correspond to

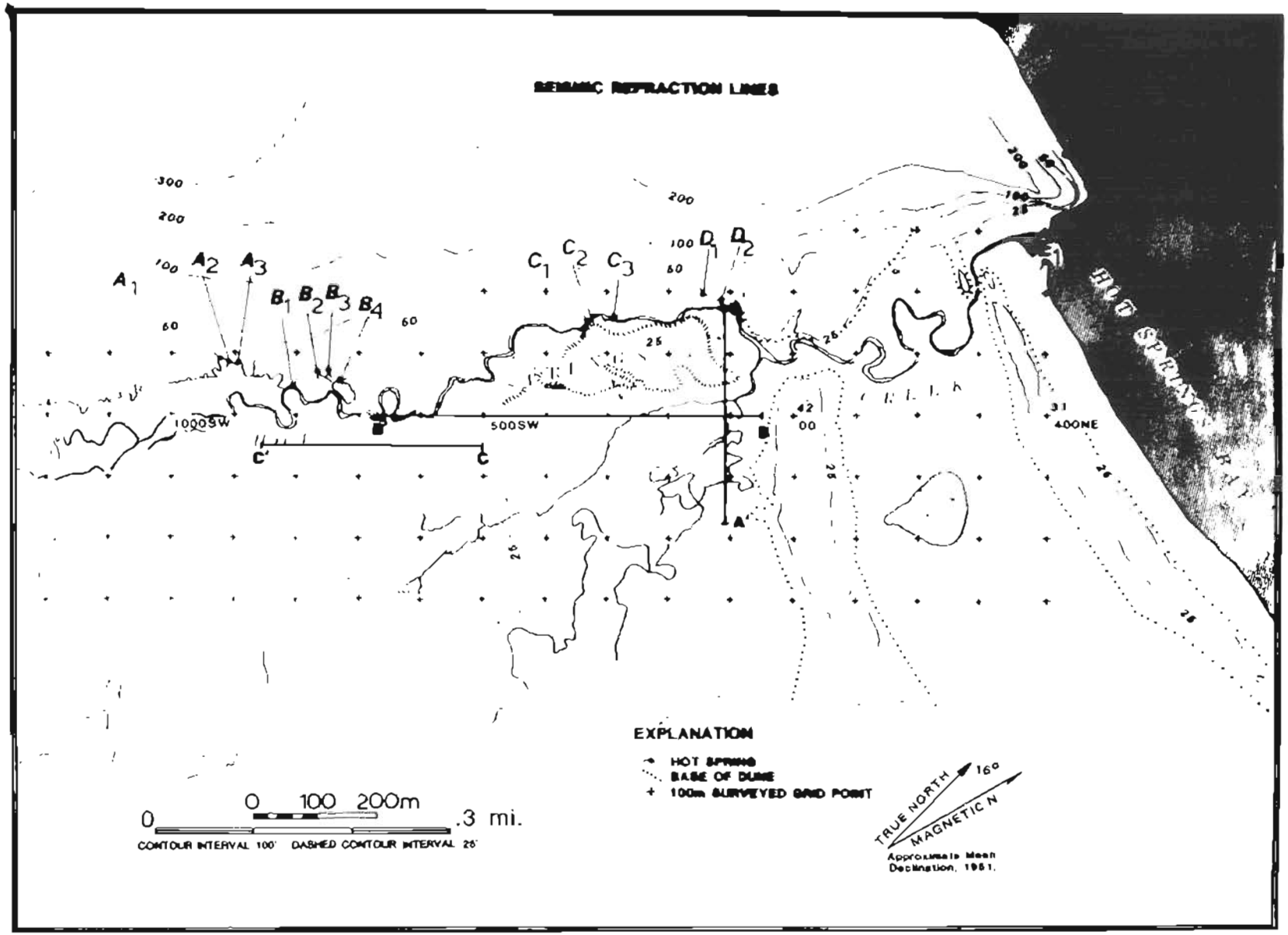

Figure 4-10. Map of Hot Springs Bay valley, Akutan Island, Alaska, showing the locations of three seismic refraction profile lines.

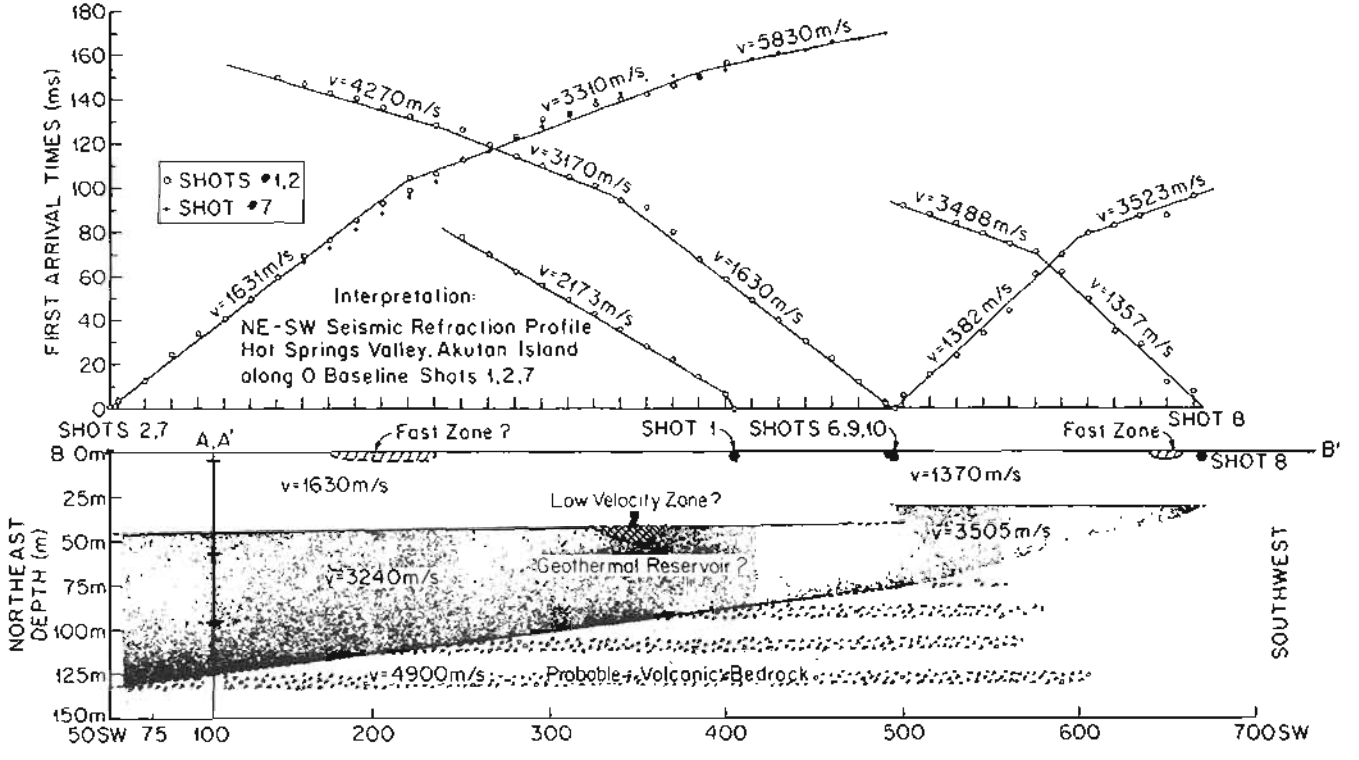

Figure 4-11. First arrival travel time curves (above) and interpreted cross section, profile B-B' parallel to valley. The layer with velocity 3,240-3,505 m/s corresponds to the low resistivity layer. Dashed portion of interface indicates zones where data are absent. Cross section shows intersection of cross valley profile A-A' with depths to corresponding seismic refractors.

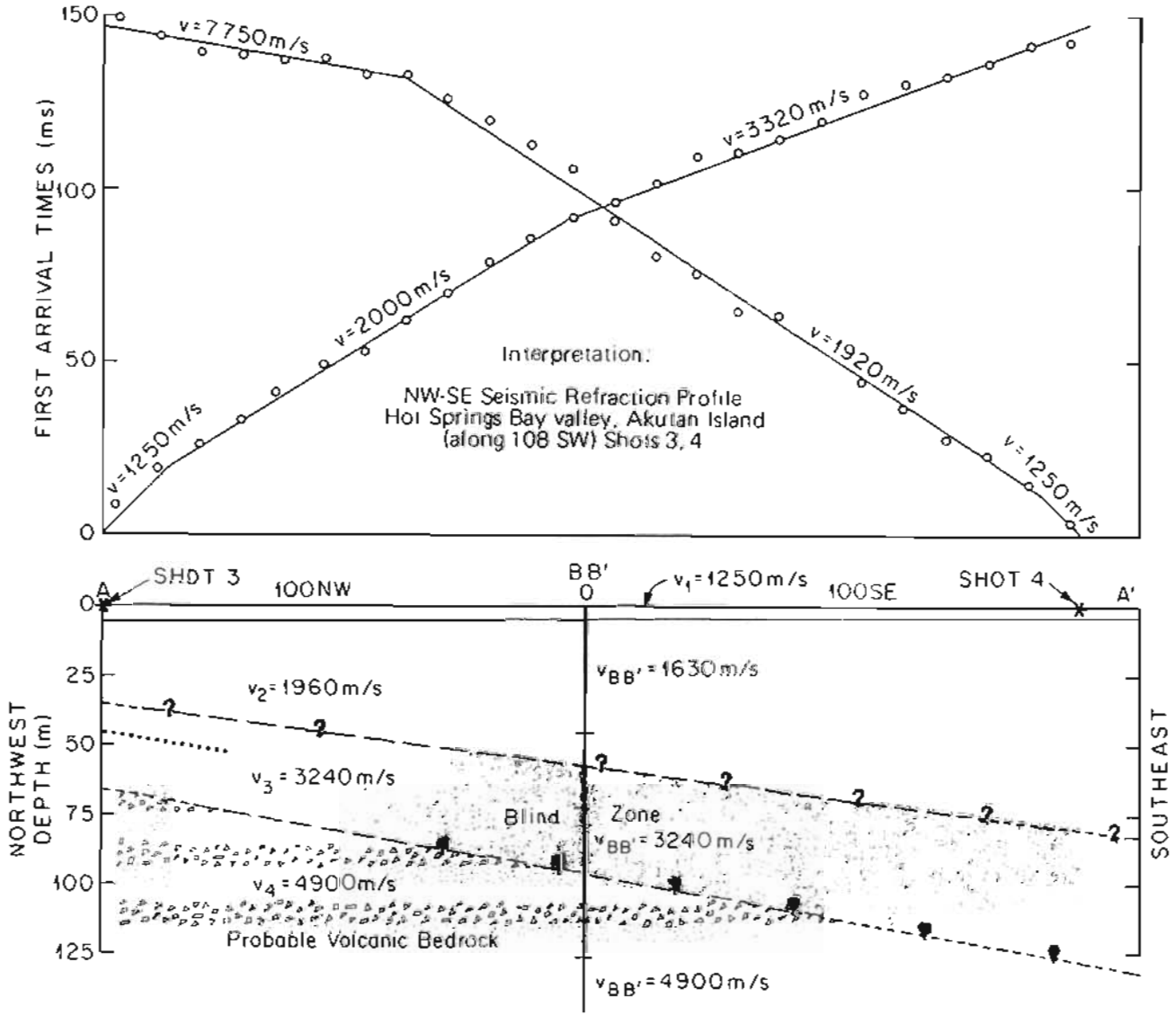

Figure 4-12. First arrival travel time curves for seismic profile A-A' (above) and interpreted cross section. The v = 3,240 m/s layer is inferred as a hidden layer which could not be seen in the first arrival travel time curves. Because it is a hidden layer the 1,960-3,240 m/s inferred interface may be more horizontal than is indicated. The steep dip of the 3,200-4,900 m/s interface suggests a glaciated surface.

the volcanic basement. However, this analysis is suspect because of the hidden layer problem discussed previously. The intermediate layer of v = 3,240-3,505 m/s seen in profile B-B' is not observed in profile A-A'. This layer can be hidden, even though its velocity is intermediate between the 1,960 m/s and 4,900 m/s, if it is not thick enough to show up on the first arrival travel time curve. It may thin towards the valley edges where profile A-A' was conducted, even though it was observed in profile B-B'.

By utilizing ray tracing techniques it is calculated that a blind zone can exist with a thickness of about 45 m, using the velocities of 3,240 and 4,900 m/s observed in profile B-B' near the intersection of AA' and BB'. The interpreted cross section, using these assumptions, is shown at each end of the cross section. The dotted line indicates the location of the interface if the hidden layer does not exist. The layer thickness and velocities where profile B-B' intersects profile A-A' are shown. The agreement in depth is not perfect but is reasonable. The apparent slope suggests that the 1,960-3,240 m/s interface may slope towards the center of the valley at about 7°, but it might be more nearly horizontal because the hidden layer problem makes the slope uncertain. The refractor interfaces are shown with shorter dashed lines where no seismic data were received as a result of ray path geometries.

Profile C-C' is located between 500 m and 950 m southwest, 50 m southeast of profile B-B', and is oriented parallel to B-B' (fig. 4-13). Again, the data seem very clean with only two major layers indicated as in Profile A-A'; the v = 3,240 m/s layer is missing (fig. 4-13). By utilizing ray tracing techniques and hidden layer nomographs (Hawkins and Maggs, 1961) it is calculated that a 17-m-thick layer of the intermediate velocity could be hidden. Other calculations indicate that a layer as thick as 25 m could be present, yet undetected, as a result of the 15-m seismometer spacing. This thickness is less than would be projected from profile B-B', but is not unexpected because of the dip towards the center of the valley in the observed profile A-A' (fig. 4-12). The interpreted profile at the bottom of figure 4-13 shows the more conservative nomograph model. The dotted lines near each end of the profile indicate the zero thickness hidden layer interface solution. Also shown by shorter dashes on the interface lines are the limits of seismic data resulting from ray path considerations.

Discussion of Seismic Results

The first arrivals indicative of a particular refractor are the waves critically refracted along the surface of the layer. Therefore, no information is available from deeper in the layer. For instance, inspection of the material from seismic shot holes, stream bank outcrops, and auger holes drilled for helium soil surveys shows that the upper portion of the layer with velocity ranging between 1,630 and 1,960 m/s is a volcanic debris flow. The entire thickness of the 1,630-1,960 m/s layer may be composed of several debris flows or might have layers of sediments of similar velocity.

The next deeper unit has a velocity about twice that of the top unit, and its upper surface is possibly an erosional surface, since it appears to slope up the valley and also up toward the walls of the valley. This unit is

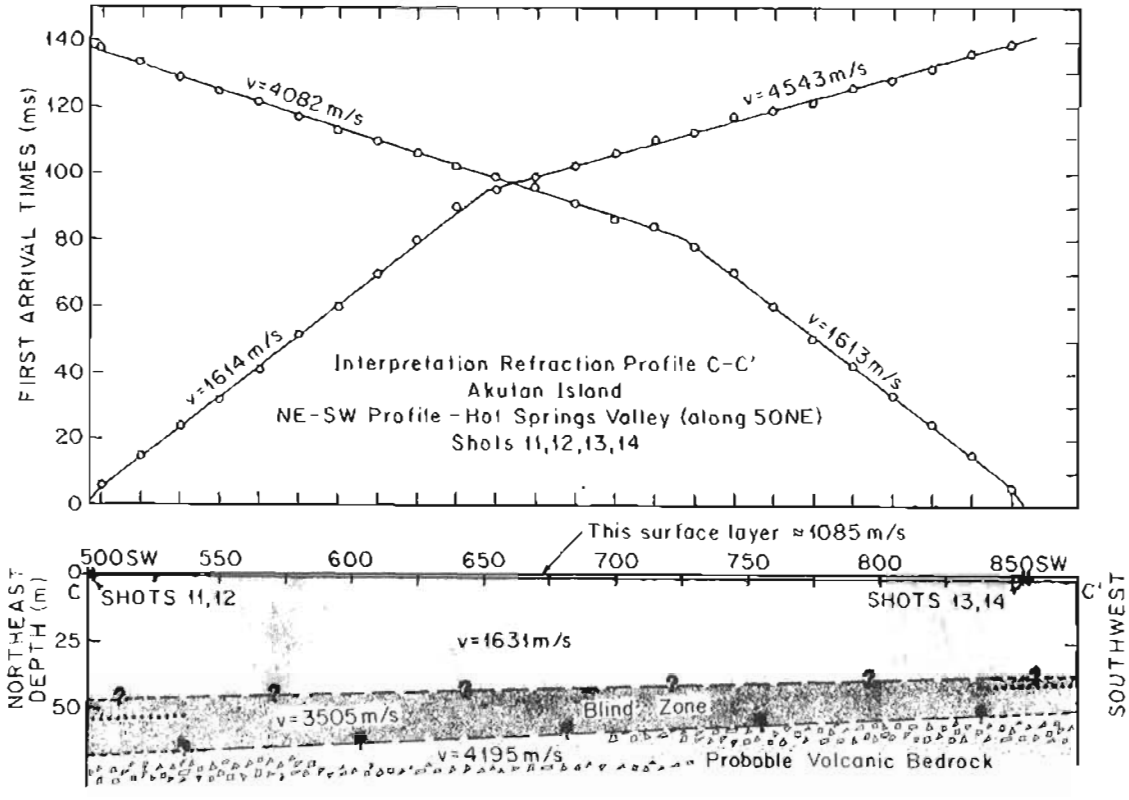

Figure 4-13. First arrival travel time curves (above) for seismic profile C-C' (see fig. 4-10 for location of seismic line) and interpreted cross section. The v = 3,505 m/s layer is inferred to be a hidden layer which could not be detected in the first arrival travel time data. Dotted lines near each end of profile show zero thickness hidden layer interface.

interpreted as a hidden layer in profiles A-A' and C-C'. The unit has low resistivity extending from the northwest valley side to near the valley center, and probably is a reservoir for hot or saline waters. Its velocity is at the upper 80 percent fiducial limit for sandstones and shales and falls at the center of the velocity distribution characteristic of limestone and dolomite, but is less than the 80 percent fiducial limit of granitic and metamorphic rocks (Grant and West, 1965); thus, the unit would appear to be a fairly rigid rock. It has a velocity slightly lower than that found by Wescott and others for the Unalaska formation under Summer Bay valley on Unalaska (unpublished data).

The basal layer with a velocity of 4,900 m/s is obviously a much more solid rock than those lying above it. The resistivity data show that the basal unit is higher in resistivity than the low resistivity unit. The unit's velocity falls near the center of the velocity distribution of granitic and metamorphic rocks (Grant and West, 1965). The basal layer could

also be an intrusive rock, a volcanic flow, a pyroclastic flow, or a well-cemented volcanic debris flow. Kienle (personal commun.) investigated seismic velocities on Augustine Volcano, Alaska, and found a unit with a similar velocity to be a sedimentary rock cemented with zeolites, presumably from hydrothermal activity.

SUMMARY AND DISCUSSION OF GEOPHYSICAL SURVEYS

Figure 4-14 shows three-dimensional perspective cross sections of the lower valley and presents a composite model of the seismic and resistivity data.

The near-surface conductivity (reciprocal resistivity) measurements show a narrow sinuous pattern about 1,500 m long near the northwest side of the valley. Assuming that there is excellent correlation between conductivity and temperature, the anomaly pattern shows where hot water occurs near the surface. No other zones of anomalous near-surface conductivity were found farther up the valley or towards the southeast part of the valley. The surface layer observed in the valley, particularly southwest of the dune near 0 m southwest, is composed of a volcanic debris flow with inferred low porosity and permeability.

For hot water to rise through this low permeability cap layer, a zone of higher permeability or a fracture system must exist. The sinuous form of the near-surface conductivity anomaly suggests the high permeability zone could be a buried stream channel.

Deeper electrical resistivity measurements with Schlumberger vertical electric soundings have led to a multi-layer resistivity model. A 2-10-m-thick near-surface layer of moderate resistivity (120 ohm-m), is underlain by a thicker (12-55 m) layer of 20-70 ohm-m resistivity which becomes thicker toward the center of the valley. This is underlain by a low resistivity layer (4.2-12 ohm-m). The depth to basement ranges from 36 m near springs C and D to 94 m near the northeast-southwest 0 baseline. The basement layer has a resistivity ranging from 514 to 1,524 ohm-m.

Motyka and others (this report) present evidence that the thermal spring waters are a complex mixture of high-enthalpy thermal waters ascending from deeper levels, low-enthalpy thermal waters derived from a shallow reservoir, and cold meteoric waters. The low-enthalpy thermal waters residing in the shallow reservoir are thought to have formed as a result of mixing of infiltrating cold meteoric waters with a portion of the ascending high-enthalpy thermal waters. The temperature of the parent thermal water is estimated to be 200°C, whereas that of the cold water fraction is estimated to be 10°C. The zone of mixing is inferred to be the region of low resistivity underlying the northwest corner of the valley (fig. 4-14), with the resulting mixed water in the shallow reservoir varying in temperature between the two end members. The higher resistivity on the southeast side of the reservoir may be due to cold water entry from that side.

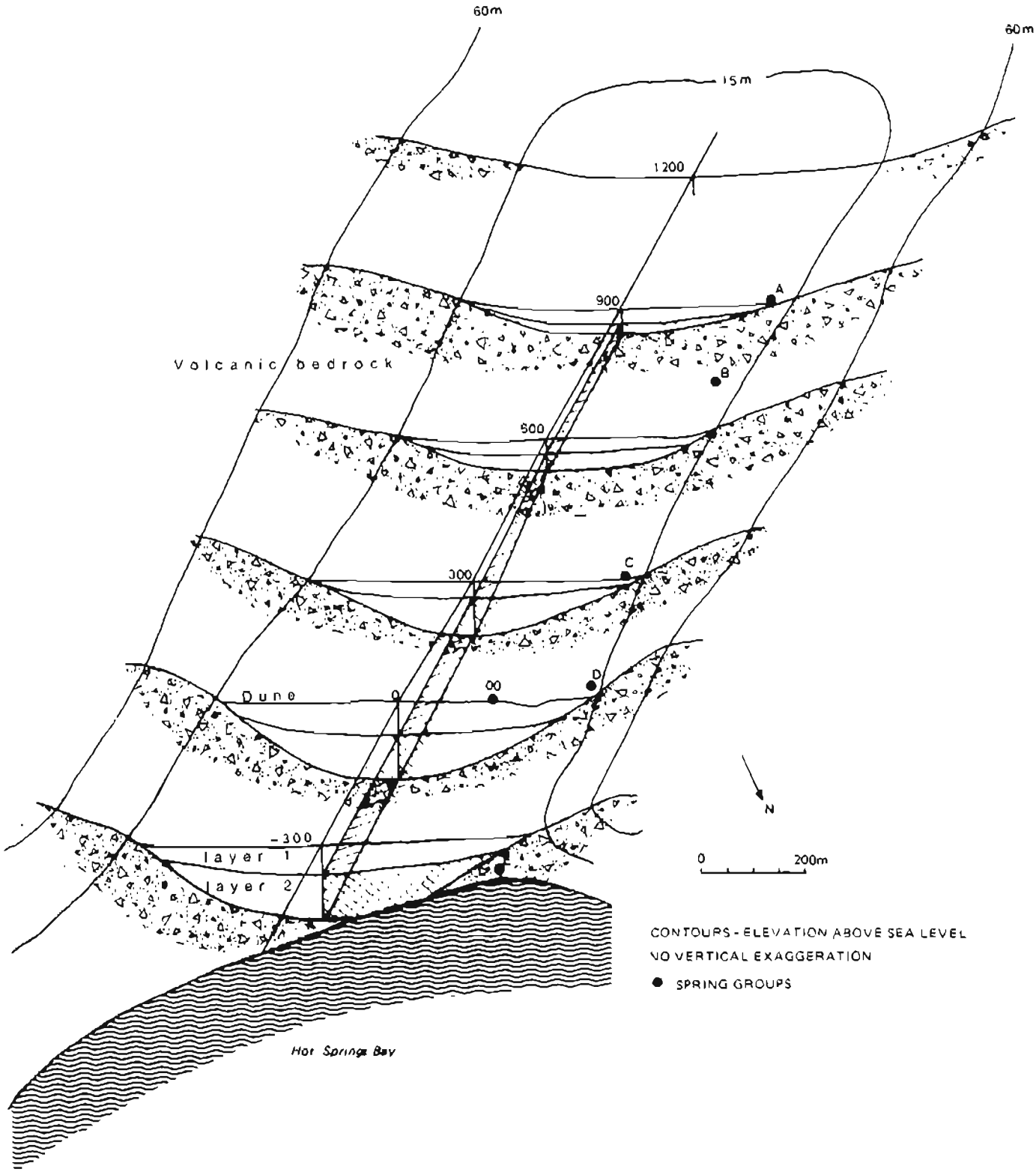

Figure 4-14. Composite cross sections showing the shallow geothermal reservoir (cross-hatched) proposed from the combination of electrical resistivity and seismic data.

By the general form of Archie's Law, the fractional porosity (Ø) of a rock can be estimated by:

$$\phi = (\rho_w/\rho_a)^{\frac{1}{2}} \qquad (4\text{-}2)$$

(Telford and others, 1976), where ρ_w is the resistivity of the formation water and ρ_a is the apparent resistivity of the bulk rock. Using the 25°C resistivity of hot spring A water, 5.63 ohm-m (Motyka and others, chap. 6, this report), the calculated resistivity of the formation water, assuming an average temperature of 100°C, is 1.96 ohm-m. Using the reservoir layer resistivity values from VES 1 and 2, of 7 and 10.5 ohm-m, respectively, the estimated porosity of the layer ranges from 43 to 53 percent. These estimates do not include the possible contribution to the resistivity of clay minerals, which would lower the calculated porosity. Keller and Frischknecht (1966) show the normal range of post-Paleozoic clastic volcanics as 10-60 percent porosity. The other important factor, permeability, cannot be estimated from the available data.

For the basement rock, using 1.53 ohm-m for the hot water resistivity, and a resistivity of 514 to 1,524 ohm-m, the estimated porosity is three to five percent.

The 100-m dipole-dipole survey produced a similar model differing somewhat in depths and resistivity. One- and two-dimensional interpretations suggest a cap rock of resistivity about 100 ohm-m and thickness of 40-70 m underlain by a reservoir layer of resistivity 3 ohm-m and perhaps having a base 150 m deep in the center of the valley. The basement resistivity was modelled using a value of 1,500 ohm-m.

Although no computer models were produced for the long northeast-southwest pseudo-section 2, it appears from the data that the reservoir layer thickens toward the northeast and thins up the valley to the southwest. From the geophysical measurements it cannot be determined whether this is an effect of the thickening of the reservoir layer to the northwest or whether there is saltwater intrusion from the ocean. R.F. Black (personal commun., 1982) argues in favor of hot water as the cause for the zone of low resistivity, stating that, "In the Aleutians, in general, sufficient precipitation occurs and enough hydraulic head is available to keep salt water out of most valleys."

The basement layer, presumed to be an extension of the Hot Springs volcanic sequence exposed in the valley walls, has high resistivity and a surface which dips toward the center of the valley and to the northeast toward the mouth of the valley. These inclinations suggest that the basement surface was glaciated into a U-shape prior to filling the valley with till, glaciofluvial deposits, debris flows and other sediments.

The seismic refraction profiling agrees fairly well with the resistivity data although the interpretation of two of the three profiles is complicated by the hidden layer problem. Three layers are inferred to exist. The uppermost layer, disregarding the shallow weathered horizon, has a range in velocity from 1,610 to 1,960 m/s and in thickness from 31 to 45 m. This layer

corresponds to the upper layer of medium resistivity seen by the resistivity measurements. The second layer, which is inferred as a hidden layer in two of the profiles, has a velocity of 3,240-3,505 m/s and corresponds to the low resistivity reservoir layer. Bedrock, with the relatively high velocity of 4,900 m/s, could be composed of volcanic debris flows or volcanic flows, intrusive rock, or possibly a well-cemented sedimentary or pyroclastic unit. The possible occurrence of hydrothermal cementation is consistent with a high-temperature deep reservoir predicted by water geochemistry (Motyka and others, chap. 6, this report).

The geophysical data cannot delineate a conduit system bringing the hot water up into the reservoir layer. Although the expression of near-surface hot water occurs in a sinuous pattern, suggesting a buried stream channel, the hot water may be entering the reservoir elsewhere.

REFERENCES CITED

Apparao, A., and Roy, A., 1973, Field results for direct-current resistivity profiling with two-electrode array: Geoexploration, v. 11, p. 21-44.

Campbell, D.L., 1981, Four or fewer dipping seismic refractors: Interpretation, in Geophysical hand calculator programs manual, HP volume: Society of Exploration Geophysics, SE 15 13-C.

Dey, A., and Morrison, H.F., 1975, Resistivity modelling for arbitrarily shaped two dimensional structures: Engineering Geoscience and Lawrence Berkeley Laboratory, University of California, p. 1-54.

East, J.S., 1982, Preliminary geothermal investigations at Manley Hot Springs, Alaska: University of Alaska, Geophysical Institute Report UAG R-290, 76 p.

Fox, R.C., Hohmann, G.W., and Rijo, L., 1978, Topographic effects in resistivity surveys: University of Utah Research Institute, Salt Lake City, report IDO/78-1701.b.3.2.1, p. A30-A38.

Grant, F.S., and West, G.F., 1965, Interpretation theory in applied geophysics: McGraw-Hill Book Co., New York, p. 8.

Hawkins, L.V., and Maggs, D., 1961, Nomograms for determining maximum errors and limiting conditions in seismic refraction survey with a blind-zone problem: Geophysical Prospecting, v. IX(4), p. 526-532.

Keller, G.V., and Frischknecht, F.C., 1966, Electrical methods in geophysical prospecting: Pergamon Press, New York, p. 492-493.

Motyka, R.J., Moorman, M.A., and Liss, S.A., 1981, Assessment of thermal spring sites, Aleutian Islands, Atka Island to Becherof Lake: Preliminary results and evaluation, Alaska Division of Geological and Geophysical Surveys Open-file Report 144, 175 p.

Osterkamp, T.E., Kawasaksi, Koji, and Gosink, J.P., 1983, Shallow magnetic induction measurements for delineating near-surface hot groundwater sources in Alaskan geothermal areas: Journal of Energy Resources Technology, v. 105, (2), p. 156-161.

Telford, W.M., Geldart, L.P., Sheriff, R.E., and Keys, D.A., 1976, Applied Geophysics: Cambridge University Press, London, p. 445.

Turner, D.L., and Forbes, R.B., 1980, eds., A geological and geophysical study of the geothermal energy potential of Pilgrim Springs, Alaska: Report UAGR-271, Geophysical Institute, University of Alaska, Fairbanks, Alaska, p. 113-135.

Wescott, E.M., and Turner, D.L., 1981, A geological and geophysical study of the Chena Hot Springs geothermal area, Alaska: Report UAG R-283, Geophysical Institute, University of Alaska, Fairbanks, Alaska, p. 31-42.

Zhody, A.R., 1974, A computer program for the automatic interpretation of Schlumberger sounding curves over horizontally stratified media: U.S. Geological Survey Report GD-74-017, p. 232.

CHAPTER 5

HELIUM AND MERCURY SOIL SURVEYS HOT SPRINGS BAY VALLEY, AKUTAN ISLAND, ALASKA

by

Eugene M. Wescott, Donald L. Turner, William Witte,
and Becky Petzinger

Geophysical Institute, University of Alaska-Fairbanks,
Fairbanks, Alaska 99775

INTRODUCTION

Concentrations of helium and mercury in soil and in water have been shown to be useful indicators of geothermal resources (Roberts, 1975; Roberts and others, 1975; Bergquist, 1980; Matlick and Buseck, 1975). In Alaska, helium and mercury surveys have shown excellent correlations with areas of upwelling of geothermal waters in the Chena Hot Springs area (Wescott and Turner, 1981a), at Pilgrim Springs (Wescott and Turner, 1981b), Summer Bay Warm Springs, Unalaska Island (Wescott and Turner, 1982; Republic Geothermal Inc., 1983), and Manley Hot Springs (East, 1982).

HELIUM SURVEY

The radioactive decay of uranium and thorium is the source of helium in the earth. Helium is chemically inert, physically stable, and quite soluble in ground water at depth, but sparingly soluble under typical near-surface conditions. Helium is practically nonabsorbable, highly mobile in geologic materials and is able to penetrate thousands of meters of overburden. Helium is present in the atmosphere at a low, yet spatially and temporally constant, abundance level of 5.239 ppm (Glueckauf, 1946; Pogorski and Quirt, 1981). The solubility of helium in water increases with temperatures above 30°C, making geothermal waters efficient scavengers of helium (Mazor, 1972). As the geothermal waters rise towards the surface, helium is released as a result of cooling and de-pressurization of the water.

Helium occurs in soil in several ways: a) trapped in the crystal lattice of soil grains; b) as gas in macro or intercrumb pore spaces; c) dissolved in the water film on soil grains; d) in micro or crumb pore spaces; e) in gas bubbles in the soil fluid; and f) dissolved in water (Pogorski and Quirt, 1981).

Helium in macro or intercrumb pore spaces was sampled by driving a hollow collection tube about 75 cm into the ground and drawing off a gas sample in a syringe. The gas was then introduced into a small evacuated steel cartridge and sealed. This technique works well only where the soil is fairly dry and free of rocks. Helium in water films on soil grains, in micro or crumb pore spaces, and in bubbles in water-filling pore spaces, was sampled by augering a soil core sampler about 75 cm into the ground, placing the bottom soil core in a steel can and sealing it.

Water samples were collected in a 500 ml sample bottle to 85 percent of volume and capped immediately with an airtight cap equipped with a septum. The bottle was shaken vigorously for 30 seconds to allow the helium dissolved in the water to equilibrate with the air space above the water, then a gas sample was drawn off by syringe through the septum and inserted into an evacuated steel cartridge as in the soil gas sampling technique. In the case of soil samples, a gas sample is drawn off from the head space in the can after sufficient time has elapsed to allow the helium in the soil to equilibrate with the air in the head space.

The helium analyses were done at Western Systems, Inc., Morrison, Colorado, by mass spectrometry accurate to 0.05 percent with a precision of ±10 ppb.

Research in the past few years has shown that helium concentration values derived from the three separate sampling methods are not simply related (Turner and Wescott, 1982; Wescott and Turner, 1985). Helium concentrations in samples derived from water are usually much higher than concentrations in soil head space or soil gas samples. In order to derive pore space concentration, soil head space concentrations must be corrected for a number of parameters: soil and air temperature, barometric pressure at the time of collection, and water content and soil density. In addition, light hydrocarbons may be generated in the soil by bacterial action after canning. The formation of gas by bacterial action after the canning must be corrected, as it alters head space pressure and therefore the equilibrium helium content in the head space, causing dilution of the helium. Only raw, uncorrected helium concentration values were used in the analysis of data from Hot Springs Bay valley; however, Wescott and Turner (1985) have shown that anomalously high raw helium values represent valid anomalies regardless of whether the corrections discussed above are made.

The average atmospheric concentration of helium is 5.239 ppm (Glueckauf, 1946). Depending on the production rate, transport rate, and soil trapping efficiency, the background pore space He concentration may vary somewhat from that value.

Aleutian basaltic and basaltic-andesitic rocks are likely to contain much less uranium and thorium than the more acidic igneous and metamorphic rocks of the interior Alaska and Seward Peninsula hot springs areas. Telford and others (1976) state that basalts, on average, have 13 percent of the Th and 15 percent of the U that is contained in granites. Thus we would expect helium anomalies in the Aleutians to be less pronounced than in other areas, and this can be illustrated by comparing the helium-concentration values obtained from four Akutan hot spring water samples with values obtained from Manley Hot Springs in the Alaskan interior. The Akutan water samples are about 22 percent above the atmospheric background: 6.56, 6.41, 6.57, and 6.05 ppm. In comparison, water samples from Manley Hot Springs at 30 ppm are 573 percent above background, consistent with the higher He production rate in the acidic plutonic and metamorphic rocks of that area (East, 1982). This result supports our suggestion that significant He anomalies on Akutan should be of less magnitude than anomalies at Manley Hot Springs or other similar Alaskan geothermal areas.

Figure 5-1 shows an enlarged portion of Hot Springs Bay valley with helium soil head-space sample concentrations and the 25- and 10-ohm-m near-surface EM-31 resistivity contours. Soil gas samples are not shown because the two types of helium sample data cannot be directly compared.

To allow for the variability of duplicate soil measurements, the variations in sampling conditions, and correction factors not included in this analysis, a soil He value of 5.40 ppm and above is defined as anomalous.

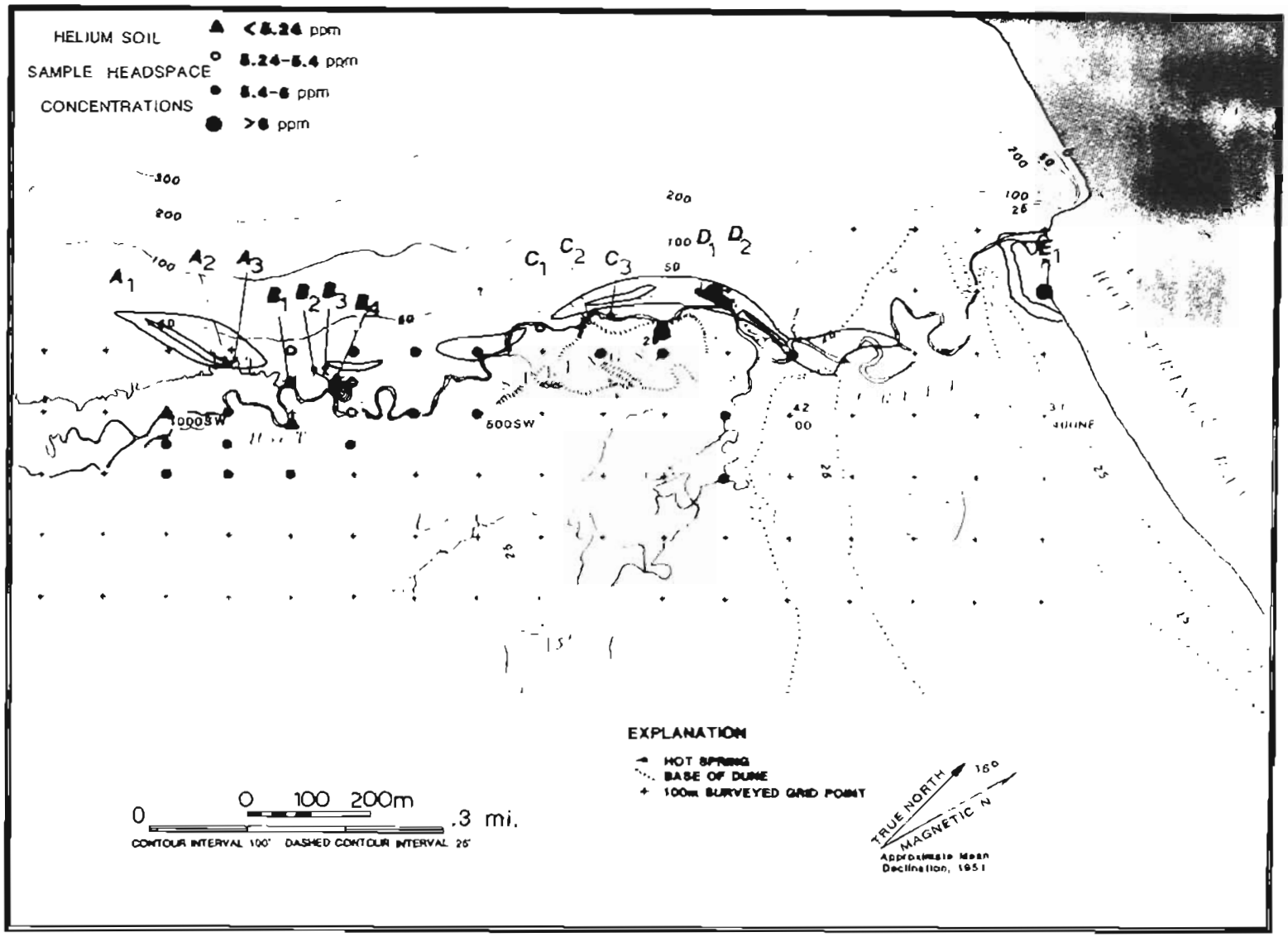

Figure 5-1. Map of Hot Springs Bay valley showing helium soil sample locations and head-space concentrations. Contours are 25 ohm-m and 10 ohm-m near-surface resistivity values from Wescott and others (this report). Anomalous concentrations occur near valley center, as well as at hot springs.

Compared to other Alaskan localities with higher U and Th backgrounds, this is a conservative value. As can be seen in figure 5-1, most of the samples are anomalous by this criterion. Several are greater than 6.0 ppm. Note that the anomalous He values extend several hundred meters towards the center of the valley away from the hot springs and the near-surface low resistivity contours.

The pattern of helium anomalies is probably distorted by the production of other gases in the organic-rich marsh. Of three samples collected which were below the atmospheric concentration of 5.24 ppm, the lowest was 4.84 ppm. Friedman (personal commun., 1981) has found similar anomalously low helium values in other surveys, and has ascribed this phenomenon to dilution of the helium content of the soil gas by other gases such as CH_4 and CO_2. Thus, since some sample sites show anomalously low values below the atmospheric value of 5.24 ppm, others which are above 5.24 ppm may also have been affected by dilution. Because the sample analysis did not include other gases, such as CO_2 and CH_4, corrections for this effect cannot be made. The effect of such a correction would only increase the magnitude of the observed anomalies.

MERCURY SURVEY

Mercury content in soils has been reported as a possible indicator of geothermal resources. Matlick and Buseck (1975) confirmed a strong association of Hg with geothermal activity in three of four areas tested (Long Valley, California; Summer Lake and Klamath Falls, Oregon). Mercury deposits often occur in regions containing evidence of hydrothermal activity, such as hot springs (White, 1967).

Mercury is highly volatile; indeed, the high mobility of Hg makes it unique among heavy metals (McNerney and Buseck, 1973). Its high vapor pressure makes it extremely mobile, and the elevated temperatures near a geothermal reservoir tend to increase this mobility. The Hg migrates upwards and outwards away from the geothermal reservoir; such aureoles are typically larger in area than corresponding geothermal helium aureoles.

Soil samples were collected at 15 locations at depths of about 10 cm below the bottom of the organic layer. The samples were air dried in the shade and sized to -80 mesh using a stainless steel sieve. The -80 mesh portions were stored in airtight glass vials for later analysis. The Hg content of each sample was determined by use of a Jerome Instrument Corp., model 301 Gold Film Mercury detector with detection limit of 0.1 nanogram of Hg. A standard volume of -80 mesh soil (0.25 cc) was placed in a quartz bulb and heated for one minute to volatilize absorbed Hg, which was then collected on a gold foil. Heating of the gold foil released the Hg for analysis as a gas in the standard manner. Calibration was accomplished by inserting a known concentration of Hg vapor with a hypodermic syringe.

The background concentration of Hg in soils varies widely from area to area, and must be determined from a large number of samples. It is generally on the order of 10 parts per billion (ppb) (Matlick and Buseck, 1975). A mean value of 139 ppb was calculated for the 15 samples collected at Hot

Springs Bay valley. The mean value was selected as the criterion for defining anomalous occurrences of Hg.

Republic Geothermal, Inc., conducted a mercury soil survey on Makushin Volcano, Unalaska Island, as part of their exploration for geothermal drilling sites (Republic Geothermal, 1983). They found an analytical range of 8-31,450 ppb for 230 soil samples, with an average value of 454 ppb, a median value of 60 ppb and a mode of 36 ppb. In their analysis, they defined 36 ppb as the background value, and contoured the data with contour interval of 3 x background (108 ppb), 5 x background (180 ppb), and 7 x background (324 ppb).

Figure 5-2 is a map of Hot Springs Bay valley with Akutan Hg values plotted on the grid system. One of the largest values of 395 ppb is at 0 NW, 100 S, several hundred meters away from the near-surface temperature anomalies. A definitive statement regarding the Hg pattern cannot be made because the grid system was not completely sampled. Most samples collected during this investigation for Hg are above the Makushin Volcano background level, and three are greater than seven times the Makushin background level.

DISCUSSION AND CONCLUSIONS

Compared to other geothermal areas where He and Hg soil concentrations have been investigated, values in Hot Springs Bay valley are anomalously high. Water sampling data yield low He values compared to Alaska continental hot springs areas, which increases the importance of the He soil anomalies. The mercury data are not sufficiently abundant to draw detailed conclusions. Compared with the Makushin Volcano surveys (Republic Geothermal, 1983) the data indicate that significant anomalies may be present.

High helium and mercury values are found both toward the center of the valley and near the hot springs and the sinuous near-surface, low resistivity patterns. Wescott and others (chap. 4, this report), have suggested the sinuous pattern represents a buried stream channel of high porosity and permeability which allows hot water to come up through the volcanic debris flow. Helium and mercury data are the only data which might indicate where the hot water from below is entering the shallow subsurface region. These data suggest the shallow subsurface region may be fed from a conduit system farther out into the valley than the buried stream channel. Additional mercury soil sampling of the Hot Springs Bay valley grid would help target a drill site for delineation of the conduit system.

REFERENCES CITED

Bergquist, L.E., 1980, Helium: An exploration tool for geothermal sites: Geothermal Resources Council Transactions, v. 3, p. 59-60.

East, J., 1982, Preliminary investigations at Manley Hot Springs, Alaska: University of Alaska, Geophysical Institute Report UAG R-290, p. 52-65.

Glueckauf, E., 1946, A micro-analysis of the helium and neon contents of air: Proceedings of the Royal Society of London, v. 185, p. 98-119.

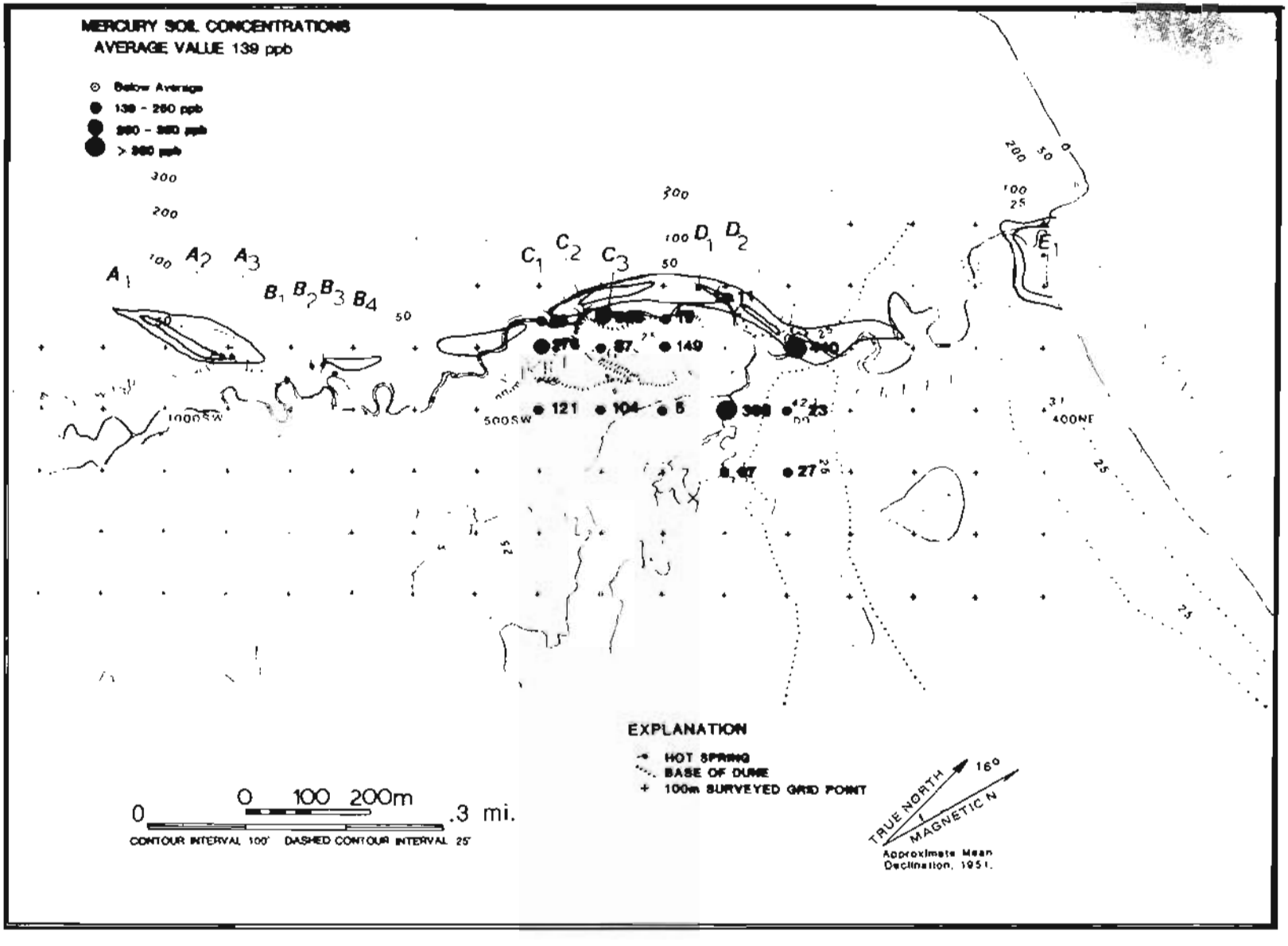

Figure 5-2. Map of Hot Springs Bay valley showing mercury soil sample locations and concentrations. The contours are 25 ohm-m and 10 ohm-m near-surface resistivity values from Wescott and others (this report). Anomalous concentrations occur in the central valley, as well as near hot springs.

Matlick, J.S., III, and Buseck, P.R., 1975, Exploration for geothermal areas using mercury: a new geochemical technique: in Proceedings, Second United Nations Symposium on the development and use of geothermal resources, v. 1, p. 785-792.

Mazor, E., 1972, Paleotemperatures and other hydrological parameters deduced from noble gases dissolved in groundwaters: Jordan Rift Valley, Israel, Geochimica et Cosmochimica Acta, v. 36, p. 1321-1326.

McNerney, J.J., and Buseck, P.R., 1973, Geochemical exploration using mercury vapor, Economic Geology, v. 68, pp. 1313-1320.

Pogorski, L.A., and Quirt, G.S., 1981, Helium emanometry in exploring for hydrocarbons: Part 1, Unconventional methods in exploring for petroleum and natural gas II, Benjamin M. Gottlieb, ed., SMU Press, Dallas, Texas, p. 124-135.

Republic Geothermal, 1983, The Unalaska Geothermal Exploration Project, Phase 1B, Final Report: Alaska Power Authority, v. 1, p. 29-36.

Roberts, A.A., 1975, Helium surveys over known geothermal resource areas in the Imperial Valley, California: U.S. Geological Survey Open-file Report, p. 75-427, 6 sheets.

Roberts, A.A., Friedman, I., Donovan T.J., and Denton, E.H., 1975, Helium survey, a possible technique for locating geothermal reservoirs: Geophysical Research Letters, 2 (6), p. 209-210.

Telford, W.M., Geldart, L.P., Sheriff, R.E., and Keys, D.A., 1976, Applied Geophysics: Cambridge University Press, London, p. 745.

Turner, D.L., and Wescott, E.M., 1982, A preliminary investigation of the geothermal energy resources of the lower Susitna Basin: University of Alaska, Geophysical Institute Report UAG R-287, 50 p.

Wescott, E.M., and Turner, D.L., 1981a, A geological and geophysical study of the Chena Hot Springs geothermal area, Alaska: University of Alaska, Geophysical Institute Report UAG R-283, p. 54-61.

Wescott, E.M., and Turner, D.L., eds., 1981b, Geothermal reconnaissance survey of the central Seward Peninsula, Alaska: University of Alaska, Geophysical Institute Report UAG R-284, p. 37-59.

Wescott, E.M., and Turner, D.L., 1982, Geothermal energy resources assessment of parts of Alaska: Final report to the Division of Geothermal Energy of U.S. DOE, under cooperative agreement DE-FC07-79-EI-27034, p. 44-46.

Wescott, E.M., and Turner, D.L., eds., 1985, Geothermal energy resource investigations in the eastern Copper River Basin, Alaska: University of Alaska, Geophysical Institute Report UAG R-302, 158 p.

White, D.E., 1967, Mercury and base-metal deposits with associated thermal and mineral waters: in Barnes, H.L., ed., Geochemistry of hydrothermal ore deposits, New York, Holt, Rinehart, and Winston, p. 575-631.

CHAPTER 6

GEOCHEMISTRY OF THERMAL SPRINGS AND FUMAROLES, HOT SPRINGS BAY VALLEY AKUTAN ISLAND, ALASKA

by

Roman J. Motyka[1], Mary A. Moorman[2], and Robert J. Poreda[3]

[1]Alaska Division of Geological and Geophysical Surveys, 400 Willoughby Ave., 3rd floor, Juneau, Alaska 99801
[2]Alaska Division of Geological and Geophysical Surveys, 794 University Ave., Suite 200, Fairbanks, Alaska 99709
[3]Isotope Laboratory, Scripps Institution of Oceanography, University of California, La Jolla, California 92037 (current address: Department of Geology, University of Rochester, Rochester, New York 14627)

INTRODUCTION

Investigations of fluids associated with the thermal springs and fumarole field located in Hot Springs Bay valley were undertaken to help assess the nature and extent of the underlying hydrothermal system, and to provide estimates of reservoir temperatures. Reconnaissance visits of the springs were made by Byers and Barth (1953), Baker and others (1977), and Motyka and others (1981). The latter study provided the impetus for selecting Akutan for the more detailed geothermal exploration which was carried out during July 1981. The springs and fumaroles were sampled once again during a one-day visit to the site on August 31, 1983.

THERMAL AREAS

The Akutan hot springs are located in lower Hot Springs Bay valley, about 4 km northwest of Akutan Harbor and 10 km northeast of Akutan volcano (fig. 6-1, sheets 1 and 2). Five separate groups of thermal springs emanate along Hot Springs Creek in a 1.5-km-long zone at the base of the west valley wall. The thermal spring waters issue from fissures in travertine-cemented volcanic debris-flow deposits exposed in stream banks (groups A, C, and D), from pools in the valley floor (groups A, B, and D), and through beach sands (group E).

The hottest springs are the southernmost, group A, with temperatures as high as 85°C. Temperatures at group B, which consists of several shallow pools, ranged from 38.5° to 50°C. Vent temperatures at group C ranged from 40° to 75°C, while vent temperatures at group D varied from 26° to 54°C. The most northerly group, group E, occurs on the shores of Hot Springs Bay in the intertidal zone east of the mouth of Hot Springs Creek (fig. 6-1). Temperatures greater than local surface waters were found at depths of 10 cm or more in the sands over a 2,500 m^2 area of intertidal beach; the highest temperatures (63°C) were adjacent to the outflow channel of Hot Springs Creek.

Temperature measurements in creek-bed gravels and analyses of chemical concentrations in stream waters showed that thermal waters also discharge directly into Hot Springs Creek and its western tributary. The stream bed of the west fork above group A measured 75.0°-83.2°C just a few cm below ground surface. Warm temperatures were also measured in gravel bars adjacent to groups C and D.

Thermal waters from springs A_1, A_2, and A_3 flow at 40, 51, 118 liters per minute (lpm), respectively, directly into the west fork channel of Hot Springs Creek. Direct measurements of individual spring discharges were not possible at other spring sites. Visual estimates of flow rates for group B were ~40 lpm, group C, ~10-20 lpm, group D ~50 lpm and group E, ~20 lpm.

A fumarole field occurs at an elevation of 350 m (1,150 ft), near the head of Hot Springs Bay valley about 3.5 km southwest of the lower valley thermal springs (sheet 1). The field consists of a series of low- to moderately-pressurized fumaroles, mildly steaming ground, and boiling acid-sulfate springs covering an area of about 5,000 m^2. Temperatures of the fumaroles

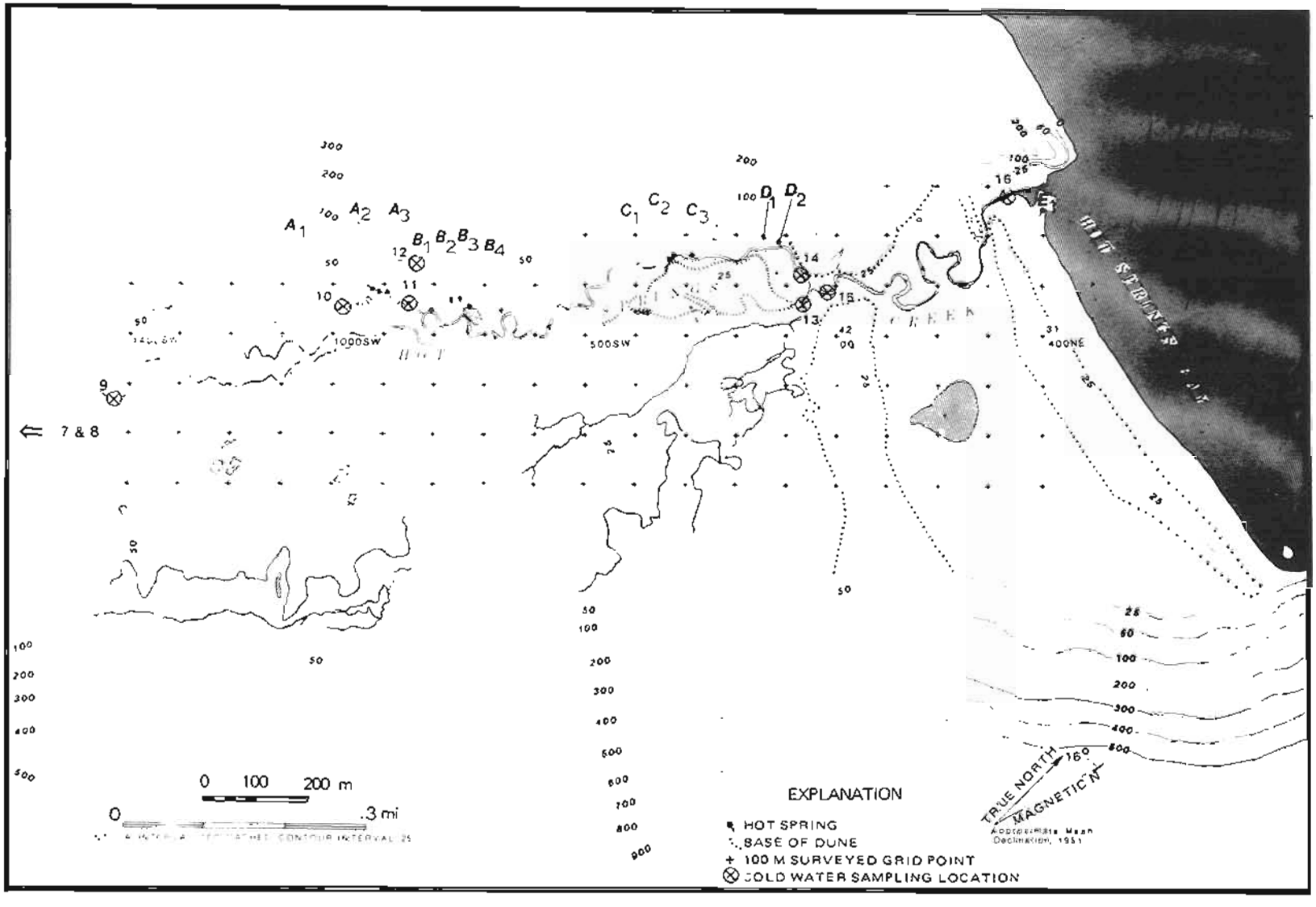

Figure 6-1. Thermal springs and stream water sampling locations in lower Hot Springs Bay valley. Sample locations 7 and 8, not shown on map, lie at the head of the valley approximately 2 and 2.5 km, respectively, from location 9.

and pools are at or near atmospheric boiling point. An aureole of argillic alteration surrounds the fumarole field.

A reconnaissance was made of the rest of the island, and visible thermal activity elsewhere appeared restricted to the active Akutan caldera and a still-warm 1978 andesitic lava flow on the north flank of the volcano.

METHODS

Samples of thermal spring waters were collected as close as possible to the issuing vent and filtered through 0.45 micron filters. The sample suite normally consisted of one liter each of filtered untreated and filtered acidified (HCl) waters, 100-ml 1:10 and 1:5 diluted samples for silica determinations, and 30-ml samples for stable isotope determinations. Additional untreated, unfiltered samples were collected for field determinations of HCO_3^-, pH, and H_2S. At spring A_3, one liter of filtered water was collected and treated with formaldehyde for $\delta^{18}O$, H_2O-SO_4 geothermometry, and one liter of untreated water was collected for tritium analysis. Representative stream and cold spring waters were also collected.

HCO_3^-, pH, and H_2S concentrations were determined in the field following methods described in Presser and Barnes (1974). The remaining constituents were analyzed at the DGGS laboratory facilities in Fairbanks except as noted in tables 6-1 and 6-2. Major and minor cation concentrations were determined using a Perkin-Elmer atomic absorption spectrometer following standard procedures outlined in Skougstad and others (1979) and in the manufacturer's manual. Sulfates were determined by the titrimetric (thorin) method; fluorides by specific ion electrode; chlorides by Mohr titration; bromides by hypochlorite oxidation and titration; and boron by colorimetric carminic acid method. Silica concentrations were determined by the molybdate blue method.

Stable isotope ratios ($^{18}O/^{16}O$ and D/H) were analyzed at Southern Methodist University, Dallas, Texas, and at U.S. Geological Survey, Menlo Park, California. Tritium concentrations were determined at the University of Miami, Miami, Florida.

Gases emanating from the fumarole field and from the lower valley hot springs were collected in 1981; fumarole gases were sampled again in 1983 during a one-day reconnaissance visit. Fumarole samples were collected by placing a plastic funnel over a pressurized vent and packing the exterior with mud to prevent air contamination. The funnel was connected with tygon tubing to a 300-ml flask charged with 50 ml of sodium hydroxide. The sampling line was purged of atmospheric air, the stopcock in the flask opened and gases allowed to bubble through the sodium hydroxide solution. Carbon dioxide and sulfur gases are absorbed by the sodium hydroxide, allowing trace gases to concentrate in the headspace of the flask. Gases from hot springs were sampled in a similar manner, except that the funnel was first immersed in a pool over a train of bubbles. Hot spring gas samples were taken by allowing the gases to displace water in the funnel, then collecting the gas in the evacuated flask.

Gases collected in 1981 were analyzed at DGGS, Fairbanks, and at the Scripps Institution of Oceanography, La Jolla, where helium isotope ratio ($^3He/^4He$) were determined. The samples collected in 1983 were analyzed at DGGS, Fairbanks, and at U.S. Geological Survey, Menlo Park, where carbon isotope ratios ($^{13}C/^{12}C$) in carbon dioxide were determined. Residual gases, that is, gases not absorbed by the sodium hydroxide solution (He, H_2, Ar, O_2, N_2, and CH_4) were analyzed on a dual-column gas chromatograph with both argon and helium carrier gases. Moles of residual gas were calculated from measured gas pressure and headspace volume. Carbon dioxide and hydrogen sulfide concentrations in the sodium hydroxide solutions were determined by titration and by ion chromatography, respectively, or by gravimetric methods using $SrCl_2$ and $BaCl_2$ to precipitate $SrCO_3$ and $BaSO_4$. A reaction of the $SrCO_3$ precipitate with phosphoric acid was used to determine carbon dioxide yield. The evolved gas was saved and analyzed for carbon isotope ratios. Steam content of the gases was determined by weight difference before and after sampling. Ammonia was analyzed by specific ion electrode method.

Adjustments were made for headspace gases dissolved in the solution using Henry's Law. Moles of each constituent collected were determined and the mole percent of each constituent was calculated. A correction was made for air contamination by using the ratio of oxygen in the sample to oxygen in air. The gas concentrations in mole percent were recalculated on an air-free basis.

The procedures used to determine helium isotope ratios and apply air corrections based on He/Ne ratios can be found in Poreda (1983).

WATER CHEMISTRY

Results of the chemical analyses of thermal spring waters are given in table 6-1; those for stream and cold spring waters are in table 6-2. Thermal spring and stream water sample locations are shown on figure 6-1. (Sample sites 7 and 8 are up-valley, southwest of the area shown in figure 6-1.) Thermal spring waters from groups A through D are moderately concentrated sodium-chloride-bicarbonate waters with significant levels of boron. Thermal waters from group E are much more saline, reflecting probable mixing with seawater in the intertidal zone. As expected, stream and cold spring waters are much more dilute, but several of the samples exhibited relatively high levels of silica; these samples were taken below thermal spring sites and probably reflect influx of thermal waters.

The percentage cation content of Hot Springs Bay valley thermal and surface waters are plotted in figure 6-2. The seawater influence on group E spring waters (sample 6) is readily apparent, as is the dilution of thermal waters with cooler surface waters at group D. The Na + K trend in stream waters reflects the sampling of stream waters up-valley of the thermal springs sites and above, near, and below individual thermal spring groups.

Thermal waters associated with the fumarole field at the head of the valley are acid-sulfate waters. The sulfate-dominated anion water chemistry is a result of dissolution of hydrogen sulfide gas in surface meteoric runoff and condensed fumarolic steam (table 6-1). The cation constituents in these

Table 6-1. Chemical and stable isotope analyses[a] of thermal waters from Hot Springs Bay valley, Akutan Island, Alaska. Values in mg/l unless otherwise specified.

	Sample[b]							
	1	2	*	3	4	5	6	Fum acid spr
Na	323	328	384	172	207	128	1660	17.0
K	28	26	26	16	16	9.3	74	3.5
Ca	12	12	12.5	15	18	11	130	32
Mg	0.9	1.0	0.9	1.5	1.6	12	320	13
Li	1.3	1.2	1.2	0.61	0.61	0.34	1.1	0.01
Sr	0.11	0.12	nd	0.10	0.22	0.09	1.2	0.05
HCO_3[c]	172	nd	89	116	118	128	161	nd
SO_4	43	41	54	22	43	26	495	1300
F	1.1	0.9	1.1	0.6	1.0	0.9	0.5	<0.1
Cl	420	410	424	220	280	140	3440	5.2
Br	1.3	nd	nd	1.3	0.3	nd	17	nd
I	0.4	nd	nd	0.1	0.6	nd	0.4	nd
SiO_2	145	135	140	103	133	91	121	220
H_2S[c]	0.50	nd	nd	nd	nd	nd	nd	nd
B	11	12	10	5.9	7.0	3.4	4.5	<0.5
Fe	0.05	0.01	nd	0.57	<0.01	0.03	0.04	41
TDS	1080	nd	1100	617	762	481	6350	1630
pH[c]	7.0	nd	8.4	6.4	6.5	6.8	7.3	2.6
T(°C)[c]	84	84	nd	47.4	73.4	58.8	67	92.3
SC[d]	1775	1500	nd	1000	1200	700	11000	3500
Date sampled	08/07/80	07/10/81	08/31/83	07/09/81	07/09/81	08/08/80	07/12/81	07/09/81
$\delta^{18}O$(SMOW)[e]	-9.2[f]	(-10.5)[g]	nd	-10.8	-10.8	-9.2	-8.8	-1.4
δD(SMOW)[e]	nd	-70	nd	-71.5	-71	-69	-59	-39
^3H(TU)	20.3±0.6	nd	nd	nd	nd	nd	nd	nd
Cl/B	38	34	42	37	40	41	764	--

[a] Chemical analyses by M.A. Moorman and R.J. Motyka, DGGS, except as otherwise noted. Isotope analysis by R. Harmon and J. Borthwick, Southern Methodist Univ., Stable Isotope Laboratory, except as otherwise noted. Tritium unit (TU) analysis by H. Goto Ostland, University of Miami, Miami, Florida.

[b] Sample location code: 1 - Hot spring A_3.
2 - Hot spring A_3.
3 - Hot spring B_1.
4 - Hot spring C_4 (upstream and adjacent to C_3).
5 - Hot springs D_2.
6 - Hot spring E.
* - Sample from hot spring A_3 analyzed by D.S. Sheppard, Department of Science and Industrial Research, New Zealand (pH and HCO_3 determined in the laboratory).

[c] Determined in the field.

[d] SC = Specific conductance (µs/cm at 25°C).

[e] SMOW = Standard mean ocean water.

[f] N. Nehring, U.S. Geological Survey, Menlo Park, California.

[g] Suspect value.

nd = not determined.

Table 6-2. Chemical and stable isotope analyses[a] of surface streams in Hot Springs Bay valley, Akutan Island, Alaska. Values in mg/l unless otherwise specified.

	Sample[b]									
	7	8	9	10	11	12	13	14	15	16
Na	6.7	4.1	4.0	9.9	37	7.3	8.6	9.1	9.4	7.3
K	0.3	0.3	0.3	1.1	3.3	<0.1	0.5	0.8	0.7	0.6
Ca	11	5.3	5.3	5.1	6.4	1.1	9.2	6.1	6.4	5.6
Mg	1.9	0.9	0.9	1.8	1.8	2.0	2.0	1.2	1.3	1.2
Li	<0.01	<0.01	<0.01	0.02	0.11	nd	<0.01	0.01	0.01	0.01
Sr	0.05	0.02	0.02	0.02	0.02	nd	0.03	0.02	0.02	0.02
SO_4	4.0	6.0	5.0	<1.0	8.0	2.0	5.0	6.0	6.0	4.0
F	<0.01	<0.1	<0.1	<0.1	<0.1	0.1	<0.1	<0.1	<0.1	<0.1
Cl	6.9	3.2	7.1	11	41	10	9.6	10	10	7.8
SiO_2	8.5	4.2	9.7	23.0	33.0	19.4	17.5	13.2	14.0	12.7
B	<0.5	<0.5	<0.5	<0.5	1.7	nd	<0.5	<0.5	<0.5	<0.5
T(°C)[c]	9	nd	nd	9	16	9	nd	8	nd	nd
SC[d]	100	100	100	100	250	65	125	nd	100	100
Date sampled	07/10/81	07/07/81	07/09/81	07/09/81	07/09/81	08/07/80	07/09/81	07/09/81	07/09/81	07/12/81
$\delta^{18}O$(SMOW)[e]	nd	-11.2 (-10.8)[f]	-11.6	-10.9 (-10.8)[f]	(-9.2)[f]	(-9.3)[f]	nd	nd	nd	-10.3
δD(SMOW)[e]	nd	-73	-75	-71 (-67)[f]	(-68)[f]	(-67)[f]	nd	nd	nd	-72

[a] Chemical analyses by M.A. Moorman and R.J. Motyka, DGGS. Isotope analysis by R. Harmon and J. Borthwick, Southern Methodist University, Stable Isotope Laboratory.

[b] Sample location codes:
7 - Stream at head of main valley.
8 - Stream at head of tributary valley.
9 - Upper west fork Hot Springs Creek.
10 - Tributary creek above springs A.
11 - Tributary creek below springs A.
12 - Cold spring near hot springs A.
13 - East fork, Hot Springs Creek above confluence.
14 - West fork, Hot Springs Creek below springs D.
15 - Hot Springs Creek below confluence.
16 - Hot Springs Creek at outlet.

[c] Determined in the field.

[d] SC = Specific conductance (µs/cm at 25°C).

[e] SMOW = Standard mean ocean water.

[f] 1980 value.

nd = not determined.

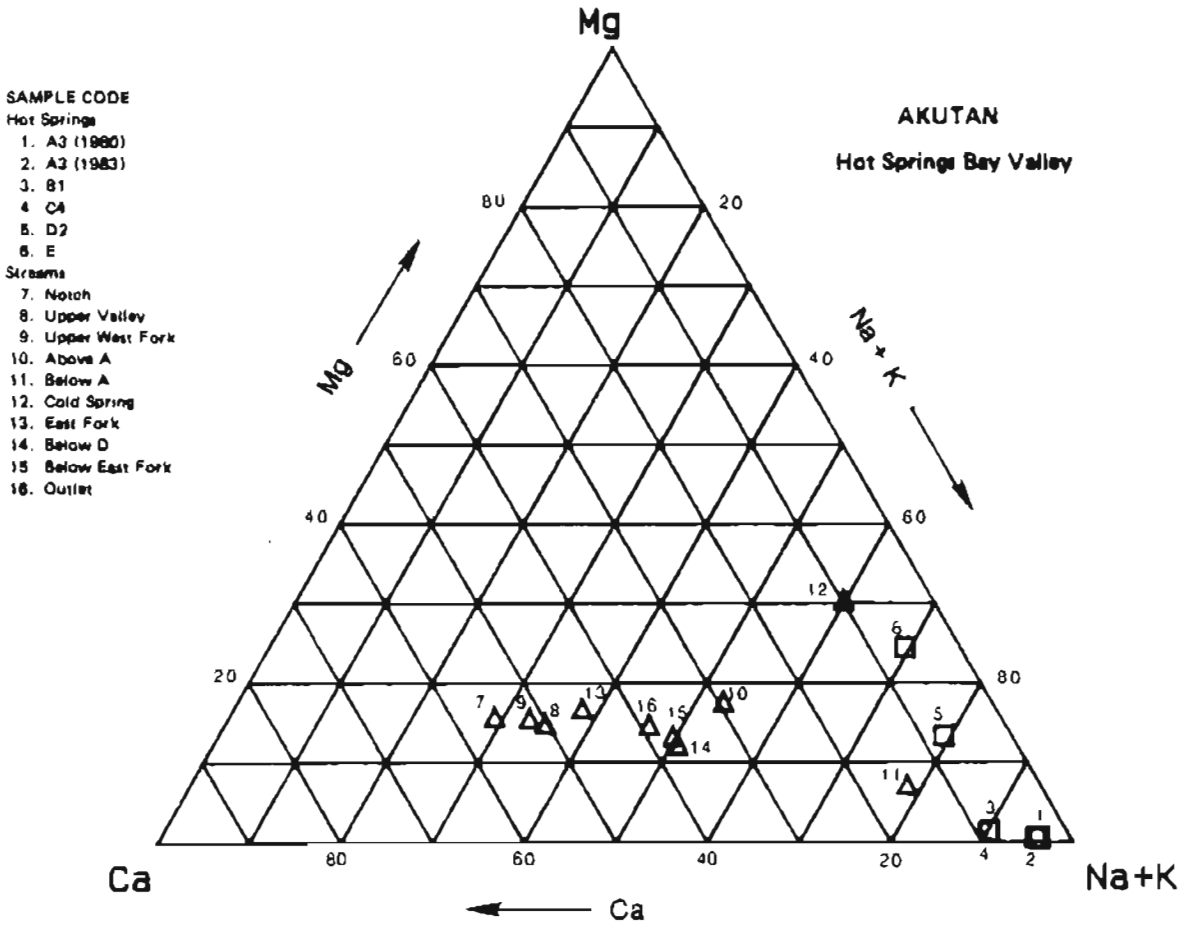

Figure 6-2. Trilateral cation diagram for waters from Hot Springs Bay valley.

thermal waters were probably leached from local rocks by the hot acid waters. The silica content of 220 ppm in one of the acid pools probably reflects the breakdown of silicates and equilibration of the waters with amorphous silica.

Stable isotope compositions of the sampled waters are given in tables 6-1 and 6-2 and plotted in figure 6-3. Also plotted are Craig's (1961) meteoric water line and the Adak precipitation line (Motyka, 1982). A marked difference exists between the 1980 and 1981 isotopic compositions. Except for sample 14, surface and thermal spring waters sampled in 1980 plot to the right of the meteoric water lines. No δD analysis is available for A_3, 1980 (sample 1), but the $\delta^{18}O$ is similar to the other 1980 samples (table 6-1). Waters sampled in 1981 are lighter, and all plot left of the meteoric water lines. The differing compositions may reflect seasonal effects or perhaps some variation in average annual meteoric water composition.

Another feature of figure 6-3 is that, except for spring A_3, the thermal spring waters are isotopically similar to the surface waters for each year. Based on similarities in isotopic compositions between deep thermal water and local meteoric water, meteoric water is considered to be the source of water charging the majority of explored hydrothermal systems (Truesdell and Hulston, 1980), and such is probably the case at Akutan. However, thermal waters derived from hot water systems (T >150°C) are commonly found to have $\delta^{18}O$ positively shifted with respect to local meteoric waters by 1-5 mils through high-temperature exchange with silicates (Truesdell and Hulston, 1980). For example, at the Makushin geothermal area on neighboring Unalaska Island, reservoir waters with temperatures of 190°C show a shift of 1.5-2 mil (Motyka and others, 1988). No comparable shift occurs for δD because of the lack of hydrogen-bearing minerals in reservoir wall-rocks.

Comparison of $\delta^{18}O$ data for 1980 and for 1981 (tables 6-1 and 6-2) suggests that A_3 waters are ~1 per mil heavier than surface waters upstream of the spring. The lack of a detectable shift in $\delta^{18}O$ in the remaining Akutan thermal spring waters suggests that the thermal waters ascending from the reservoir are being diluted with meteoric water before emerging at the surface, or that the reservoir temperatures are insufficient to produce significant exchanges, or both.

Another feature of the isotope geochemistry is the distinctly heavier composition of water from spring E, which probably reflects the influence of seawater mixing. Not plotted in figure 6-2 is the isotopic composition of waters from a fumarole field acid-sulfate pool (table 6-1). The isotopically heavier composition of these waters probably reflects evaporative concentration of heavy isotopes in the surface pool waters.

GAS CHEMISTRY

The results of the gas analyses in mole percent are given in table 6-3. Sample AL-11 is from hot spring A_3. Sample AL-9 is from an acid-sulfate spring, and samples BN4, BN14, and RM3 are from fumaroles in the fumarole field (sheet 1). The much higher percentages of nitrogen and argon gases in hot spring A_3 gases vs. the fumarole gases probably reflects a greater proportion of air being dissolved in the thermal spring waters with oxygen selectively removed through oxidation reactions. The N_2/Ar ratio in the spring gases (~44) is near that of air-saturated water (~37). The N_2/Ar ratios in most of the fumarole field gases are considerably higher, suggesting that N_2 being emitted from the fumarole is additionally derived from sedimentary and perhaps mantle sources.

The fumarole samples have relatively high gas-to-steam ratios (2-3 percent) and are similar to each other in their proportions of major, minor, and trace gases, with carbon dioxide and hydrogen sulfide being the predominant dry-gas components. All the fumarole samples contain relatively large proportions of methane with very similar hydrogen-methane (H_2/CH_4) ratios. By comparison, the majority of fumaroles at the Makushin geothermal area have methane in only trace amounts and are very water-rich with gas-steam ratios ~1 percent (Motyka and others, 1983; Motyka and others, 1988).

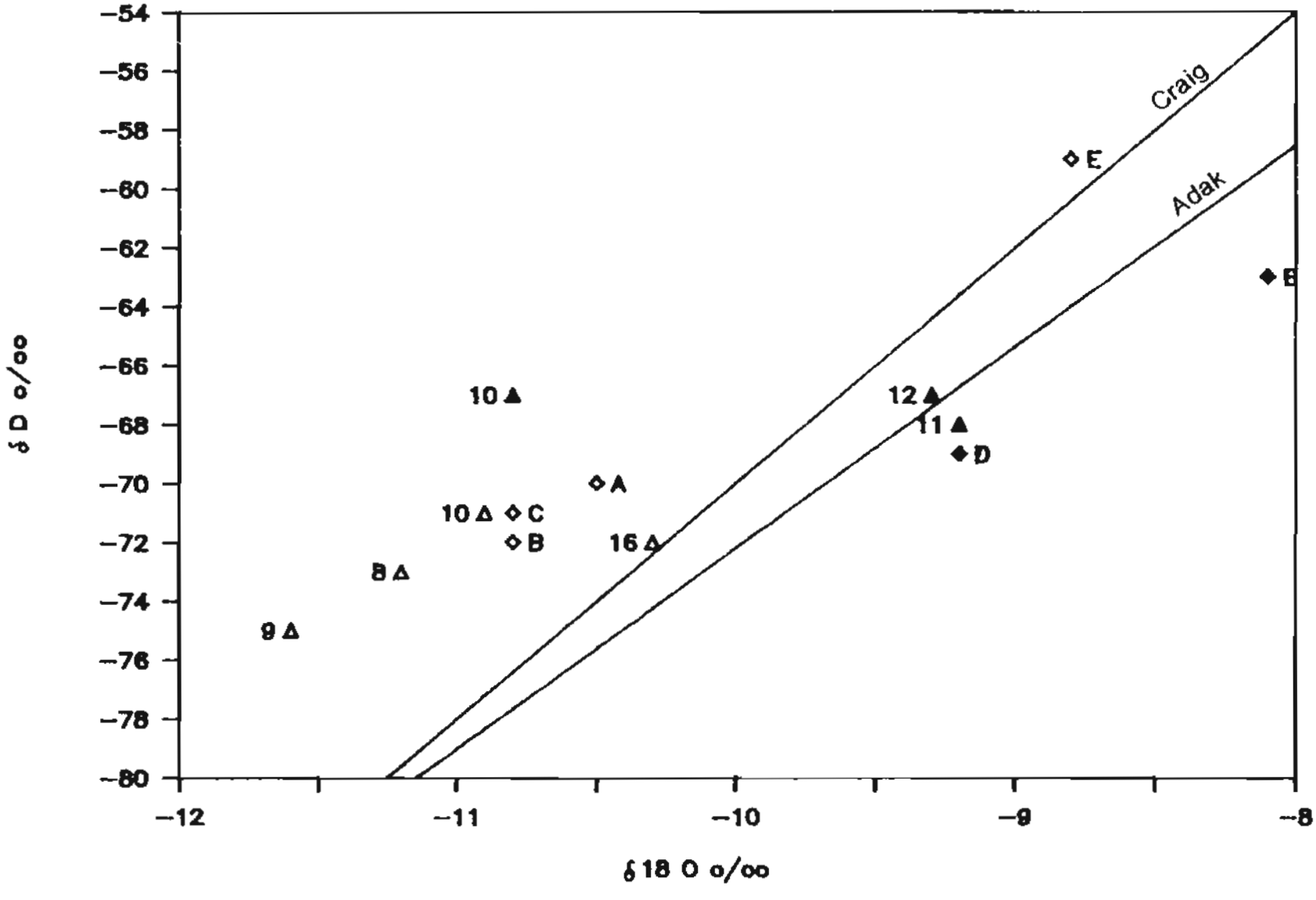

Figure 6-3. Diagram of stable isotope compositions (plotted from data in tables 6-1 and 6-2) of thermal spring (◇) and stream waters (Δ) from Hot Springs Bay valley, Akutan Island. Solid symbols = 1980; open symbols = 1981.

Table 6-3. Analyses of fumarolic and hot spring gases, Hot Springs Bay valley, Akutan, Alaska.

Sample (vent type)	Date sampled	T(°C) (surface)	RO_2[a]	Air-corrected analyses, mole %: Xg[b]	CO_2	H_2S	H_2	CH_4	NH_3	N_2	Ar	He	Ratios: N_2/Ar	C/S	H_2/CH_4	T(°C)[c]	$\delta^{13}C$-CO_2[d]	$\delta^{13}C$-CH_4[d]	Rc/Ra[e]
AL-11[f] (alkali-chloride hot spring)	07/09/81	84.5	0.000	--	10.27	6.26	0.45	4.58	nd	76.68	1.73	0.0012	44	24	0.10	--	-18.1	-39.2	6.0-6.3
AL-9[f] (acidic-sulphate hot spring)	07/07/81	86.6	0.000	--	92.53	2.83	0.34	1.32	nd	2.96	0.02	0.0007	148	33	0.26	208	-11.2	-34.9	7.1
BN4[g] (fumarole)	08/31/83	98.5	0.000	2.06	95.47	1.44	0.20	0.92	0.004	1.96	0.009	tr	215	67	0.21	189	-10.9	nd	nd
BN14[g] (fumarole)	08/31/83	98.5	0.002	2.40	94.35	1.41	0.19	0.91	0.004	3.07	0.021	tr	154	68	0.21	189	-10.8	nd	nd
RM3[h] (fumarole)	08/31/83	98.5	0.001	2.72	95.03	1.28	0.21	1.05	0.016	2.29	0.097	bd	23	75	0.20	188	nd	nd	nd

[a] Ratio of mole % O_2 in sample to mole % O_2 in air.
[b] Gas-steam ratio, moles gas/moles steam in percent.
[c] Gas geothermometer of D'Amore and Panichi (1980); PCO_2 assumed to be 1 bar.
[d] $\delta^{13}C$ in per mil referenced to "PDB" (Fritz and Fontes, 1980).
[e] Ratio of $^3He/^4He$ in sample (air-corrected) to $^3He/^4He$ in atmosphere (Poreda, 1983).
[f] Collected by R. Poreda and R. Motyka. Analyzed by R. Poreda and J. Welhan, Scripps Institution of Oceanographic, La Jolla, California, and R. Motyka, Alaska Division of Geological and Geophysical Surveys (Fairbanks, Alaska).
[g] Collected and analyzed by D. Sheppard, Department of Science and Industry Research, New Zealand.
[h] Collected by D. Sheppard; analyzed by R. Motyka.
nd = no data.

Methane and hydrogen concentrations can be controlled by the reaction

$$CH_4 + 2H_2O \rightleftharpoons CO_2 + 4H_2 \qquad (6\text{-}1)$$

with higher temperatures favoring the right side of the equation (Giggenbach, 1980). Thus the high methane content and low H_2/CH_4 ratio could indicate a cooler geothermal system than at Makushin, where reservoir temperature estimates range from 200° to 250°C. Alternatively, the higher methane content could reflect thermogenic breakdown of carbonaceous sediments. The carbon-13 compositions of the fumarolic carbon dioxide and methane are -11 and -35 per mil, respectively. Mantle-derived carbon dioxide is estimated to have carbon-13 compositions ranging from -4 to -9 per mil (Truesdell and Hulston, 1980), and mantle methane is estimated to range from -14 to -20 per mil (Welhan, 1981). Carbon dioxide derived from organic-sedimentary sources has carbon-13 compositions ranging from -12 to less than -20 per mil (Truesdell and Hulston, 1980); thermogenically derived methane has carbon-13 compositions ranging from -35 to -50 per mil (Schoell, 1980). Thus, the fumarolic methane may be primarily from thermogenic breakdown of organic sediments and the carbon dioxide primarily mantle-derived, with a small component of carbon dioxide from sedimentary sources.

The high helium isotope ratios for both the springs (~6.0) and the fumaroles (~7.0) and the proximity of these hydrothermal vents to Akutan volcano do indicate a magmatic influence on the hydrothermal system. Enrichments in ^3He with respect to atmospheric levels have been correlated with magmatic activity on a worldwide basis, and the excess ^3He is thought to be derived from the mantle (Craig and Lupton, 1981). Enrichments in $^3He/^4He$ for Akutan fumarole and hot springs gases compared to atmospheric ratios (R/Ra) are typical of other island arc settings which range from 5 to 8 (Poreda, 1983). The excess $^3He/^4He$ ratio in gases from hydrothermal systems suggests a more direct connection to magmatic sources with little crustal contamination, although it may also result from leaching of young volcanic rock (Truesdell and Hulston, 1980), while lower values indicate a crustal influence of radiogenic ^4He.

A potential source of thermogenically produced methane and carbon dioxide could be deep-lying marine sandstones and shales which are thought to underlie the Aleutian Islands (Marlow and others, 1973). Circulation of thermal fluids through such rocks could promote thermogenic reactions giving rise to the methane and the organic-sedimentary component of carbon dioxide found in the fumarole gases. The contribution of gases from thermogenic breakdown of organic material must be greater at the hot springs than at the fumarole field because of the larger proportion of methane, and the lower carbon-13 compositions of the carbon dioxide (-18 per mil) and methane (-39 per mil) in the hot spring gases. An additional source region for the increased organic component could be the near-surface region beneath the valley floor where organic material may have become entrapped during infilling of the valley following glaciation. Subsequent circulation of thermal waters through these recent valley sediments would have heated the organic material, causing the thermogenic breakdown.

CONVECTIVE HEAT DISCHARGE BY SPRINGFLOW

The convective heat discharge by springflow can be computed from

$$Q = M + \Delta h \qquad (6\text{-}2)$$

where M = mass discharge of hot water and Δh = net enthalpy per unit mass of discharge from each spring or spring group. The net enthalpy is calculated as the difference between the enthalpy of the water at the discharge temperature and the enthalpy of water at the mean annual temperature at the land surface, which for Hot Springs Bay valley is estimated to be 10°C (Selkregg, 1976).

Chemistries of stream waters above and below group A springs and measurement of stream flow provide a means of estimating the total amount of thermal water (hot springs plus direct) being discharged into the west fork channel of Hot Springs Creek in the vicinity of group A. Assuming the increase in chemical constituents downstream of group A is due solely to the addition of thermal waters, the hot-water fraction of total stream flow can be determined using

$$X = (C_m - C_c) \; / \; (C_h - C_c) \qquad (6\text{-}3)$$

where X is the hot-water fraction, and C is the concentration of chemical constituents in the hot (h), cold (c), and resulting mixed water (m), respectively. Thermal water from spring A_3 is the hottest of the group and sample 2, obtained on July 10, 1981 (table 6-1), was chosen to represent the hot-water fraction. Samples 10 and 11 (table 6-2) were obtained from the stream on July 9, 1981 above and below spring group A with the latter sample being taken at the site of the stream flow measurement. Water flow in the creek just below group A measured 4,265 lpm ± 5 percent.

Because chloride is a conservative, highly soluble ion and normally found only in trace amounts in rocks, chloride concentrations in the waters are less likely to be affected by chemical reactions, precipitation, or leaching from stream gravels then any of the other major or minor constituents present in the water. Using chloride concentrations for C, the resultant hot-water fraction is 0.075. In contrast, using the sum of all analyzed constituents for C gives a hot-water fraction of 0.094.

Stream temperatures above and below site A measured 9.7° and 16.0°C, respectively. The enthalpy of the hot-water fraction can be calculated from the equation

$$h_h = h_c + (h_m - h_c) \; / \; X \qquad (6\text{-}4)$$

where h_h, h_m, and h_c are the enthalpies of the hot, mixed, and cold-water fractions, respectively, and X is the hot-water fraction computed from equation (6-3). Using the temperature-enthalpy tables for water found in Keenan and others (1978) and X = 0.075, one arrives at an estimated temperature of ~94°C for the hot-water fraction, compared to 84.5°C, the hottest

spring vent temperature measured at spring group A. In comparison, a value of X = 0.094 gives a temperature of ~77°C.

Using the more conservative value of 0.075 for the hot-water fraction gives an estimated total hot-water discharge from group A of 320 lpm. The heat loss represented by this hot-water discharge using equation (6-1) is about 1.6 MW. A similar analysis of hot-water discharge at spring group A made in August 1980 gave nearly identical results (Motyka and others, 1981).

Determination of the total discharge of thermal waters in the area was attempted by measuring the stream flow in Hot Springs Creek below group D springs and comparing chemical characteristics of the stream water above group A springs to characteristics of water below group D springs (analyses 9 and 14, respectively, in table 6-2). Unfortunately, the thermal water in the stream is highly diluted by the large cold-water fraction, and only a crude estimate of overall heat discharge can be made. Using equation (6-3) and analysis 2 (table 6-1) for the hot-water component, the computed hot-water fraction at sampling point 14 is 0.015, based on total analyzed constituents, and 0.008, using chloride concentrations. The total stream flow below spring group D was measured to be 52,700 lpm ± 5 percent, so the corresponding hot water discharge estimates above this point are 790 and 420 lpm, respectively. If the hot-water fraction is assumed to be 84°C, then the corresponding estimated heat discharges are 4.1 and 2.2 MW, respectively. The estimated flow from group A alone was ~320 lpm, so it appears that using chloride concentrations to calculate the hot-water fraction below group D gives too low an estimate, and the more probable heat discharge lies between 4.1 and 2.2 MW. A substantial amount of thermal water is probably also discharging at and beyond the beach, as evidenced by spring group E and the elevated temperatures measured in the surrounding sands.

GEOTHERMOMETRY

Chemical geothermometers, which are based on temperature-sensitive chemical reactions in hydrothermal fluids, are commonly used to estimate subsurface temperatures at sites where data from drilling are not available (see Fournier, 1981, for review). These reactions may control either the absolute amount of an element (for example, cations) or fractionation of isotopes. By comparing the results of reactions under known conditions with results of analyses of hydrothermal fluids, an estimated reservoir temperature can be calculated. The estimated temperatures derived from geothermometry calculations may represent actual subsurface temperatures if several assumptions about the nature of an individual hydrothermal system are satisfied.

Application of the more commonly used and accepted geothermometers to the Hot Springs Bay valley thermal spring waters is given in table 6-4. Thermal water from spring A_3 has the highest vent temperature and flow rate and is therefore considered to be the most representative of reservoir chemistry. Estimates of reservoir temperature range from about 180° to 200°C, based on analytical results for spring A_3 using the Na^+-K^+, $Na^+-K^+-Ca^{++}$ the single water-sulfate oxygen-isotope geothermometers. Application of the magnesium correction (Fournier and Potter, 1978) lowers the reservior

Table 6-4. Geothermometry of thermal waters in Hot Springs Bay valley, Akutan Island, Alaska. (Temperatures in °C.)

Spring sampled	Date sampled	Geothermometer used: Quartz[a]	Chalcedony[b]	Na/K[b]	Na-K-Ca[c]	Na-K-Ca[d] with mg corr.	$\delta^{18}O$ H_2O-SO_4[e]
A_3	8/07/80	159	135	204	188	169	186[f]
A_3	7/10/81	155	130	198	184	163	nd
A_3	8/31/83	157	133	186	178	162	nd
B_1	7/09/81	139	112	212	181	139	nd
C_4[g]	7/09/81	154	129	198	173	139	nd
D_2	8/08/80	132	105	191	164	11	nd
E	7/12/81	148	123	156	161	2	nd

[a] Fournier and Potter, 1982b.
[b] Fournier, 1981.
[c] Fournier and Truesdell, 1973.
[d] Fournier and Potter, 1978.
[e] McKenzie and Truesdell, 1977.
[f] N. Nehring, U.S. Geological Survey, Menlo Park, California.
[g] Upstream and adjacent to C_3 on fig. 6-1.
nd = not determined.

temperature predicted by the Na^+-K^+-Ca^{++} geothermometer by approximately 20°C. However, use of the Mg^{++} correction is ambiguous because of the likelihood that the magnesium present in the thermal spring waters is acquired from colder waters mixing with ascending thermal waters.

Fournier (1981) reports that in most natural waters above 150°C, and in some waters below that temperature, quartz appears to control the dissolved silica concentration; therefore, the quartz geothermometer is used for the Akutan hot spring waters. In contrast to the other geothermometers, the quartz geothermometer yields substantially lower temperature estimates, averaging about 157°C for spring A_3 (table 6-4). However, the quartz geothermometer is particularly susceptible to dilution; thus, if mixing occurs the quartz geothermometer would predict only minimum temperatures.

D'Amore and Panichi (1980) have suggested a gas geothermometer for estimating reservoir temperatures, based on the proportions of CO_2, H_2S, H_2, and CH_4 in fumarolic gases. Application of this geothermometer to the gas analyses of upper Hot Springs Bay valley fumaroles gives estimated reservoir temperatures ranging from 188 to 208°C (table 6-3), which is consistent with the cation and the water-sulfate oxygen-isotope geothermometry for spring A_3.

EVIDENCE FOR MIXING

Several lines of evidence indicate that the thermal waters ascending from the hot-water reservoir predicted by geothermometry mix with, and are diluted

by, colder waters before emerging at the surface in lower Hot Springs Bay Bay valley. First, the significantly lower reservoir temperatures predicted by the quartz geothermometer vs. the cation and the water-sulfate oxygen isotope geothermometers is itself a clue that mixing may be occurring. Second, mixing with cold meteoric waters is suggested by the similarities in stable isotope compositions between the thermal spring waters and the locally derived meteoric waters (fig. 6-3).

Another indication of mixing is the tritium content of 20.3 tritium units (TU) found in a water sample collected from spring A_3. Panichi and Gonfiantini (1978) have reviewed the use of tritium as an indicator of age and mixing in geothermal systems. Tritium was introduced into the atmosphere in large quantities during the years of thermo-nuclear weapons testing following 1952. Since the test ban treaty of 1963, tritium in the atmosphere has steadily declined, but still remains at levels much greater than pre-1952. Because of its relatively short half-life (12.3 yr), tritium provides a good marker for waters recently exposed to the atmosphere. Tritium data from the Makushin geothermal area (Motyka and others, 1988) and almost all other investigated hot water systems indicate that residence times of recharging meteoric waters in geothermal reservoirs are far greater than 25 years.

As a comparison to waters from Akutan spring A_3, the weighted-average tritium concentration of precipitation in Anchorage in 1980 was 29 TU, with seasonal variation ranging from the winter minimum of 16 TU to the late-spring maximum of 51 TU (source of data: International Atomic Energy Agency). Samples of waters thought to be wholly or partially of recent meteoric origin collected in July 1982 from the Makushin geothermal area on Unalaska Island varied from 6 TU to 37 TU, in contrast to thermal reservoir waters collected from the Makushin test well, which had a tritium content of only 0.10 TU (Motyka and others, 1988). The high tritium content of waters emerging from spring A_3 are therefore indicative of a significant component of young meteoric waters in the thermal spring waters.

Lastly, in order to account for the difference in temperature between the reservoir and the spring vents, the ascending thermal water must cool in one or a combination of three ways: 1) by conduction to wallrock surrounding the conduit; 2) by adiabatic expansion (boiling); or 3) by mixing with cooler waters. Calculations by Truesdell and others (1977) indicate that for hot spring waters ascending from a 200°C reservoir 1 km deep, conductive cooling will reduce water temperatures to 100°C only for flows less than 30 lpm. Total discharge at the group A springs is estimated at 320 lpm, several times greater than the preceding estimate for cooling by conduction alone. Thus, since vent temperatures are below boiling, cooling of the ascending waters must be at least partially due to mixing.

MIXING MODELS

In this section, enthalpy diagrams for silica and chloride are examined following procedures outlined by Fournier and Truesdell (1974) and Fournier (1979), to help deduce mixing patterns among the various spring waters.

Mixing trends appear best defined for waters from groups A and B while the histories of waters from groups C and D are more difficult to establish.

Figure 6-4 presents a plot of the concentration of silica in the thermal spring waters vs. the enthalpy of the emergent waters. The quartz solubility curve (QSC) of Fournier and Potter (1982a) is also shown. Point A is the average of the three analyses for spring A_3 (table 6-1). Point S represents local meteoric water assumed to have SiO_2 = 10 ppm and T = 10°C. Lines M_1 and M_2 represent two simple mixing models consistent with the range of cation and water-sulfate oxygen-isotope geothermometer temperature estimates for the underlying hot-water reservoir (180°-200°C) and with infiltrating surface water as the cold-water end member. None of the thermal spring waters falls near either of these two simple mixing trends, which indicates that the water compositions and temperatures result from other mixing trends or from more complex processes.

If either M_1 or M_2 is valid, then the high level of dissolved silica and low temperature of the waters relative to these mixing lines require that they have cooled appreciably by conduction after mixing (for example, from A' or A" to A, fig. 6-4) or dissolved additional silica by reactions with glassy rock after mixing. (Because of high discharge rates, at least for spring group A waters, conductive cooling following mixup seems unlikely unless there is a substantial component of horizontal flow.) Conductive cooling following mixing seems unlikely, at least for spring group A waters, unless there is a substantial component of horizontal flow. Conductive cooling also seems inconsistent with chloride-enthalpy data for waters from groups C and D as discussed below. Glassy rocks are not found in any of the bedrock exposures in the adjacent valley walls (Swanson and Romick, this report). Glass was not found to be a constituent of debris flow deposits examined in Hot Springs Bay valley (Swanson and others, this report), but the composition of subsurface valley filling deposits is unknown and may include glassy rocks or ash.

Line M_{AB}, drawn through points A and B, represents an alternative and possibly more accurate mixing model (fig. 6-4). Point A was chosen because the temperature and flow rate of spring A_3 indicate this spring is the least likely to have been affected by conductive cooling; point B was chosen because the proximity of spring group B to spring group A made it the most likely to be directly related to spring group A water. M_{AB} intersects QSC at a temperature equivalent of ~200°C, consistent with the high end of the geothermometer estimates of reservoir temperature. Although point D falls below M_{AB}, points C and E do fall on or near this mixing line, providing additional credence for this model. Spring group D waters could have been produced by secondary mixing of water having a composition similar to A with cold dilute waters similar to S.

M_{AB} intersects the silica axis at 53 ppm, a concentration which is substantially higher than silica concentrations in any of the cold surface waters unaffected by thermal discharges. If mixing model M_{AB} is valid, then the relatively high silica concentration for the 'cold' water end member suggests the end member may actually be a low-enthalpy thermal water (10° <T >90°C). Magnesium is usually removed from high-temperature waters (T >150°C)

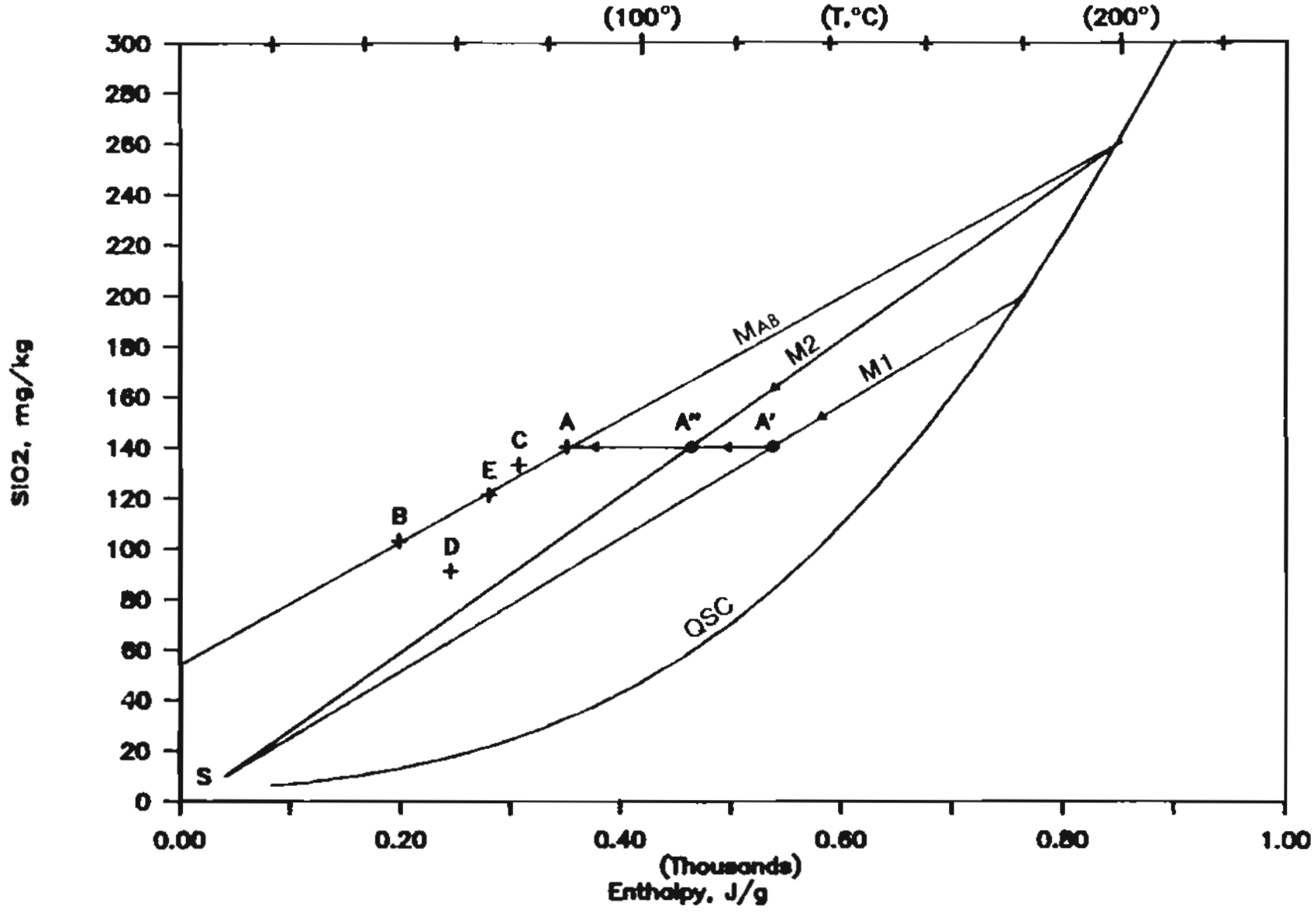

Figure 6-4. Silica-enthalpy relationships for Hot Springs Bay valley thermal spring waters. Quartz solubility curve (QSC) from Fournier and Potter (1982a). Mixing lines M_{AB}, M_1, and M_2 explained in text.

through hydrothermal reactions (Fournier, 1981). Thus, the presence of magnesium in all the spring waters could also be indicative of the low- to moderate-enthalpy water component although the Mg^{++} may have been acquired after mixing by dissolution of basic volcanic rocks.

The relative amounts of mixing of low- and high-enthalpy waters needed to produce the various spring waters can be estimated only approximately from M_{AB}, because the temperature and silica concentration of the low-enthalpy component can be interpolated at best to lie somewhere along the M_{AB} mixing line between the silica axis and point B. Assuming the high-enthalpy component is represented by the intersection of M_{AB} with QSC, the hot-water fraction comprising spring A_3 water would range from a maximum of 40 percent for a 'zero' enthalpy water component to a minimum of 23 percent for a low-enthalpy thermal water similar to B.

No clear mixing trend emerges from an examination of thermal spring data on a plot of chloride vs. enthalpy (fig. 6-5). Spring group E is excluded because of the probable mixing of high-chloride seawater at this site. Line L_{AB} represents a possible mixing model for producing A and B waters by mixing S, an end member with chloride concentration and enthalpy similar to local surface waters, with a high-enthalpy component such as represented by R. Points C and D plot substantially above L_{AB} and, in contrast to M_1 and M_2 on the silica vs. enthalpy diagram, the location of these two points relative to L_{AB} cannot be the result of conductive cooling. Heat would have to be added and waters on L_{AB} would have to mix with a relatively high-enthalpy, low-chloride 'cold' water component in order to produce C and D waters. This low-chloride, 'cold' water component could be normal cold ground water heated by steam or perhaps by conduction from the underlying hot-water reservoir.

Waters from groups C and D could also have formed by mixing with a hot-water component having a substantially lower concentration of chloride than the hot-water component for groups A and B. However, the similarity in the ratio of the conservative elements Cl/B (~40, table 6-1) suggests that the hot-water components of springs from groups A, B, C, and D (and probably E) are all derived from the same parent reservoir. A model for deriving hot-water end members with differing chloride concentrations consistent with a single parent reservoir is represented by line X, a hypothetical boiling line for a parent hot water assumed to have a temperature of ~200°C, from which steam is continually separated. The resulting residual water becomes increasingly more concentrated in chlorides. Such models have been discussed in detail by Fournier (1979). The dashed rays show potential pathways by which the different spring waters may have formed. However, none of the lower valley hot springs are at boiling point, and the closest fumaroles are 4 km away, an improbable distance for separating steam to travel without significant cooling. Mixing with hot-water components derived from a boiling line such as L_X is therefore deemed to be an unlikely model for producing the Akutan hot springs.

To summarize, the data are insufficient to fully determine which, if any, of the above mixing models is accurate. A mixing trend for waters from spring groups A and B appears to be the best-defined. Line M_{AB} predicts a 'cold' water end member with a relatively high concentration of silica. To

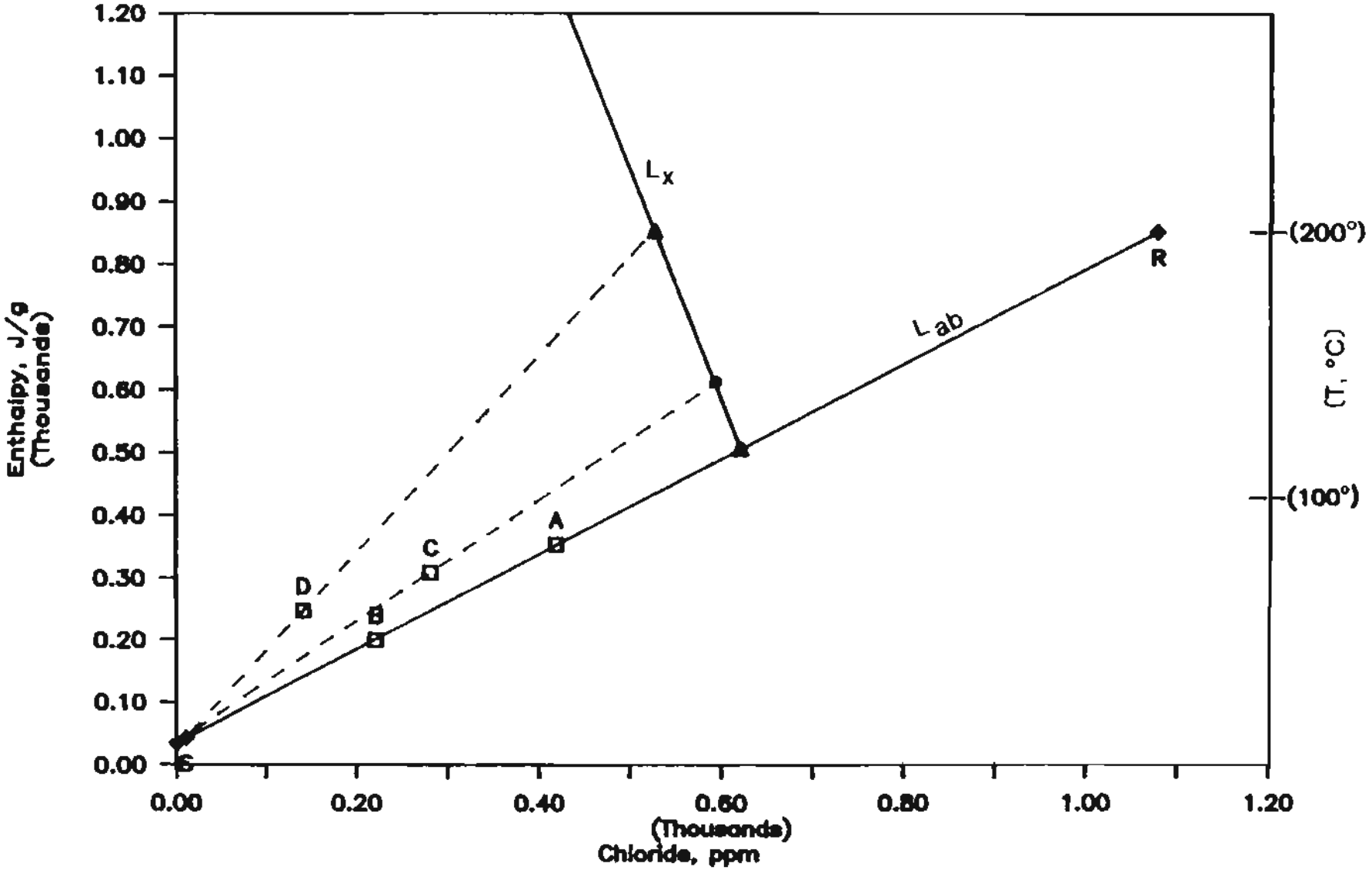

Figure 6-5. Chloride-enthalpy relationships for Hot Spring Bay valley thermal spring waters. Mixing lines L_{AB} and boiling line L_X explained in text.

be consistent with the silica mixing model M_{AB}, the 'cold' water end member on the chloride-enthalpy mixing line L_{AB} would be construed to lie between points S and B. If the hot-water end member is presumed to have a temperature of ~200°C, extension of line L_{AB} gives a corresponding chloride concentration of ~1,100 ppm (point R). Additional implications imposed by these mixing lines are examined in the next section which discusses the hydrothermal system.

HYDROTHERMAL SYSTEM

Deep Reservoir

Evidence from geothermometry, silica mixing models, and Cl/B ratios indicates that the thermal waters feeding the springs in lower Hot Springs Bay valley are at least partially derived from a parent hot-water reservoir. The depth of this reservoir is unknown, but based on the exploration of the Makushin geothermal area on neighboring Unalaska Island (Motyka and others, 1988), the reservoir could lie within 1 km of the surface. The gases and steam emanating from the fumarole field at the head of the valley probably also originate from the boiling of a subsurface hot-water reservoir. Similarities between the compositions of the lower valley hot spring gases and upper valley fumarole gases, $^3He/^4He$ ratios, and the geothermometric estimates of reservoir temperatures suggests that the thermal fluids supplying the two zones are derived from the same reservoir. If so, the reservoir may span a length of 4 km or more.

Evidence has been presented to indicate that thermal waters ascending from this parent reservoir are substantially diluted before they emerge from springs in the lower valley. The effects of this dilution on the various geothermometers were examined to refine estimates of reservoir temperature. The quartz geothermometer is particularly susceptible to dilution, but as illustrated above, the parent hot-water temperature can be estimated by using silica mixing models. The preferred silica-enthalpy mixing line (M_{AB}, fig. 6-4) intersects QSC at a temperature equivalent of ~200°C, an estimate for the hot-water component that is substantially above temperatures predicted by the quartz conductive geothermometer.

The Na^+/K^+ geothermometer, which is based on the ratio of Na^+ to K^+, is relatively unaffected by dilution unless the diluting waters have significant concentrations of Na^+ or K^+. Excluding spring group E water, which probably contains Na^+ and K^+ derived from seawater, the Na^+/K^+ estimates range from 186° to 212°C with an average of ~200°C, similar to the temperature predicted by the silica mixing model.

Dilution can affect the Na^+-K^+-Ca^{++} geothermometer. Based on calculations made by Fournier (1981) the estimated dilutions of the hot-water component along line M_{AB} would cause the Na^+-K^+-Ca^{++} geothermometer to underestimate reservoir temperatures by 10°-20°C.

Dilutions can also affect the water-sulfate oxygen-isotope geothermometer because the diluting water can mask the $\delta^{18}O$ composition of the hot-water fraction (McKenzie and Truesdell, 1977). If the fraction of the

parent hot water can be calculated and the $\delta^{18}O$ compositions of the diluting water and the spring water are determined, then the $\delta^{18}O$ composition of the parent thermal water before dilution can be calculated using an equation similar in form to equation (6-4). From mixing line M_{AB} (fig. 6-4), the hot-water fraction was estimated to be between 23 and 40 percent. Comparison of $\delta^{18}O$ data for 1980 and for 1981 (tables 6-1 and 6-2) suggests that spring A_3 waters are ~1 per mil heavier than surface waters upstream. A value of 40 percent for the hot-water fraction and an assumed difference of 1 per mil between the diluting water and the spring water result in a hot-water component ~1.5 per mil heavier than spring A_3 water and a water-sulfate oxygen-isotope geothermometer estimate of ~214°C.

Taking into account the effects of dilution, the temperature of the parent reservoir is most likely to be at least 200°C, if not higher, consistent with the gas geothermometry for the fumarolic emissions. Silica- and chloride-enthalpy diagrams suggest concentrations of ~260 ppm for SiO_2, and ~1,100 ppm for Cl^- in the reservoir waters. The similarity in stable isotope compositions between the thermal spring waters and surface stream waters indicates meteoric water is the likely source of recharge for the reservoir. Consideration of dilution suggests the $\delta^{18}O$ composition of the recharging meteoric water is subsequently shifted by + 2.5 per mil, probably through high-temperature isotopic exchange reactions with reservoir wall rocks.

The carbon-13 data for carbon dioxide and methane and the relatively large proportion of methane present in the gases collected from the fumaroles and hot springs indicate thermogenic breakdown of organic sediments in the reservoir to be one of the sources of carbon in the hydrothermal system. The relatively heavy carbon-13 composition of the fumarolic carbon dioxide and the $^3He/^4He$ ratios of 6.0:7.0 reflect a probable mantle influence on the geothermal system and suggest that a magmatic intrusive, perhaps associated with the active volcanism at nearby Akutan volcano, is the source of heat driving the hydrothermal system.

Shallow Reservoir and Zone of Mixing

Substantial evidence has been presented to indicate that thermal waters ascending from the deep reservoir encounter and mix with 'colder' waters prior to their emergence from springs in the lower valley. The preferred silica-enthalpy mixing line (M_{AB}, fig. 6-4) predicts a relatively high concentration of silica in the 'cold' water end member. One model which could account for this high silica concentration is that a portion of the ascending high-enthalpy waters are mixing with cold meteoric waters that infiltrate into the subsurface to form a shallow reservoir of mixed moderate-enthalpy water. Additional evidence for a shallow reservoir of warm water comes from the geophysical survey work of Wescott and others (this report) who were able to infer the existence of a seismically-recognizable low-resistivity layer which lies 30-100 m below the surface along the western part of the lower valley.

Figure 6-6 shows a schematic cross-section of suggested hydrologic pathways where two separate but interconnected stages of mixing are envisioned. A relatively impermeable capping debris flow layer (Swanson and others, this

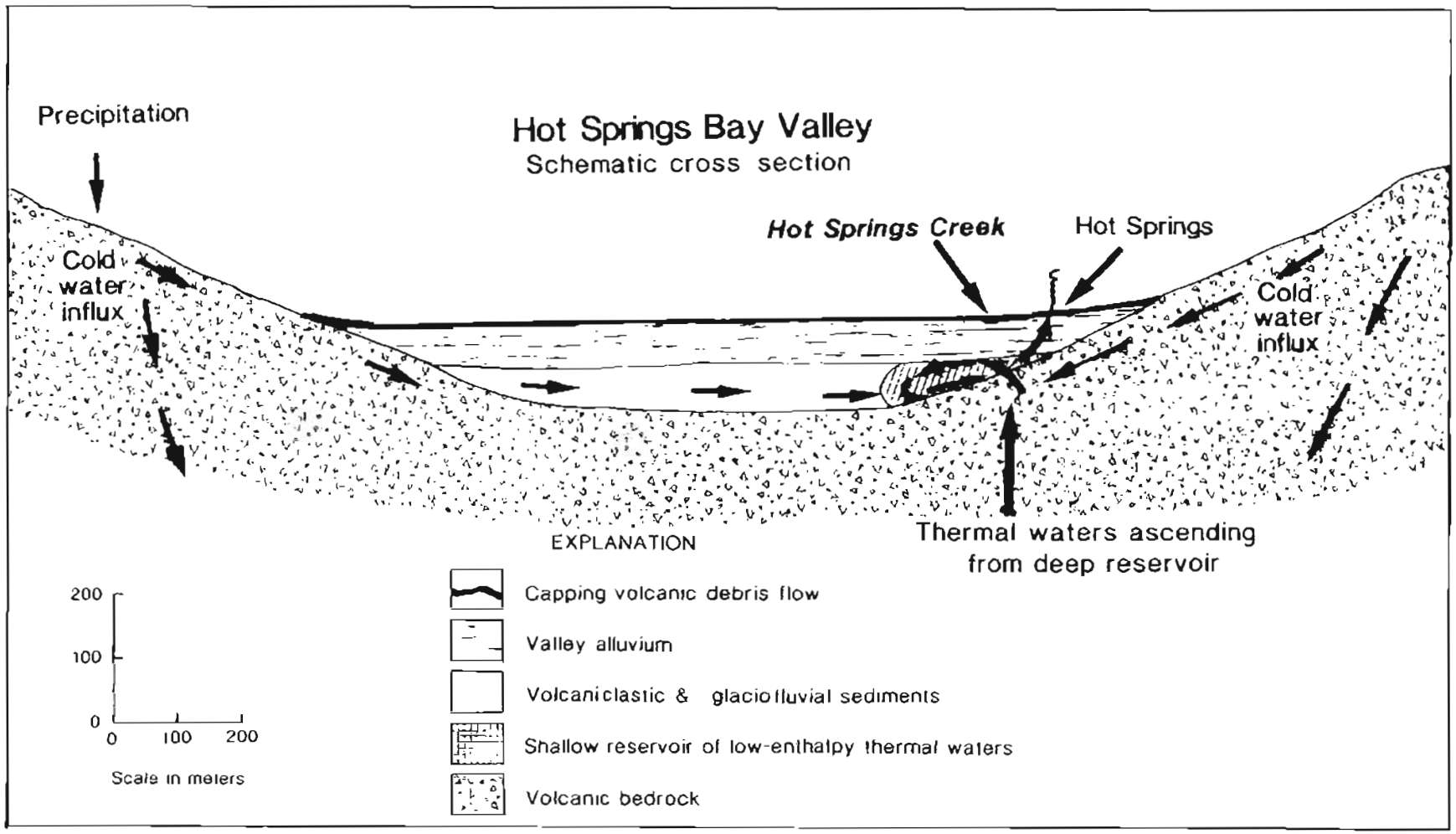

Figure 6-6. Schematic cross section (looking up valley) of lower Hot Springs Bay valley showing suggested hydrologic pathways for cold and hot waters. Mixing with upwelling thermal water is thought to occur in a zone of low resistivity found to underlie the western part of the lower valley. Subsurface boundaries are inferred from seismic and electrical resistivity surveys (Wescott and others, this report).

report) substantially limits direct downward percolation of surface waters through the valley floor. In the first stage, cold meteoric waters infiltrate along the valley walls and migrate down-valley and laterally into the shallow reservoir and mix with hot waters ascending from the deep reservoir. This mixing stage is assumed to follow mixing line M_2 in fig. 6-4. The second stage of mixing occurs when ascending hot waters flow through and mix with the previously formed stage one low-enthalpy waters before emerging at the surface. This mixing stage follows line M_{AB} in fig. 6-4.

Assuming there is no loss or gain of silica through deposition or dissolution and that the minimum concentration of silica in the low-enthalpy shallow-reservoir water is at least 53 ppm, and using 260 ppm and 10 ppm for the concentration of silica in the hot and cold waters, respectively, the minimum proportion of hot water making up the shallow reservoir is computed from equation (6-3) to be 17 percent. The corresponding minimum temperature of the mixed water is estimated at ~43°C, using equation (6-4), the temperature-enthalpy tables for water (Keenan and others, 1978), and 10° and 200°C for the cold- and hot-water fractions, respectively. To be consistent with mixing line M_{AB}, the low-enthalpy waters envisioned to have formed along mixing line M_2 must cool substantially by conduction before mixing with hot waters to produce the various spring waters. Such cooling could occur during convective overturn within the shallow reservoir, particularly if there is a substantial component of shallow horizontal flow.

Water flow within the shallow reservoir is likely to be relatively dynamic. Residence time for the low-enthalpy waters in the shallow reservoir must be short (<2 yr) to account for the relatively high concentration of tritium in the A_3 spring waters; hot water entering the shallow reservoir would begin boiling at a depth of 140-150 m under a normal hydrostatic gradient. Boiling probably is quenched largely by mixing with colder waters, although a portion of the steam may separate and heat ground waters underlying spring groups C and D. Temperatures within the shallow reservoir can thus vary from ~200°C where hot waters enter to ~10°C around the lateral margins of the system, where cold meteoric waters are infiltrating, and such large variations in temperatures could correspond to the variations in resistivity estimated for the subsurface layers in models developed by Wescott and others (this report).

SUMMARY AND CONCLUSIONS

The results of fluid analyses, geothermometry, and application of mixing models provide evidence that thermal fluids emanating at the surface of Hot Springs Bay valley are derived in part from a deep hot-water reservoir having a temperature of ~200°C. Silica- and chloride-enthalpy analyses indicate that thermal spring waters emerging in the lower valley, particularly spring group D, have had differing heritages, but similarities in the ratio of the conservative elements Cl/B suggest a common parent for the deep thermal water component. Similarities in gas composition, $^3He/^4He$ ratios, and geothermometric temperature estimates suggest that the reservoirs supplying thermal fluids to the fumaroles and the hot springs are interconnected. If so, the deep reservoir system may extend over a distance of over 4 km. Depth to the reservoir is unknown, but based on exploration at Makushin geothermal area on

neighboring Unalaska Island, the reservoir may lie within 1 km or less of the surface.

Thermal spring water chemistry and mixing models suggest that the reservoir contains moderately concentrated NaCl waters with Cl^- concentrations of ~1,100 ppm and silica concentrations of ~260 ppm. The similarity in stable isotope composition of thermal spring waters to surface stream waters indicates the deep reservoir is recharged by local meteoric waters. The carbon-13 data for carbon dioxide and methane and the relatively large proportion of methane present in the gases collected from the fumaroles and hot springs indicate that thermogenic breakdown of organic sediments is one of the sources of carbon in the system. The relatively heavy carbon-13 composition of the fumarolic carbon dioxide and the $^3He/^4He$ ratios of 6.0:7.0 reflect a probable magmatic influence on the geothermal system, perhaps associated with the active volcanism at nearby Akutan Volcano.

Fumaroles at the head of the valley are probably fed directly by gases and steam boiling off the deep hot-water reservoir. Thermal waters ascending from the reservoir in the lower part of the valley pass through and mix with low-enthalpy thermal waters contained in a shallow reservoir, located below a capping volcano debris flow layer, before emerging from springs. Geophysical evidence for the existence of this shallow reservoir is provided by Wescott and others (this report). The low-enthalpy thermal water in the shallow reservoir is thought to be derived from the mixing of cold meteoric waters infiltrating beneath the valley floor with thermal waters ascending from the deep reservoir. Residence time for waters in the shallow reservoir must be relatively short to account for the high tritium content in spring waters emerging from spring A_3. The mixed waters then cool further by conduction during convective overturn and shallow horizontal flow.

Conductive heat losses for thermal waters emerging from spring group A are considered minor in view of the high rate of thermal spring discharge. Cooling of the thermal waters ascending from the reservoir and feeding spring group A is accomplished primarily through mixing with the low-enthalpy thermal waters in the shallow reservoir. Any boiling that may take place in the ascending thermal waters is probably quenched during the mixing stage, although some steam may separate and heat ground water in spring groups C and D.

Heat discharge at the surface by spring flow from spring groups A through D, referenced to 10°C, is estimated at 2.2-4.1 MW. Substantially more thermal water is likely to discharge at the beach and directly into the sea beyond the limit of the volcanic debris flow confining unit.

REFERENCES CITED

Baker, R.O, Lebida, R.C., Pyle, W.D., and Britch, R.P., 1977, An investigation of selected Alaska geothermal spring sources as possible salmon hatchery sites: National Technical Information Service IDO/1624-1, 173 p.

Byers, F.M., Jr., and Barth, T.F.W., 1953, Volcanic activity on Akun and Akutan Islands: Pacific Science Congress, 7th, New Zealand, 1949 Proceedings, v. 2, p. 382-397.

Craig, Harmon, 1961, Isotope variations in meteoric waters: Science, v. 133, p. 1702-1703.

Craig, Harmon, and Lupton, J.E., 1981, Helium-3 and mantle volatiles in the ocean and the oceanic crust: The Oceanic Lithosphere: vol. 7, The Sea, New York, John Wiley & Sons, p. 391-428.

D'Amore, Franco and Panichi, Costanzo, 1980, Evaluation of deep temperatures of hydrothermal systems by a new gas geothermometer: Geochimica et Cosmochimica Acta, v. 44, p. 549-556.

Fournier, R.O., 1979, Geochemical and hydrologic considerations and the use of enthalpy-chloride diagrams in the prediction of underground conditions of hot-springs systems: Journal of Volcanology and Geothermal Research, v. 5, p. 1-16.

Fournier, R.O., 1981, Application of water chemistry to geothermal exploration and reservoir engineering, in Ryback, L., and Muffler, L.J.P., eds., Geothermal systems: Principles and case histories: New York, John Wiley and Sons, p. 109-144.

Fournier, R.O., and Potter, R.W., 1978, A magnesium correction for the Na-K-Ca chemical geothermometer: U.S. Geological Survey Open-file Report 78-468, 24 p.

Fournier, R.O., and Potter, R.W., II, 1982a, An equation correlating the solubility of quartz in water from 25° to 900°C at pressures up to 10,000 bars: Geochimica et Cosmochimica Acta, v. 46, p. 1969-1974.

Fournier, R.O., and Potter, R.W., II, 1982b, A revised and expanded silica (quartz) geothermometer: Geothermal Resources Council Bulletin, v. 11, p. 3-12.

Fournier, R.O., and Truesdell, A.H., 1973, An empirical Na-K-Ca geothermometer for natural waters: Geochimica et Cosmochimica Acta, v. 37, p. 1255-1275.

_____, 1974, Geochemical indicators of subsurface temperature, pt. 2 of Estimation of temperature in fraction of hot water mixed with cold water: Journal of Research, U.S. Geological Survey, v. 2, p. 263-278.

Fritz, Peter, and Fontes, J.C., eds., 1980, Handbook of environmental isotope geochemistry: New York, Elsevier, p. 11-13.

Giggenbach, W.F., 1980, Geothermal gas equilibria: Geochimica et Cosmochimica Acta, v. 44, p. 2021-2130.

Keenan, J.H., Keyes, F.G., Hill, P.G., and Moore, J.G., 1978, Steam Tables: Thermodynamic properties of water including vapor, liquid, and solid phases, John Wiley & Sons, New York, 156 p.

Marlow, M.S., Scholl, D.S., Buffington, D.S., and Alpha, T.R., 1973, Tectonic history of the central Aleutian arc: Geological Society of America Bulletin, v. 84, p. 1555-1574.

McKenzie, W.F., and Truesdell, A.H., 1977, Geothermal reservoir temperatures estimated from the oxygen compositions of dissolved sulfate in water from hot springs and shallow drillholes: Geothermics, v. 5, p. 51-61.

Motyka, R.J., 1982, High temperature hydrothermal resources in the Aleutian arc: Alaska Geological Society Symposium on Western Alaska Geology and Resource Potential, Anchorage, Proceedings, p. 87-99.

Motyka, R.J., Moorman, M.A., and Liss, S.A., 1981, Assessment of thermal spring sites, Aleutian arc, Atka Island to Becharof Lake - preliminary results and evaluation: Alaska Division of Geological and Geophysical Surveys Open-file Report 144, 173 p.

Motyka, R.J., Moorman, M.A., and Poreda, R., 1983, Progress report-thermal fluid investigations of the Makushin geothermal area: Alaska Division of Geological and Geophysical Surveys Report of Investigations 83-15, 48 p.

Motyka, R.J., Queen, L.D., Janik, C.J., Sheppard, D.S., Poreda, R.J., and Liss, S.A., 1988, Fluid geochemistry and fluid-mineral equilibria in test wells and thermal gradient holes of the Makushin geothermal area, Unalaska Island, Alaska: Alaska Division of Geological and Geophysical Surveys, Report of Investigations [in preparation].

Panichi, Costanzo, and Gonfiantini, R., 1978, Environmental isotopes in geothermal studies: Geothermics, v. 6, p. 143-161.

Poreda, R.J., 1983, Helium, neon, water and carbon in volcanic rocks and gases: University of California, San Diego, Ph.D. thesis, 215 p.

Presser, T.S., and Barnes, Ivan, 1974, Special techniques for determining chemical properties of geothermal waters: U.S. Geological Survey Water Resources Investigations 22-74, 11 p.

Schoell, Martin, 1980, The hydrogen and carbon isotopic composition of methane from natural gases of various origins: Geochimica et Cosmochimica Acta, v. 44, p. 649-661.

Selkregg, L.L., ed., 1976, Alaska Regional Profiles, Volume III, Southwest Region: University of Alaska, Arctic Environmental Information and Data Center, Anchorage, Alaska, 313 p.

Skougstad, M.W., Fishman, M.J., Friedman, M.J., Erdmann, D.E., and Duncan, S.S., eds., 1979, Methods for determination of inorganic substances in water and fluvial sediments: U.S. Geological Survey Techniques of Water - Resources Investigations, book 5, chapter A1, p. 626.

Truesdell, A.H., and Hulston, J.R., 1980, Isotopic evidence on environments of geothermal systems, in Fritz, P., and Fontes, J.Ch., eds., Handbook of environmental isotope geochemistry: New York, Elsevier, p. 179-219.

Truesdell, A.H., Nathenson, Manual, and Rye, R.O., 1977, The effects of subsurface boiling and dilution on the isotopic compositions of Yellowstone thermal waters: Journal of Geophysical Research, v. 82, p. 3694-3703.

Welhan, J.A., 1981, Carbon and hydrogen gases in hydrothermal systems: The search for a mantle source: University of California, San Diego, Ph.D. thesis, 182 p.

CHAPTER 7

APPRAISAL OF GEOTHERMAL POTENTIAL OF HOT SPRINGS BAY VALLEY AKUTAN ISLAND, ALASKA

by

Roman J. Motyka,[1] Eugene M. Wescott,[2] Donald L. Turner,[2] and Samuel E. Swanson[2]

[1]Alaska Division of Geological and Geophysical Surveys, 400 Willoughby Ave., 3rd floor, Juneau, Alaska 99801
[2]Geophysical Institute, University of Alaska-Fairbanks, Fairbanks, Alaska 99775

CONCEPTUAL MODEL OF AKUTAN GEOTHERMAL SYSTEM

The results of investigations described in this report allow development of a conceptual model of the geothermal regime at Hot Springs Bay valley as depicted in figure 7-1. Seismic and resistivity surveys have delineated three units in the valley: 1) an upper layer, 30–70 m thick with seismic velocity of 1,630–1,960 m/s and resistivity of 100 ohm-m; 2) an intermediate-velocity layer (about 3,240 m/s) 0–75 m thick which contains a region of low resistivity (3 ohm-m); and 3) a deep high-velocity (4,900 m/s), high-resistivity (1,500 ohm-m) unit presumed to be volcanic bedrock similar to the older volcanic breccias which form the steep valley walls. Detailed resistivity measurements suggest the existence of more complicated layering within the three fundamental units.

Key features of the hydrothermal system are: 1) a deep hydrothermal reservoir at a temperature of 200°C from which thermal fluids ascend to shallower levels; 2) a shallow reservoir of low-enthalpy thermal waters underlying the northwest corner of the valley; 3) the fumarole field at the head of the valley; and 4) the hot springs along the lower western margin of the valley.

The hydrothermal system is assumed to be driven by magmatic heat associated with nearby Akutan Volcano as suggested by petrologic and geochemical data and helium isotope ratios.

Hydrothermal Cap

Geophysical surveys have inferred the existence of an intermediate-resistivity, low-velocity upper layer which is 40–70 m thick near the valley center and which thins up-valley and toward the valley margins. The uppermost unit in this layer was found to be a volcanic debris flow of relatively recent age (<3,000 ybp). By inference, the remainder of this layer is presumed to be composed of similar debris flows (such as are exposed in adjacent valleys), interbedded with valley alluvium. This layer appears to act as a low-permeability cap on the shallow subsurface hydrothermal system.

The thermal springs all occur along the lower west valley margin. Although searched for, no geologic or geophysical evidence could be found for fault control of the spring flow or fumarole emissions. The sinuous low-resistivity pattern of shallow-ground EM-31 measurements suggests that the thermal spring waters are migrating along older stream channel gravels. The thermal springs presently occur on or very near stream banks, and thermal waters are also discharging through stream-bed gravels directly into Hot Springs Creek. The creek has apparently cut through the uppermost volcanic debris flow layer which is probably thinnest along the valley margins. Interconnection with stream-cut channels embedded in the older debris flows would allow thermal waters under artesian pressure in the shallow mixing reservoir to migrate upward through permeable gravels and emerge at the surface.

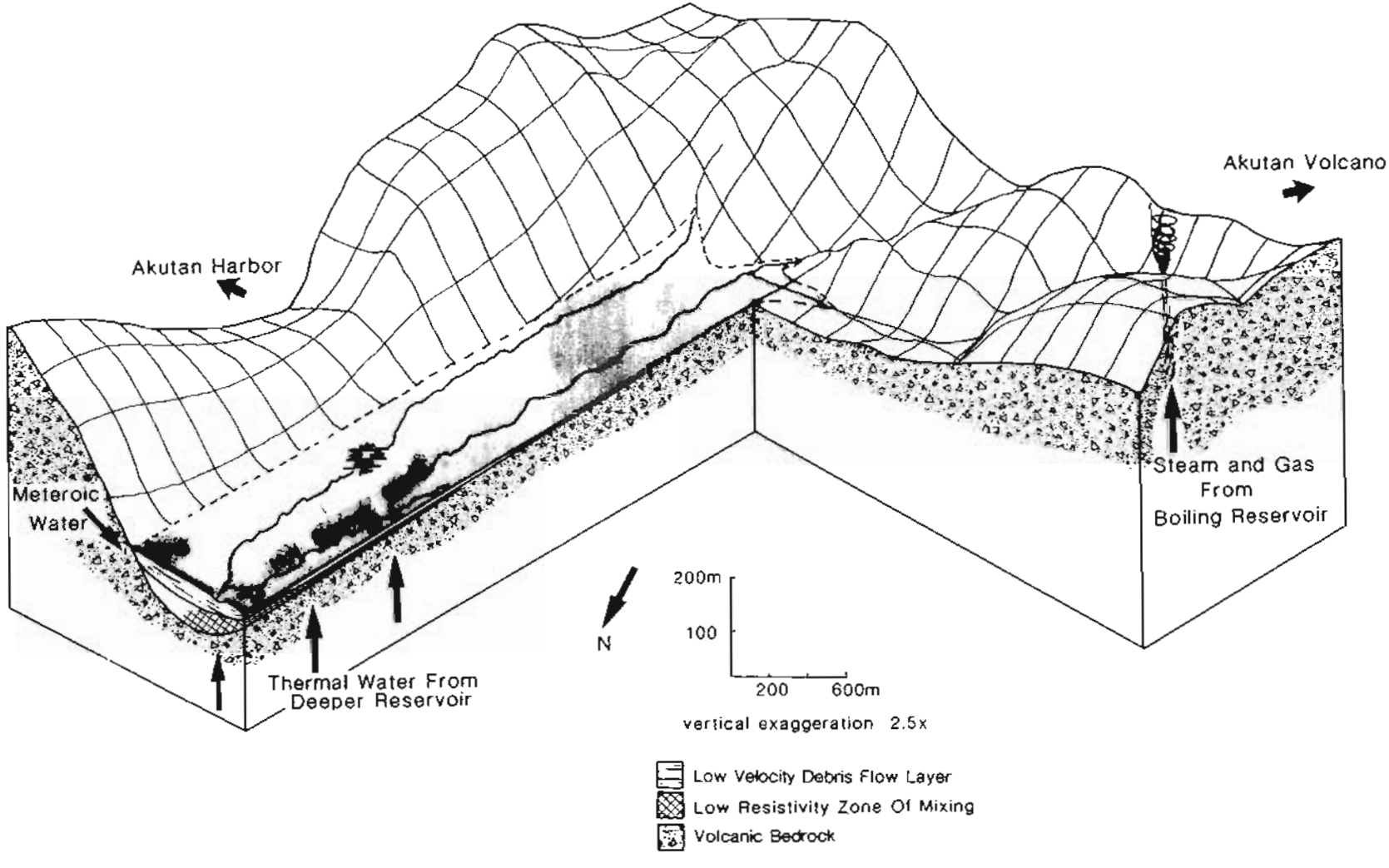

Figure 7-1. Conceptual model of geothermal system at Hot Springs Bay valley, Akutan Island, Alaska. Thermal waters from deep reservoirs ascend into a porous layer underlying the lower valley. The thermal waters are diluted with infiltrating cold meteoric waters in a zone of mixing and ascend and emanate as hot springs. Steam and other gases evolving from either the same reservoirs or different reservoirs feed fumaroles at the head of the valley. The underlying driving force is assumed to be a shallow-lying body of magma associated with active Akutan volcano.

Shallow Reservoir-Low Resistivity Zone of Mixing

The longitudinal seismic refraction survey BB' delineated a middle layer in the lower valley having a thickness of ~100 m near the ancient dune and thinning rapidly to less than 40 m, 500 m up-valley from the dune. The upper surface of this layer dips gently down-valley and lies at depths of 30-40 m. The interface of the layer with underlying valley bedrock has a comparatively steeper slope, with a depth to bedrock at the dune of 130 m vs. 75 m at 500 m up-valley.

This intermediate layer was not detected by the down-valley transverse seismic survey AA' nor by the longitudinal survey CC' taken up-valley from BB'. However, Wescott and others (this report) have argued that a hidden layer up to 25 or 45 m thick could exist and go undetected by the seismic surveys. Furthermore the three-layer model is in general agreement with the deep-sounding electrical resistivity surveys.

The composition of the intermediate layer is uncertain. The relatively high seismic velocity of this layer indicates a fairly rigid rock, while electrical resistivity indicates a fairly porous or, alternatively, a clay-rich unit. Seismic profiles suggest that the lower valley bedrock was glacially carved. The intermediate layer could thus be composed of till and glaciofluvial outwash deposited during the waning stages of the Wisconsinan Glaciation. The rigidity of the layer could arise from subsequent hydrothermal cementation. Alternatively, the layer could be composed of partially cemented ash flow tuffs, which could account for both rigidity and porosity. Either case is consistent with the inference that the intermediate layer is required to have sufficient permeability to allow migration, mixing and upwelling of thermal waters.

The low resistivity of the intermediate layer has several possible causes. The depth to bedrock near the ancient dune is 120 m below present mean sea level. Worldwide eustatic sea-level depression during the Wisconsinan maximum is estimated to have been 75-100 m below the present mean sea level (Clark and Lingle, 1979). Relative sea levels and sea-level changes during the late stages of the Wisconsinan Glaciation and during the Holocene in the Aleutians are not well-known because of the complications involved in unraveling isostatic, eustatic and tectonic processes (Black, 1980). However, it does appear possible that glaciofluvial sediments were deposited in a marine environment in Hot Springs Bay valley during the waning stages of the Wisconsinan Glaciation. Thus, the low resistivity could be a result of the salinity of pore waters in glacio-marine sediments that have not been flushed by fresh waters. The low carbon-13 compositions of the carbon dioxide and methane and the large proportion of methane in hot springs gases indicate that a source of organic material exists in the near-surface region of the valley, but whether the material is of marine or terrestial origin cannot be distinguished.

A second possible cause of low resistivity of the intermediate layer is that coastal saltwater currently exists in the intermediate layer as a result of modern-day hydrodynamic conditions. Both these possibilities are rejected

in favor of a hypothesis of the presence of low-resistivity thermal waters for the following reasons:

1. The hydraulic head and the constant flow of meteoric and thermal water through the valley fill are probably sufficient to keep the valley flushed of salt water and cleansed of salts from any early Quaternary marine sedimentation.

2. The region of low resistivity is confined to the west side of the valley and extends to within 30 m of the surface at 1 km from the present coast. If the low resistivity were due to pore waters in glacio-marine sediments or the occurrence of natural salt water bodies, the low resistivity would be expected to extend across the entire width of the valley. It also seems improbable that salt water would penetrate as far inland as 1 km or as shallow as 30 m.

3. The most compelling reason for ascribing the low resistivity to thermal waters is the proximity of this zone to the location of hot springs.

Further evidence for the existence of shallow thermal waters is the anomalously high helium and mercury values in soil samples obtained near the valley center (Wescott and others, this report).

Evidence from fluid geochemistry mixing models suggests the existence of a shallow reservoir of low-enthalpy thermal waters formed by the mixing of ascending high-enthalpy thermal waters and infiltrating cold meteoric waters. The zone of mixing is inferred to be the region of low resistivity within the intermediate layer. The ascending parent thermal waters are estimated to be at a temperature of ~200°C. Under normal hydrostatic pressure these waters would normally begin boiling when they reached depths of ~150 m, but meteoric waters infiltrating into the intermediate layer from the east side and from up-valley probably intercept the hot waters and either quench the boiling or prevent boiling from occurring at all. The mixed waters are further cooled during convective flow and horizontal movement within the shallow reservoir.

Deep Reservoir

The high resistivity, high velocity bedrock underlying the valley is inferred to be a continuation of the Hot Springs Bay volcanics exposed in the valley walls. What underlies the volcanics is unknown. The depth of penetration of the geophysical surveys was insufficient to delineate conduits supplying geothermal fluids to the intermediate layer and, although the existence of a deep reservoir can be inferred from fluid geochemistry, the depth to the reservoir is unknown. At the Makushin geothermal area on neighboring Unalaska Island, an exploration well sited at 370 m (1,200 ft) above sea level encountered a producing fracture in a hot-water system at a depth of 600 m (2,000 ft), about 240 m below sea level. The potentiometric surface of the Makushin hot-water system itself is estimated to be at about 120 m above sea level (Motyka and others, 1988). Thus it seems reasonable to assume that the reservoirs at Akutan lie within 1 km of the surface and are perhaps as shallow as 300 m below the valley floor.

Similarities between the compositions of the lower valley hot spring gases and upper valley fumarole gases, $^3He/^4He$ ratios, and the geothermometric estimates of reservoir temperatures suggest that the thermal fluids supplying the two zones are derived from the same reservoir. If so, the reservoir may span a distance of over 4 km in length. The temperature of the deep reservoir is estimated to be at least 200°C, while silica and chloride-enthalpy diagrams suggest concentrations of 260 ppm for SiO_2, and 1,100 ppm for Cl^- in the reservoir waters. The similarity in stable isotope compositions of thermal spring waters to surface stream waters indicates meteoric water to be the likely source of recharge for the reservoir.

The relatively heavy carbon-13 composition of the fumarolic carbon dioxide and the $^3He/^4He$ ratios of 6.0-7.0 reflect a probable mantle influence on the geothermal system, and suggest that a magmatic intrusive, perhaps associated with the active volcanism of nearby Akutan volcano, is the source of heat driving the hydrothermal system. Akutan is a young volcano with a small caldera indicative of movement and storage of magma in the shallow crustal region of Akutan Island. Geochemistry and petrology of volcanic rocks at Akutan volcano are also consistent with fractional crystallization of a single shallow magma system.

GEOTHERMAL POTENTIAL

The available information about Hot Springs Bay valley is sufficiently detailed to allow estimation of the energy potential of the geothermal resources. The estimates are necessarily crude because precise determination of parameters required for rigorous resource assessment, such as reservoir depth, volume, permeability, and temperature, can be obtained only through an exploration drilling program.

Natural Heat Discharge

The heat being discharged at the surface in a hydrothermal system's natural state is a useful indicator of long-term extractable energy. The rate at which heat is being discharged from the Hot Springs Bay valley geothermal system by natural fluid flow in the lower valley was estimated at 2.1-4.4 MW (Motyka and others, this report). This estimate is based on thermal spring flow measurements, estimates of thermal water discharge directly into Hot Springs Creek, and the discharge of thermal waters at and beyond the Hot Springs Bay beach. The heat being discharged from the fumaroles located at the head of the valley was not measured but is judged to be in excess of 1 MW.

If the hydrothermal system is assumed to be in a state of equilibrium, that is, heat discharged at the land surface is being replenished by heat from deeper in the system, then the estimates of heat discharge represent the rate at which heat could theoretically be extracted from the system indefinitely without significant drawdown or depletion of reservoir energy. In practice, operation of a geothermal well could, depending on reservoir characteristics, result in significant drawdown and depletion of energy.

Reservoir

Methodology

The methodology developed by Brook and others (1979) for assessing geothermal reservoirs which have not yet been drilled is adapted here. The accessible geothermal resource base of a reservoir, or the total amount of thermal energy stored in the reservoir, is expressed by:

$$Q_r = \rho c \; V \; (T - T_{ref}) \qquad (7\text{-}1)$$

where

Q_r = accessible reservoir thermal energy in joules

ρc = volumetric specific heat of rock plus water

V = reservoir volume

T = reservoir temperature

T_{ref} = reference temperature.

The recoverable geothermal energy, that is, the amount of heat that can actually be extracted at the wellhead (Q_{wh}), is estimated by Nathenson and Muffler (1975) to be approximately 25 percent of the stored energy. In making this estimate, Nathenson and Muffler have assumed that thermal energy in the reservoir can be additionally extracted by a sweep process involving injection of cold water into the reservoir to replace the original hot water withdrawn during production. If cold-water reinjection is not done, the recoverable energy would be somewhat less, although cooler ground water would still be expected to replace some of the extracted thermal water.

Electricity is produced from geothermal resources by converting part of the thermal energy into mechanical energy (work) and using this work to generate electrical energy. The change in fluid enthalpy minus the waste heat involved in the process is the work that is available, W_a.

The ratio of work to the accessible energy base, W_a/Q_r, has been calculated by Brook and others (1979) for hot-water systems for a broad range of temperatures and for reservoir depths of 1 and 3 km using a number of simplifying assumptions. The reader is referred to Brook and others (1979) for details on the calculations and assumptions made. For a reservoir depth of 1 km and temperature of 200°C, conditions we might expect for the deeper reservoirs at Akutan, the ratio W_a/Q_r from Brook and others (1979) is 0.058.

The electrical energy E obtainable from a geothermal reservoir is given by the equation:

$$E = W_a \; . \; U \qquad (7\text{-}2)$$

in which U is a utilization factor less than one, to account for mechanical and other losses that occur in a new power cycle. For hot-water systems a value of 0.4 is representative (Nathenson, 1975).

Assessment of Stored and Wellhead Energy Potential

Results of thermal fluid geothermometry indicate that the hydrothermal reservoir has a temperature of ~200°C (Motyka and others, this report). As discussed previously, geothermal drilling at neighboring Unalaska Island intersected a producing hot-water fracture zone at a depth of approximately 600 m below the surface at the point of drilling. It thus seems reasonable to assume that the reservoir at Akutan lies within 1 km of the surface and may perhaps be shallower. If the thermal fluids emanating from the lower valley hot springs and the upper valley fumarole field are derived from the same reservoir, then the reservoir could span a length of 4 km or more. Based on the results of explored geothermal systems, Brook and others (1979) estimate that the width and thickness of a geothermal reservoir are likely to be at least 1 km. Using these dimensions, the total volume of the Hot Springs Bay valley reservoir is estimated to be ~4 km^3.

The reference temperature, T_{ref}, is taken to be the mean annual surface temperature, ~10°C (Selkregg, 1976). The type and porosity of rock housing the geothermal reservoir at Hot Springs Bay valley are unknown. Candidates for reservoir rock include deep-seated marine sandstones and shales (Motyka and others, this report), Hot Springs Bay volcanics, and gabbroic intrusives (Swanson and Romick, this report). Following the recommendations of Brook and others (1979) for unexplored systems, the volumetric specific heat, ρc, is assumed to be 2.7 $J/cm^3/°C$ based on a rock volumetric specific heat of 2.5 $J/cm^3/°C$ and a reservoir porosity of 15 percent, which are average values for explored systems.

Table 7-1 presents the estimated geothermal energy potential of Hot Springs Bay valley based on the preceding reservoir parameters. The wellhead energy potential is ~5.1×10^{17} J. If this energy were to be converted entirely to electrical energy the estimated average electrical power generation capacity for a 30-year period is ~12.7 MW, more than sufficient to meet the energy needs of the Akutan community for the foreseeable future.

SUGGESTIONS FOR RESOURCE DEVELOPMENT

The proximity of the Hot Springs Bay valley geothermal resource area to Akutan village and the harbor make this resource a particularly attractive one for continued exploration and development. The resource area lies near the coast and is accessible by sea. Exploration and drilling equipment can be brought to the site by barge and tractor, with little or no helicopter support. Development of the resource could be tailored to the needs of the Akutan community; the estimated wellhead energy potential should be more than adequate to meet their electrical power, district heating and industrial direct heating needs. Sampling and analysis of fluids produced from the well would be required to identify potential environmental problems.

Prior to development of the geothermal resource the following exploration program is suggested:

Table 7-1. Estimates of geothermal energy potential of Hot Springs Bay valley, Akutan Island, Alaska.

Temperature	200°C
Assumed volume	4 km^3
Stored energy, Q_r	20.5×10^{17} J
Wellhead energy, Q_{wh}	5.1×10^{17} J
Work available, W_a	0.30×10^{17} J
Electrical energy, E	0.12×10^{17} J
Electrical power production (30-yr period)	12.7 MW

Phase 1

1) Conduct an electrical resistivity survey of the entire valley, extending northeastward over the pass towards Akutan Village and Harbor with depths of penetration of over 1 km (sheet 1). A 2-km transmitting dipole for a controlled source audio-magneto-telluric survey could be installed in Broad Bight valley on the south side of the island for these measurements.
2) Conduct a detailed helium and mercury soil-survey of the valley.
3) Conduct a self-potential survey of the valley.
4) Continue monitoring thermal springs and fumaroles to refine mixing models and provide better estimates of deep reservoir temperatures.

Phase 2

1) Site an exploratory test well based on results of Phase 1.
2) Drill well to appropriate depth.
3) Sample and analyze thermal fluids from well.
4) Test well and reservoir for well efficiency and hydrologic parameters.

The goal of the first phase is to look for connections between fumaroles and hot springs, to refine estimates of reservoir size and temperature, and to determine the locations and depths of potential reservoirs and conduit systems in order to guide the siting and design of exploration and production wells. The exploration well could possibly be converted into a production well, depending on the results of well and reservoir testing.

REFERENCES CITED

Black, R.F., 1980, Isostatic, tectonic, and eustatic movements of sea level in the Aleutian Islands, Alaska, in Nils Axel Morner, ed., Earth rheology, isostasy and eustasy: J. Wiley and Sons, p. 231-248.

Brook, C.A., Mariner, R.H., Mabey, D.R., Swanson, J.R., Guffacti, Marianne, and Muffler, L.J.P., 1979, Hydrothermal convection systems with reservoir temperatures >90°C, in Muffler, L.J.P., ed., Assessment of geothermal resources of the United States - 1978: U.S. Geological Survey Circular 790, p. 18-85.

Clark, J.A., and Lingle, C.S., 1979, Predicted relative sea-level changes (18,000 years B.P. to present) caused by late-glacial retreat of the Antarctic ice sheet: Quaternary Research, v. 11, p. 279-298.

Motyka, R.J., Queen, L.D., Janik, C.J., Sheppard, D.S., Poreda, R.J., and Liss, S.A., 1988, Fluid geochemistry and fluid-mineral equilibria in test wells and thermal gradient holes of the Makushin geothermal area, Unalaska Island, Alaska: Alaska Division of Geological and Geophysical Surveys, Report of Investigations [in preparation].

Nathenson, Manuel, 1975, Physical factors determining the fraction of stored energy recoverable from hydrothermal convection systems and conduction-dominated areas: U.S. Geological Survey Open-file Report 75-525, 35 p.

Nathenson, Manuel, and Muffler, L.J.P., 1975, Geothermal resources in hydrothermal convection systems and conduction-dominated areas, in White, D.E., and Williams, D.L., eds., Assessment of geothermal resources of the United States - 1975: U.S. Geological Survey Circular 726, p. 104-121.

Selkregg, L.L., ed., 1976, Alaska Regional Profiles, Volume III, Southwest Region: University of Alaska, Arctic Environmental Information and Data Center, Anchorage, Alaska, 313 p.